2018

Methods To Identify And Develop Drugs For Cryptosporidiosis

Rajiv Satish Jumani
University of Vermont

METHODS TO IDENTIFY AND DEVELOP DRUGS FOR CRYPTOSPORIDIOSIS

A Dissertation Presented

by

Rajiv Satish Jumani

to

The Faculty of the Graduate College

of

The University of Vermont

In Partial Fulfillment of the Requirements
for the Degree of Doctor of Philosophy
Specializing in Cellular, Molecular and Biomedical Sciences

May, 2018

Defense Date: February 27, 2018
Dissertation Examination Committee:

Christopher D. Huston, M.D., Advisor
Johnathan E. Boyson, Ph.D., Chairperson
Wolfgang Dostmann, Ph.D.
Markus Thali, Ph.D.
Gary E. Ward, Ph.D.
Cynthia J. Forehand, Ph.D., Dean of the Graduate College

ABSTRACT

Cryptosporidiosis is a common diarrheal disease caused by intestinal infection with the apicomplexan parasite *Cryptosporidium*, in humans usually either with *C. hominis* or *C. parvum*. Unfortunately, given a large burden of disease in children and immunocompromised people like AIDS patients, the only currently approved treatment, nitazoxanide, is unreliable for these patient populations. To address the urgent need for new drugs for the most vulnerable populations, large phenotypic screening efforts have been established to identify anti-*Cryptosporidium* growth inhibitors *in vitro* (hits). However, in the absence of a gold standard drug, the *in vitro* and *in vivo* characteristics that should be used to prioritize screening hits are not known. This thesis is focused on identifying promising anti-*Cryptosporidium* hits and drug leads, and using them to establish validated methods to guide hit-to-lead studies for anti-*Cryptosporidium* drug development.

A re-analysis of our phenotypic screen of the Medicines for Malaria Venture Open Access Malaria Box identified a promising *C. parvum* growth inhibitor, MMV665917. It had similar *in vitro* activity against *C. hominis*, *C. parvum* Iowa, and *C. parvum* field strains, and it was amenable to preliminary structural activity relationship studies using commercially available variants, with one variant demonstrating nanomolar potency. Furthermore, MMV665917 was effective *in vivo* in an acute interferon-γ mouse model of cryptosporidiosis; and it appeared to cure an established infection in the chronic NOD SCID gamma (NSG) mouse model, unlike nitazoxanide, paromomycin, and clofazimine. We hypothesized that anti-*Cryptosporidium* activity in the highly immunocompromised chronic NSG mouse model might relate to compounds being capable of killing and eliminating parasites (cidal), rather than only preventing growth (static). To test this, we developed a novel *in vitro* parasite persistence assay that showed that MMV665917 was potentially cidal, whereas nitazoxanide, paromomycin and clofazimine appeared static. This pharmacodynamic assay also provided the concentration of compound required to maximize rate of parasite elimination, which could help design *in vivo* experiments.

To further characterize compounds based on mechanism of action, we developed a range of *in vitro* medium-throughput life-stage assays. To validate and gain value from the assays, a "learner set" of compounds from our in-house screens and collaborations were tested in all of the *in vitro* assays and in the *in vivo* NSG mouse model. Using these assays, it was possible to group molecules based on chemical class/mechanism of action. Because compounds from distinct groups showed activity in the NSG mouse model, these methods could be used to obtain a diverse set of early-stage *Cryptosporidium* inhibitors for prioritization. Furthermore, compounds that appeared static in the *in vitro* parasite persistence assay did not have activity in the NSG mouse model. In summary, we report the identification and development of a highly promising initial lead, MMV665917, and report a range of *in vitro* assays that can be used to prioritize anti-*Cryptosporidium* hits and leads.

CITATIONS

Material from this dissertation has been published in the following form:

Jumani R.S., Bessoff K., Love M.S., Miller P., Stebbins E.E., Teixeira J.E., Campbell M.A., Meyers M.J., Zambriski J.A., Nunez V., Woods A.K., McNamara C.W., Huston C.D.. (2018). A Novel Piperazine-Based Drug Lead for Cryptosporidiosis from the Medicine for Malaria Venture Open Access Malaria Box. Antimicrobial Agents and Chemotherapy, 62, e01505-17.

ACKNOWLEDGEMENTS

First and foremost I would like to thank my advisor, Dr. Christopher D. Huston. No words can justify my gratitude for him. A long time ago, when I was rotating in his lab he mentioned to me that motivating students is not his strength; but his constant motivation all these years is the one thing that has kept me going all along, including the herculean task of writing this dissertation. Even at times when I lost confidence in my abilities, Chris has been extremely patient with me, finding innovative ways to help me. He has not only been a personal and professional guide and mentor, but I owe most of my personal and professional success to him. It is common saying that graduate students subconsciously take after their mentors; I would honestly consider myself very fortunate to have inherited his virtues. His values and teachings have not only made me a good scientist but a better human being as well.

I am extremely thankful to my thesis committee for guiding me all through these years. Their critical insight have taught me so much that I always looked forward to learning from them at the committee meetings, while at the same time dreading that I am not smart enough. Dr. Jon Boyson has always provided very thorough and meaningful insights that have been extremely vital to the success of my training and thesis. Dr. Wolfgang Dostmann has not only taught me all the organic and medicinal chemistry knowledge I know, but also been like a beacon, guiding me with invaluable personal and professional advice at every critical juncture. Dr. Markus Thali was the first faculty that I got in touch with during my applications,

and I have had some extremely memorable conversations with him. He is one of the main reasons why I love Switzerland and Swiss chocolates – thank you again for introducing me to Lindor! Dr. Gary Ward's love for science and rigor has been contagious. I have always looked up to his professionalism, teaching and presentation skills.

I would like to thank my labmates: Adam, Alvee, Connor, Erin, Kovi, Liam, Peter and Ze, who have been like a family to me. This thesis would have not happened without all of you. Kovi is an amazing personality and taught me all the Crypto; Adam's been the prodigy scientific big brother; Ze is a scientific genius; Peter is extremely hard working and provides the most critical insights; Liam is extremely kind and smart; Connor is always lively, and a programming genius; Alvee is one of the most intelligent people I have known; and Erin is one of the smartest and kindest person I have met. The CMB, NGP and medicine department folks have always been there and made things happen; thank you Erin Montgomery, Carrie, Kristin, Jessica, Hayley, Ashley and Pam. Dozens of people inside and outside UVM have taught me immensely, and although too many to name here, I am extremely grateful to them.

I am extremely fortunate to have such a loving and supportive wife, family and friends, who have been my pillar of support. This thesis is dedicated to my mother, Mrs. Meena S. Jumani, who is the real reason and inspiration behind my endeavors.

TABLE OF CONTENTS

Page

LIST OF TABLES

Table Page

LIST OF FIGURES

Figure Page

CHAPTER 1

CHAPTER 2

CHAPTER 3

APPENDIX I

APPENDIX II

CHAPTER 1: COMPREHENSIVE LITERATURE REVIEW

1.1. Introduction

The goal of this thesis is to identify and develop anti-*Cryptosporidium* compounds, with a major focus to develop relatively inexpensive *in vitro* assays to rationally aide the initial stages of *Cryptosporidium* drug discovery and development. This Chapter provides a background about the medical importance of the disease, followed by early stage drug development strategies used for other neglected tropical diseases, and how we have adapted them in part for anti-*Cryptosporidium* drug development.

Cryptosporidiosis is a water-borne diarrheal disease that is caused by eukaryotic *Cryptosporidium* parasites, of which there are many species. *Cryptosporidium* belongs to the phylum Apicomplexa, which also includes other well-studied and medically important parasites like *Toxoplasma* and *Plasmodium* species (Perkins, Barta, Clopton, Peirce, & Upton, 2000).

1.2. Historical Perspective

Although first reported in the peptic glands of the common mouse by Ernest Edward Tyzzer in 1907 (Tyzzer, 1907, 1910), *Cryptosporidium* was reported to cause disease in animals only in 1955 after the identification of *C. meleagridis* in turkeys (Slavin, 1955). Medical and agricultural interest in *Cryptosporidium* grew after reports of its ability to cause disease in cattle in the early 1970s (Meuten, Van Kruiningen, & Lein, 1974; Panciera, Thomassen, & Garner, 1971). Soon after, two separate human

reports of watery diarrhea caused by intestinal *Cryptosporidium* infection in a 3-year-old child and a 39-year-old immunosuppressed patient with exposure to cattle, emerged in 1976 (Meisel, Perera, Meligro, & Rubin, 1976; Nime, Burek, Page, Holscher, & Yardley, 1976). In 1979 two more immunosuppressed human cryptosporidiosis cases were published, wherein the patients did not live on a farm and the source of infection was unclear (Lasser, Lewin, & Ryning, 1979; Weisburger et al., 1979). These reports suggested a possible link between immunosuppression and cryptosporidiosis. During the same period, several *Cryptosporidium* species were identified in animals ranging from snakes and rabbits to sheep and monkeys. However, the role of *Cryptosporidium* infection in humans came to prominence after the discovery of the human immunodeficiency virus (HIV) in the 1980's. The Centers for Disease Control and Prevention (CDC) reported several cases of untreated chronic and prolonged diarrhea caused by *Cryptosporidium* infections in acquired immunodeficiency syndrome (AIDS) patients ("Cryptosporidiosis: assessment of chemotherapy of males with acquired immune deficiency syndrome (AIDS)," 1982). In the same decade several cases of shorter term, self-resolving diarrheal cases of cryptosporidiosis in immunocompromised patients were also described, along with transmission of the parasite to humans from infected farm cattle ("Human cryptosporidiosis--Alabama," 1982; Reese, Current, Ernst, & Bailey, 1982). In the developing world, cryptosporidiosis was reported not only to be a common cause of chronic diarrhea, but also associated with malnutrition in young children (Macfarlane & Horner-Bryce, 1987).

Research in the field was still highly limited until the United States' largest recorded waterborne outbreak caused more than 400,000 people to fall sick with cryptosporidiosis in Milwaukee in 1993 (Mac Kenzie et al., 1994). Despite numerous reports documenting cryptosporidiosis in immunosuppressed children in developing countries, *Cryptosporidium* was not considered a major pathogen until most recently after the report of the Bill and Melinda Gates Foundation funded the Global Enteric Multicenter Study (GEMS) (Kotloff et al., 2013). GEMS was the largest and most comprehensive study of childhood diarrhea, involving seven sites in Africa and Asia, and it identified cryptosporidiosis as the third most common cause of severe diarrhea in young children (J. Liu et al., 2016). The GEMS study used more sensitive detection techniques to identify *Cryptosporidium* species and corrected for co-infections with various other pathogens to find the pathogen responsible for the disease (Kotloff et al., 2013; J. Liu et al., 2016). Cryptosporidiosis was not considered a major pathogen for a long time and hence, the true extent of spread had never previously been thoroughly examined. All these factors combined with the fact that the earlier human studies have used less-sensitive methods of detection (Chalmers & Katzer, 2013) make it difficult to comprehend the true extent of infection.

1.3. Transmission

The predominant mode of infection is thought to be the fecal-oral route, as several logs per gram of environmentally stable oocysts are shed in the feces of infected individuals and calves, and as little as 9 oocysts of some virulent strains are sufficient

to cause disease in ~50% of the healthy volunteers (ID_{50}) (DuPont et al., 1995). The thick-walled oocysts shed in the feces are also highly stable in water for several months and are resistant to bleach, making water treatment complicated in developed countries as well (Rose, Huffman, & Gennaccaro, 2002). This has led to several outbreaks in the US and Europe, including the Milwaukee outbreak in the US that was mainly caused due to malfunction in the municipal water filtration unit. Frequent outbreaks in developed countries also occur due to infections from recreational water in swimming pools and playgrounds (Hlavsa et al., 2011).

C. parvum and *C. hominis* are the *Cryptosporidium* species that account for more than 90% of the infections in humans (Cacciò, 2005; Checkley et al., 2015). *C. hominis* is the species that is associated with majority of the waterborne outbreaks and was also responsible for most of the infections in children in the GEMS study (Sow et al., 2016). Although *C. hominis* can infect calves as well (Akiyoshi, Feng, Buckholt, Widmer, & Tzipori, 2002), *C. hominis* infections in humans are thought to be predominantly spread from other symptomatic and/or asymptomatic human carriers (Chalmers & Katzer, 2013; Hunter & Thompson, 2005). On the other hand, *C. parvum* can be transmitted from infected calves and humans (Hunter & Thompson, 2005).

1.4. Epidemiology

1.4.1. Children

Diarrhea is the second leading cause of death in children below 5 years of age, causing more than 499,000 deaths in 2015 (Disease, Injury, & Prevalence, 2016).

Shockingly, this is similar to the number of deaths due to all the cancers combined in the United Sates (U.S. Cancer Statistics Working Group, 2017). Although the number of deaths caused by diarrhea is on a steady decline, the decrease in incidence of diarrhea has been marginal, with the low- and middle- income regions of South Asia and sub-Saharan Africa worst affected (Disease et al., 2016; Mortality & Causes of Death, 2016). Cryptosporidiosis is a leading cause of infectious diarrhea in children (Kotloff et al., 2013; Jie Liu et al., 2016; Platts-Mills et al., 2015). Apart from being fatal, diarrhea is detrimental to the health of children, leading to long term developmental and growth defects (Bushen et al., 2007; Guerrant et al., 1999; Korpe et al., 2016; Kotloff et al., 2013). There is also a strong correlation between *Cryptosporidium* infections and malnutrition in children, although it is not clear if cryptosporidiosis is the predominant cause of malnutrition or if malnourished children are predisposed to cryptosporidiosis; both may be true (Macfarlane & Horner-Bryce, 1987; Shirley, Moonah, & Kotloff, 2012). It is also not known if during infections in infants, especially malnourished and immunocompromised children, the disease is only limited to the gastrointestinal tract.

1.4.2. Immunocompetent and Immunocompromised Adults

Cryptosporidiosis is self-limiting in immunocompetent adults, with infections ranging from asymptomatic to 2 weeks or longer of diarrhea (Chen, Keithly, Paya, & LaRusso, 2002). The infections are predominantly limited to the gastrointestinal tract with only a few cases of extra-intestinal infection reported in immunocompetent

patients with *C. hominis* (Hunter et al., 2004). In contrast, the infection is more likely to extend beyond the intestine in individuals with limited or no cell-mediated immunity, like AIDS patients and organ transplant recipients (Chen et al., 2002; Malebranche et al., 1983; Navin et al., 1999). The biliary tract usually gets infected in these patients and is thought to be a reservoir of infection (Chen et al., 2002). Most AIDS patients experience prolonged diarrhea, which lasts more than two months. Only about 4% of the patients shed the parasite without showing diarrhea symptoms. The symptoms in AIDS patients are inversely proportionate to the CD4+ T-cell counts, and treatment with highly active anti-retroviral therapy (HAART) can restore health (Flanigan et al., 1992).

1.5. Life Cycle

Cryptosporidium completes its life cycle in one host (monoxenous) (refer Figure 1 for schematic). The ingested thick-walled oocysts are triggered for excystation by the acid in the stomach followed by the bile salts, temperature and pH change in the intestine. A suture in the oocyst wall opens to release the infectious motile sporozoites. Sporozoites attach and invade the intestinal epithelial cells lining the lumen to form an unusual intracellular but extra-cytoplasmic niche called the parasitophorous vacuole (PV). This niche gives the parasite the advantage to steal nutrients from the lumen of the intestine as well as the cytoplasm of the host cell. The initial uninucleate intracellular form is called a trophozoite. The trophozoites undergo asexual replication (merogony) to form type I meronts, each containing six to eight

merozoites. The merozoites egress out of the PV to infect more epithelial cells. Each merozoite is thought to form a new trophozoite that can undergo merogony to form type I or type II meronts (containing only 4 nuclei). Type I meronts are thought to repeat the asexual replication cycle, while Type II meronts are believed to give rise to the sexual stages of microgamonts and macrogamonts. Each microgamont contains several motile microgametes (sperm equivalent), which upon release find and fertilize the uninucleate macrogamont (egg cell equivalent) to form thin- or thick-walled oocysts that sporulate *in situ*. The thin-walled oocysts are presumed to cause further local infection in the same host, while thick-walled oocysts are secreted in the feces for dissemination (Current & Reese, 1986; Fayer & Xiao, 2007). The life-cycle of *Cryptosporidium* is primarily based on visualization of stages using histology and/or electron microscopy techniques, and has not been validated by genetic or molecular approaches.

1.6. Current Treatment Options

There are no vaccines for cryptosporidiosis. The only U.S. Food and Drug Administration (FDA) approved medicine, nitazoxanide, has variably efficacy, with poor activity in the most affected populations. A placebo controlled study in HIV positive patients with cryptosporidiosis showed nitazoxanide to be completely ineffective (Abubakar, Aliyu, Arumugam, Hunter, & Usman, 2007). In a study with malnourished children with chronic cryptosporidiosis, nitazoxanide cured the diarrhea symptoms at day 7 in 56% of the patients, as opposed to the 23% of cured cases with

placebo alone (B. Amadi et al., 2009). Nitazoxanide is most effective in immunocompetent individuals, in whom it speeds up recovery (Beatrice Amadi et al., 2002). Paromomycin has shown good efficacy in mouse models of cryptosporidiosis, but is not useful in AIDS patients with cryptosporidiosis. Several other molecules including azithromycin, spiramycin, and immunoglobulin have proven ineffective against cryptosporidiosis in AIDS patients (Cabada & White, 2010; Checkley et al., 2015). Even with HAART therapy in AIDS patients, significant mortality is observed early on (Dillingham et al., 2009). Halofuginone is approved in Europe for use as a prophylactic drug for cryptosporidiosis in calves (Trotz-Williams, Jarvie, Peregrine, Duffield, & Leslie, 2011), but not in humans, due to its toxicity and side effects (Pham et al., 2014). There is a clear and desperate need for better treatments for cryptosporidiosis in the most vulnerable populations.

1.7. An Overview of Drug Discovery and Development

A general drug discovery and development scheme involves multiple stages that progress from identifying an active compound *in vitro* to activity in animal models to patient populations. Drug development generally happens at a pharmaceutical company wherein the efforts are well coordinated between diverse groups of people with specific expertise who are provided with clear go/no-go decisions set at every stage of drug development. An overview of the key stages is discussed below.

The initial discovery phase starts with a basic R&D exploratory stage that requires understanding biology of the disease. This is followed by development of a

reliable and robust screening assay with a goal to obtain diverse chemical scaffolds with desired activity against the disease. When available, a high-throughput screening assay is generally preferred, which could be a target-based or phenotype-based screening assay. In the phenotype-based approach, a collection of small molecules is tested for their effect on a biological process, for example, inhibition of asexual replication of a parasite in an *in vitro* cell based assay. On the other hand, a target-based approach involves screening of small molecules that alter the activity of a natural or recombinant protein that is crucial to the disease. The second approach requires the target be validated and activity of the molecules reconfirmed against intact cells. Although several recent advancements in genomics and computer-based modelling have dramatically aided target-based screening, it is unclear which of the screening approaches is more productive, as several successful drugs have been developed with both methodologies and it is not mandatory to know the target for a drug to be approved.

Screening data are analyzed to identify molecules with desired effects (hits). The hits need to be further validated based on biological, physical and chemical properties. Drug development in general has a very high attrition rate that depends a lot on the quality of the initial molecules. Furthermore, the investment for drug development increases dramatically following hit identification, demanding prioritization of quality hits. Prioritized hits with favorable pharmacodynamic (PD) and pharmacokinetic (PK) properties are tested for toxicity and efficacy in an animal model, which hopefully gives rise to an early lead molecule. The early leads undergo

several rounds of structural optimization for selectivity, potency, and PK-PD among other parameters to give rise to a drug candidate.

The drug candidate is further developed and tested in the preclinical development stage. This stage includes the study of process chemistry factors such as assessment of cost of goods, compound stability and further comprehensive preclinical safety studies in animals under Good Laboratory Practices (GLP) conditions. Once an investigational new drug application (IND) has been successfully accepted by a regulatory agency such as the US FDA, the molecule goes into preliminary Phase I clinical trials. Upon successful completion of Phase I, dosing regimens are optimized in Phase II, followed by a study against the comparator product in Phase III. If the molecule is successful in the clinical trials, a Marketing Authorization Application (MAA) is submitted to request full approval. There are numerous reasons that drug candidates fail. The lack of efficacy has contributed to 21% of the failures, while 21% have failed due to toxicity. Biopharmaceutical properties like oral bioavailability and formulation issues account for 39% of failures (Nwaka & Ridley, 2003).

The *Cryptosporidium* drug development pathway is not very well established (Huston et al., 2015; Manjunatha, Chao, Leong, & Diagana, 2016), with the first medium-throughput phenotypic screening assay published in 2013 (Bessoff, Sateriale, Lee, & Huston, 2013). The following sections are going to discuss some of the key aspects of the initial stages of drug development up to lead identification successfully used for other neglected infectious diseases, followed by a discussion of how these could be applied for *Cryptosporidium* drug development.

1.8. Neglected Disease Drug Development

Neglected tropical diseases (NTDs) are a group of infectious diseases that predominantly affect low-income populations in the less-developed world. The infections are widespread, causing severe morbidity and mortality while also costing developing economies billions of dollars every year. The lack of a market incentive along with challenging drug R&D and the high financial cost of drug development has hindered pharmaceutical investment for NTDs. Although NTDs account for more than 11% of the global disease burden, less than 1% of the approved drugs from 1975-2004 were for neglected tropical diseases (Trouiller et al., 2002). Since then, the formation of public-private partnerships (PPPs) and product development programs (PDPs) along with philanthropic and government funding has significantly improved the efforts towards developing therapeutics for NTDs. The PDP model involves a collaborative approach for drug development. PDPs essentially provide the oversight framework for drug discovery and development in a non-profit neglected disease setting. They provide structure in the form of disease specific goals based on patient needs, facilitate key collaborations fostering sharing and openness, and require standardized assays that enable logical go/no-go decisions, which results in appropriate prioritization and resource distribution. Some of the salient strategies used by PDPs like the Medicines for Malaria Venture (MMV), TB alliance, the Drug development for Neglected Disease Initiative (DNDi) for Chagas and visceral leishmaniasis are discussed below (Katsuno et al., 2015).

Setting clear goals for NTD drug development by understanding patient populations and needs has been successful in many instances. Target candidate profiles (TCP) are put in place to guide development of new molecules and target product profiles (TPP) for new medicines (Katsuno et al., 2015). There can be multiple TPPs and TCPs, and these keep evolving based on the need, since drug development usually takes a decade to complete during which disease landscape and patient needs can change, and major technological improvements in drug development may occur. For example, malaria drug development has two TPPs and five TCPs, with TCPs used to prioritize hits based on rate of action of compounds and life stage activity with clear gold standards used for every assay (Burrows et al., 2017; Burrows, van Huijsduijnen, Mohrle, Oeuvray, & Wells, 2013). The TPP for TB focuses on developing new drugs that are active against the drug-sensitive and drug-resistant TB, and reduce the duration of current treatments (Katsuno et al., 2015). The minimum requirement for visceral leishmaniasis includes greater than 90% clinical efficacy in a ten-day treatment regimen with activity against all resistant strains of *L. donovani*, along with no drug-drug interaction issues with malaria, TB and HIV treatments (Chatelain & Ioset, 2011). The TPP for Chagas disease at a minimum demands superiority to the current standard of care, benznidazole (Chatelain & Ioset, 2011). The presence of a gold standard drug has greatly helped set clear goals for TPPs and TCPs for these diseases.

Apart from the high-cost, there are several unique challenges facing drug development for NTDs. A high proportion of the patients reside in areas with poor infrastructure and highly limited healthcare resources. Therefore, the drugs need to be

stable under high-temperature and humidity conditions for long durations. Furthermore, drugs should be administered with no or limited oversight for dosing. Hence, oral drugs with minimal doses are favored. Co-infections are common in the tropical areas requiring a potential for multiple treatments at the same time requiring drugs with low drug-drug interactions so that there is no interference with other medicines.

1.8.1. Assay development

In general, it is unclear if target or phenotype-based screening is more fruitful (Eder, Sedrani, & Wiesmann, 2014; Swinney, 2013). There are several advantages to using a target-based screen. The knowledge of a target is exceptionally helpful in that it can aid in optimization of a chemical scaffold for selectivity towards the pathogen over the human host. Medicinal chemistry is also much easier to perform to improve potency, pharmacokinetic and pharmacodynamics properties. Knowledge of the target at the start can also help predict any toxicity issues that might come up later in the process. In disease areas where drugs with different mechanisms of action are desired, it is beneficial to know the target. Genome sequencing considerably eased the process for target identification, but target validation can be challenging, especially in the case of poorly studied NTDs. Furthermore, there is an added requirement to test the feasibility of the compound against the intact whole pathogens. In some cases, discrepancies have been observed between *in vitro* target inhibition studies and activity against whole pathogens for NTD drug development. There could be discrepancies

between activity against a target versus whole cell due to several reasons, such as inaccessibility of the target due to membrane permeability issues, off-target effects, alternate compensatory pathways, etc. (Nwaka & Hudson, 2006).

On the other hand, phenotypic screens are performed against the whole pathogen. Phenotypic screens are not biased and have the potential to quickly provide a large number of diverse hits, although the success of the hit and its druggability cannot be determined until later on. Recent improvement in genetics and molecular biology techniques, especially omics technologies, can aid in figuring out targets after phenotypic screening. Furthermore, phenotypic assays have been more productive for anti-bacterial drug development (Payne, Gwynn, Holmes, & Pompliano, 2007). Phenotype-based screens also provide a resource to screen and identify hits from a larger chemical space as compared to target-based screens. For these reasons, phenotypic screens have been more widely used for NTDs. For an efficient and reliable high throughput screen (medium throughput screen at the minimum), the assay needs to be robust with a good signal to noise ratio, which is often assessed using statistical metrics such as the Z and Z' scores (Zhang, 1999). Apart from the primary screening assay, several other follow-up assays aide in prioritization of hits with respect to TCPs and TPPs.

The *in vitro* culture of asexual blood stages of all major species of *Plasmodium* has been extremely important for malarial drug development (Schuster, 2002). Further breakthroughs in assays for the different life stages have been key in obtaining diversity and addressing specific needs such as activity against liver stages of species that

establish dormancy (Burrows et al., 2013). To directly compare compounds and avoid discrepancies between groups, MMV contracts out each of these assays to experts at specific locations for testing all the molecules under similar conditions.

1.8.2. Screening compound source

The quality of starting chemical entities is extremely important, especially for NTDs, wherein there is an urgent medical need, but the resources are highly limited. Pharmaceutical and biotech companies have a rich source of unique chemical compounds and associated expertise. PDPs utilize the collaborative model, wherein pharmaceutical and biotech industries contribute sets of diverse small molecules containing annotated analogues along with the knowledge and expertise associated with it (Chatelain & Ioset, 2011). MMV has also gone a step further and put together libraries of compounds with analogues from pharmaceutical companies and made them freely available for NTD research. To add further value, MMV asks for the screening data to be made available to the public in return for the compounds. The libraries include the 'Malaria Box', which is a set of 400 unique and diverse compounds active against blood stage of *P. falciparum* from phenotypic screens of over 6 million compounds performed by GlaxoSmithKline (GSK), the Genomics Institute of the Novartis Research Foundation (GNF), and St. Jude Children's Research Hospital (Van Voorhis et al., 2016). Furthermore, all the 400 compounds are commercially available and there is significant data shared for safety including: host cell toxicity using several cell lines and zebrafish; absorption, distribution, metabolism and elimination (ADME);

PK; and activity against several different pathogens. MMV has also recently put together a 'Pathogen Box', which includes 400 molecules with activity against at least one of several different pathogens that cause NTDs, including malaria, TB, kinetoplastids, helminths, cryptosporidiosis, toxoplasmosis and dengue virus (Duffy et al., 2017). Similar to the Malaria Box collection, significant investment has been made for these compounds, with data for host cell toxicity, ADME properties and PK made available. These data are extremely valuable for follow-up, saving time and resources while accelerating drug development for NTDs. For some of the compounds the biological targets are known, and this can aid in use of these molecules as chemical probes to explore the biology of the less-studied NTDs. PDPs have also initiated collaborations with pharmaceutical companies to obtain libraries of classes of inhibitors along with analogues that inhibit a specific known biochemical pathway of importance (Chatelain & Ioset, 2011).

There has been some success in repurposing existing drugs or compounds with significant previous investment for NTDs, especially compounds that have been taken into clinical trials, as it reduces the associated financial risk. For example, eflornithine was initially developed as an anti-cancer drug, but was later found to have great activity for treating Human African Trypanasomaisis (HAT). Miltefosine was initially taken to human trials for its anti-cancer properties, but then was taken for clinical trials for leishmaniasis due to its superior efficacy compared to existing treatments in the rodent model (Andrews, Fisher, & Skinner-Adams, 2014). The NIH clinical collection library serves as a useful source for repurposing, as it is composed of FDA-approved drugs and

molecules that have been taken into clinical trials (Bessoff et al., 2013). A major concern with repurposing already existing profit-making drugs is that the companies owning the drugs could be unwilling to share them in fear of identification of new safety concerns or other issues that might affect existing use (Pink, Hudson, Mouries, & Bendig, 2005).

1.8.3. Hit Identification

Phenotypic screens against the whole pathogen make it possible to screen thousands to millions of compounds in a short amount of time. There is no single formula or global potency threshold cut-off to identify hits from the screens, as the potency depends on several factors, including the assay type, assay set-up conditions (serum concentration, detection methods, compound concentration etc.), nature of the chemical library, and the pathogen under study. Several assays can be used as primary screens that can yield different results. For visceral leishmaniasis, a direct comparison of the axenic assays with adapted extracellular amastigotes that are thought to mimic intracellular stages gave a higher false-positive hit rate than the *L. donovanii* amastigote intracellular assay (De Rycker et al., 2013). The *P. falciparum* intracellular blood stage assay is the most widely used assay for primary screening for malaria. But the different TCPs could require alternate primary screening assays, like a malaria liver schizonticidal assay used to identify compounds active against latent liver stages that complicate treatment of malaria (Burrows et al., 2017; Burrows et al., 2013). PDPs

focus towards standardizing primary screening or follow-up potency assays for disease types so that compounds identified from various sources can be directly compared.

The hit cut-off can vary dramatically between pathogens due to differences in the biology of the diseases. For example, asexual blood stages of *Plasmodium* involve processes like host membrane re-arrangement that are targeted by the general drug-like molecules. On the other hand, *L. donovanii* has its intracellular stage inside acidic compartments of the phagolysosome of macrophages that are hard to access and retain drug activity in (Katsuno et al., 2015).

1.8.4. Hit Validation

The initial hits from the primary screen need to be further tested for several general and disease specific parameters to be considered a validated hit. The compound needs to be re-synthesized/re-purified with a conventionally decided purity of greater than 90% and tested against the pathogen to confirm its activity. Dose response curves should be performed against the pathogen to determine the half-maximal inhibitory concentration (EC_{50}), with the compound able to attain 100% inhibitory activity (usually demonstrating a sigmoidal concentration versus growth inhibition curve with a Hill coefficient ideally between 0.5 and 1.8). Potency varies with disease with a reasonable cut-off selected based on other compounds identified. For example, for malaria where it has been relatively easy to identify hits, a cut-off of 1-2 µM is used (Gamo et al., 2010; Guiguemde et al., 2010; Plouffe et al., 2008). It should be noted that potency has little to do with potential efficacy, but has a large

impact on manufacturing costs. The molecule should have at least greater than a 10-fold selectivity window over a relevant mammalian cell line. Keeping in line with lower manufacturing costs, the molecule should be easy to synthesize, ideally in less than 5 steps with acceptable yield. Preliminary structural-activity relationship studies (SAR) should show potential for medicinal chemistry changes and the molecule should not have any unstable or highly reactive moieties in the core pharmacophore (Katsuno et al., 2015; Nwaka & Hudson, 2006; Nwaka et al., 2009).

1.8.5. Hit-to-lead and Early Lead Identification

An early lead compound should demonstrate acceptable *in vivo* PK, toxicity and efficacy in a relevant animal model of the disease. The hit-to-lead prioritization is an extremely crucial step in NTD drug development as the finances, time and resources are highly limited. Added on, the high attrition rate of drug development is inversely proportionate to the quality of the chemical entities. Furthermore, since the investment in cost and time dramatically increases as one goes further in drug development, it is critical that quality lead compounds are prioritized (Khanna, 2012; Nwaka & Hudson, 2006). Hit-to-lead prioritization is generally guided by clear go/no-go decisions based on the TPPs and TCPs. In general, a diverse set of molecules with different mechanisms of action are preferred, as this gives a better chance for at least one molecule to make it all the way, rather than prioritizing all compounds with similar profiles (Katsuno et al., 2015).

For example, malarial drug development has clear TCPs based on life stage mechanism of action studies. The validated hits are screened against all the life stage assays along with key mechanistic assays and these results are used for further prioritization of compounds. The presence of gold standard compounds for comparison in each assay dramatically helps in characterizing the compounds (Burrows et al., 2017; Burrows et al., 2013).

The choice of *in vivo* model is extremely important. This was particularly true for a recent promising drug candidate, posaconazole, for Chagas disease. Posaconazole was highly promising *in vitro*, in an animal model for Chagas and preclinical efficacy studies. It also had a different mode of action from the only approved class of nitroheterocyclics. But the compounds failed during clinical treatment, as it performed poorer than the approved benznidazole nitroheterocycle class. Looking back, posaconazole was only tested in the acute disease mouse model, while the chronic stage is an important cause of disease, underscoring the importance of using the correct models (Chatelain, 2015; Molina et al., 2014).

1.9. Anti-*Cryptosporidium* Drug Development

The only FDA approved drug for cryptosporidiosis, nitazoxanide, is not very effective in young children and immunocompromised patients, but the reasons for its failures are not known. The lack of a highly efficacious drug complicates drug development, since there is no standard to follow.

Cryptosporidium biology is poorly understood, as there is no continuous *in vitro* culture system. A few rounds of asexual replication followed by formation of gamonts can be achieved *in vitro*, after which the culture crashes. Based on visualization techniques, it is thought that the parasite needs to undergo asexual followed by sexual replication to sustain an infection *in vivo*, but such details of the life cycle have not been confirmed by genetics or molecular methods. Based on the few rounds of asexual growth *in vitro*, a medium-throughput cell based phenotypic screening assay using the *C. parvum* Iowa isolate was developed for the first time and published in 2013. Prior to this, most of the drug development efforts were hypothesis driven or random, with a few groups taking advantage of genomic data and using target-based screening efforts. Due to the lack of genetic tools for *Cryptosporidium*, none of the targets were effectively validated. After the GEMS reports demonstrating cryptosporidiosis as a leading cause of severe diarrhea in children, there has been a lot of interest in *Cryptosporidium* drug development efforts including from pharmaceutical companies, and funding from the Bill and Melinda Gates Foundation. PATH, a non-profit organization, has also started an accelerator for *Cryptosporidium* research and drug development to reduce child mortality (ACCORD) program to facilitate the development of new therapeutics for cryptosporidiosis (Shoultz, de Hostos, & Choy, 2016).

1.9.1. Target Product Profile

The first TPP for cryptosporidiosis was published by Huston et. al. in 2015 (Huston et al., 2015). This has been followed up by a slightly modified TPP put forward by Majunatha et. al. in 2016 (Manjunatha et al., 2016), demonstrating the evolving nature of the TPPs. The profiles are predominantly similar with major differences in the duration of desired treatment regimen, method of treatment, and desired microbial and clinical efficacy, including extra-gastrointestinal infections. Both the publications put forward minimum and ideal TPPs for cryptosporidiosis. Since developing drugs and performing clinical trials on infants < 6 months of age is complicated, the initial idea is to first focus on *C. hominis* or *C. parvum* infected infants 6-24 months old that do not have HIV. It is assumed that a drug effective in infants would also work in immunocompetent children and adults. Ideally, the target populations would include children greater than 1 month of age with or without HIV and immunocompromised adults. Huston et. al. recommends a new drug should at least have microbial (clear fecal parasite shedding) and clinical efficacy (resolution of clinical diarrhea symptoms) that is superior to nitazoxanide in malnourished children, and similar to nitazoxanide in immunocompetent individuals. Ideally, the drug should be able to clear fecal parasite shedding quickly (e.g. < 2 days) and have > 90% efficacy in all patient populations. Manjunatha et. al. suggest that the drug needs to show clinical and microbial efficacy by 4 days of treatment with > 90% efficacy in the minimum target population and > 95% efficacy in the ideal case target population with clearance of extra-gastrointestinal infections. Microbial efficacy is achieved when fecal

parasite test is negative for 2 consecutive days. Huston et. al., recommend an oral treatment that is at the minimum of superiority over nitazoxanide in the vulnerable populations, while ideally a single dose cure is preferred. Manjunatha et. al., call for a 3-day dosing cure with a maximum of thrice a day dosing regimen, and acceptance of a parenteral dosing regimen in a hospital setting. Based on market analysis and the desired public health benefit, the cost of the complete treatment should not be more than US$2.00, which is the cost of a complete treatment with nitazoxanide in India. Ideally, the treatment should cost US$0.50 (Huston et al., 2015).

1.9.2. Hit Identification and validation

The medium-throughput screening assay has been further optimized by the California Institute for Biomedical Research (Calibr) into a high-throughput screening assay with more than 1,000,000 compounds screened to date ((Love et al., 2017) and personal communication). There are several different assays developed along with different isolates of *C. parvum* Iowa strain used for potency studies (Bessoff et al., 2014; Castellanos-Gonzalez et al., 2013; Chao et al., 2018; Gorla et al., 2014; Love et al., 2017; Manjunatha et al., 2017; Ndao et al., 2013). The differences between assays or a standardized assay needs to be finalized in order to directly compare hits and leads. With the lack of a better standard, *in vitro* potency requirements are based on nitazoxanide with a recommended EC_{50} equal to or less than that of nitazoxanide along with at least a 10-fold selectivity window against the HCT-8 mammalian cell line that is routinely used for screening (Huston et al., 2015).

1.9.3. Hit-to-lead and Early Lead Identification

C. parvum Iowa isolates have been passed in calves with several logs of oocysts shed per gram feces during peak infection. This has provided a constant supply of oocysts for *in vitro* studies, as the parasite cannot be continuously cultured using a simple *in vitro* system (Arrowood, 2002). On the other hand, the laboratory strain of *C. hominis*, TU502 whose genome has been sequenced, has been maintained in gnotobiotic piglets that require expensive special housing and maintenance with poorer yields compared to calves. Furthermore, isolated *C. parvum* oocysts are stable at 4 °C for up to 4-5 months in phosphate buffered saline, whereas, *C. hominis* TU502 are highly unstable, retaining *in vitro* viability only a few days after shedding. This has made *C. parvum* the strain of choice for *in vitro* studies. Even though a substantial portion of the human infections are caused by *C. hominis*. Therefore, it is imperative that compounds be tested for activity against *C. hominis* as well. Furthermore, the infectious dose and *in vitro* drug susceptibility for field isolates is known to vary. Hence, it is extremely beneficial to test hits against at least *C. parvum* farm field isolates to avoid unexpected concerns further in the drug development process.

Learning from other NTD drug development strategies, development of several other assays has been suggested by Huston et. al. as part of the hit-to-lead prioritization cascade. These include: *in vitro* rate of action; static versus cidality; tendency to develop resistance; and life stage activity and other mechanistic assays to differentiate between hits and help select a diverse set of compounds despite the lack of knowledge

of molecular mechanism of action (Huston et al., 2015). Poor understanding of *Cryptosporidium* biology, unavailability of reliable markers and gold standard controls, lack of a continuous culture system, and asynchronous *in vitro* infections with mixed parasite populations are some of the factors that have made development of these assays very challenging. It is not clear if the sexual stages of the parasite have to also be affected to clear an infection, and/or if the sexual stage alone can be targeted to clear infection. Recently, the first report of genetic manipulation of *Cryptosporidium* was published. The method is not very convenient yet, as it involves making mutants by performing surgeries in mice and maintenance of oocysts *in vivo*, but it provides a great potential to help in understanding biology and developing assays along with identifying and validating targets (Pawlowic, Vinayak, Sateriale, Brooks, & Striepen, 2017; Vinayak et al., 2015).

Cryptosporidium has an unusual intracellular but extra-cytoplasmic niche with access to the intestinal lumen as well as the cytoplasm of the cell. Generally, for intracellular infections drugs with good oral bioavailability are preferred as the drug gets absorbed and accumulates in the blood and then reaches inside the infected cells. For an extracellular pathogen in the intestine, it is preferred that the drug does not get absorbed and rather stays in the intestine and locally acts on the pathogen. *Cryptosporidium* has this in-between niche, making it unclear if a drug needs to be absorbed or stay in the intestine. It is more likely that the PK characteristics desired will vary based on the drug and its mechanism of action. It is very likely that the PV membrane is selective, allowing only certain molecules to pass through. Also, an

effective anti-*Cryptosporidium* drug could potentially target a process in the host cell that is crucial for the parasite's survival (but not critical for the host), as *Cryptosporidium* is thought to rely heavily on the host. For extra-intestinal infections, systemic exposures would likely be important to clear the pathogen.

Several acute and chronic rodent models of cryptosporidiosis have been used to test only microbial efficacy of hits, as the rodent models do not get diarrhea (Gorla et al., 2014; Love et al., 2017; Manjunatha et al., 2017; Ndao et al., 2013). The acute models resolve infection after a few days, giving a small window for testing hits. The chronic mouse model includes the IFN-gamma knockout model, but its infection outcome varies between different groups, from self-resolving to lethal infections (Love et al., 2017; Manjunatha et al., 2017; Ndao et al., 2013). Nitazoxanide does not have any activity in the rodent models tested. In part due to the lack of a gold standard drug, it is not clear which of the rodent models best reflects disease in humans. Infection of calves with *C. parvum* is used as a clinical model for diarrhea symptoms and microbial efficacy (Manjunatha et al., 2017; Schaefer et al., 2016; Stebbins et al., 2018). Although extremely expensive, gnotobiotic piglets are used for microbial and clinical efficacy studies of *C. hominis* TU502 (Theodos, Griffiths, D'Onfro, Fairfield, & Tzipori, 1998).

1.9.4. Our Strategy

A key gap exists in the nascent *Cryptosporidium* drug development pipeline between screening to identify potential starting points and testing in rodents. As noted

above, methods are needed for prioritization according to the likelihood of *in vivo* success, and to maintain mechanistic diversity. Development of such key methods is the focus of this thesis. Since no gold standard drug exists and very few leads have been reported to date, our strategy was to collaborate and obtain as many leads as possible from various groups with a goal to obtain a diverse set of "learner hits and leads" to test and validate the value of our prioritization assays.

Our group was the first to report a robust cell-based screening assay for *Cryptosporidium*. We have collaborated with various groups performing target- and phenotype-based anti-*Cryptosporidium* drug development and provided a cell-based screening facility using our assay to directly compare the potency of all of the compounds (Figure 2). We have also developed a highly immunocompromised NOD SCID gamma (NSG) mouse model that represents chronic cryptosporidiosis, as in AIDS patients, providing the ability to test the effect of a molecule on an established infection, and also follow-up for relapse after cessation of treatment. In line with the *in vitro* assays, these compounds were tested in the same animal model providing for direct comparison between all these assays. These results formed the basis to directly compare the molecules in the established *in vitro* prioritization assays. Chapter two describes prioritization of a promising hit identified from the Malaria Box screen to an early lead compound with activity in the NSG and IFN-gamma knockout mouse model. The chapter also demonstrates that a parasite persistence assay to identify potentially static versus cidal compounds by comparing the rate of parasite kill *in vitro* is a valuable tool to differentiate compounds. Chapter three describes a range of life stage

assays that can differentiate hits based on mode of action and can be used as a tool to obtain a diverse set of compounds.

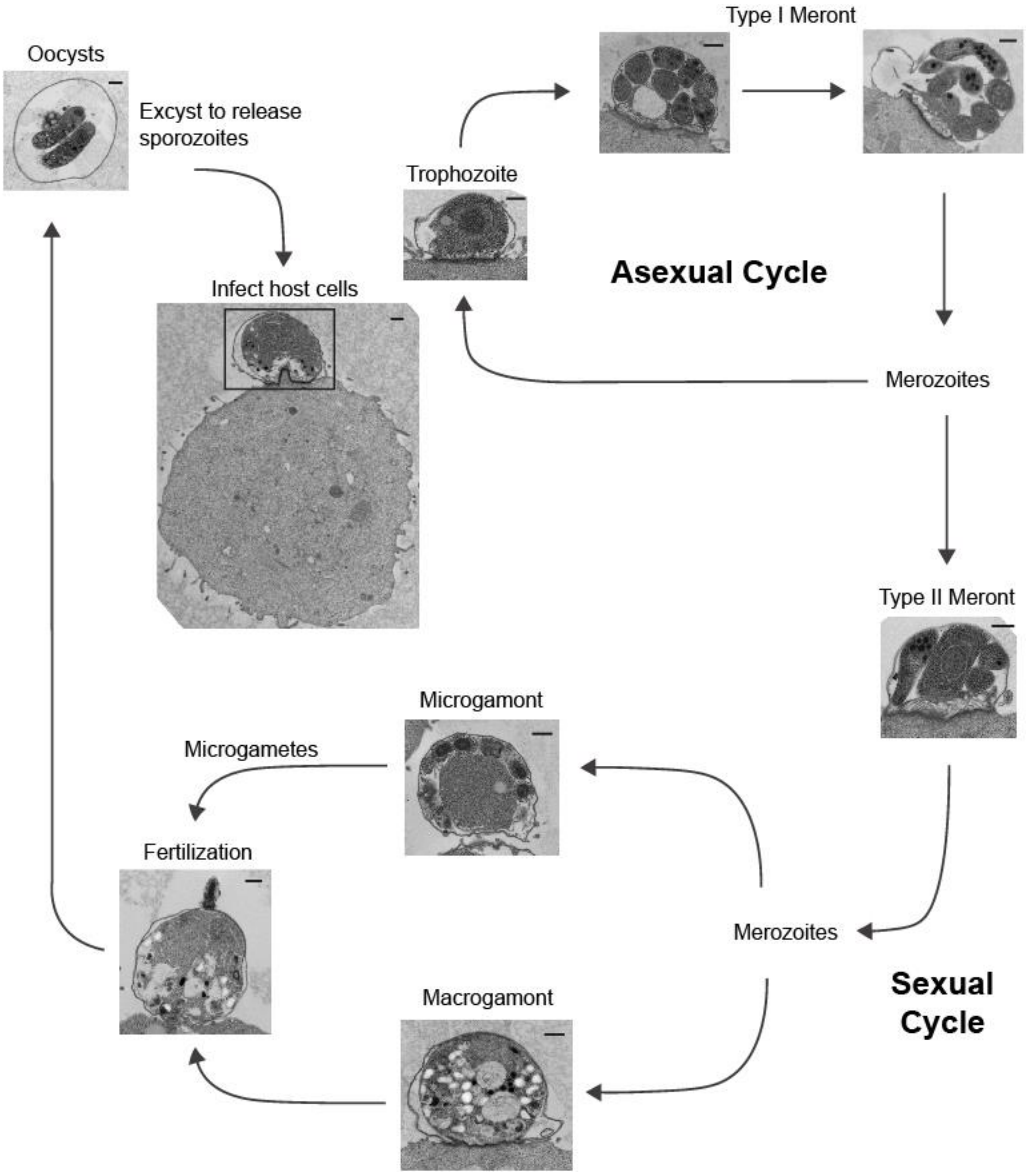

Figure 1. Life cycle of *Cryptosporidium parvum* depicted using transmission electron microscopy pictures.

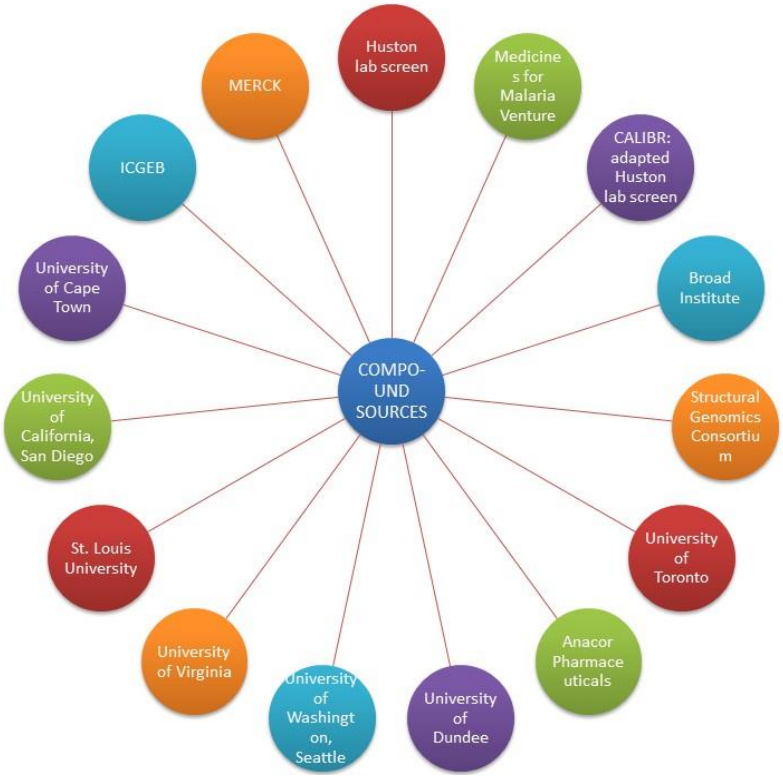

Figure 2. Collaborations and source of anti-*Cryptosporidium* hits and leads used in this thesis.

1.10. References

Abubakar, I., Aliyu, S. H., Arumugam, C., Hunter, P. R., & Usman, N. K. (2007). Prevention and treatment of cryptosporidiosis in immunocompromised patients. *Cochrane Database Syst Rev*(1), CD004932. doi:10.1002/14651858.CD004932.pub2

Akiyoshi, D. E., Feng, X., Buckholt, M. A., Widmer, G., & Tzipori, S. (2002). Genetic analysis of a Cryptosporidium parvum human genotype 1 isolate passaged through different host species. *Infect Immun, 70*(10), 5670-5675.

Amadi, B., Mwiya, M., Musuku, J., Watuka, A., Sianongo, S., Ayoub, A., & Kelly, P. (2002). Effect of nitazoxanide on morbidity and mortality in Zambian children with cryptosporidiosis: a randomised controlled trial. *The Lancet, 360*(9343), 1375-1380. doi:10.1016/s0140-6736(02)11401-2

Amadi, B., Mwiya, M., Sianongo, S., Payne, L., Watuka, A., Katubulushi, M., & Kelly, P. (2009). High dose prolonged treatment with nitazoxanide is not effective for cryptosporidiosis in HIV positive Zambian children: a randomised controlled trial. *BMC infectious diseases, 9*, 195. doi:10.1186/1471-2334-9-195

Andrews, K. T., Fisher, G., & Skinner-Adams, T. S. (2014). Drug repurposing and human parasitic protozoan diseases. *Int J Parasitol Drugs Drug Resist, 4*(2), 95-111. doi:10.1016/j.ijpddr.2014.02.002

Arrowood, M. J. (2002). In vitro cultivation of cryptosporidium species. *Clin Microbiol Rev, 15*(3), 390-400.

Bessoff, K., Sateriale, A., Lee, K. K., & Huston, C. D. (2013). Drug repurposing screen reveals FDA-approved inhibitors of human HMG-CoA reductase and isoprenoid synthesis that block Cryptosporidium parvum growth. *Antimicrob Agents Chemother, 57*(4), 1804-1814. doi:10.1128/AAC.02460-12

Bessoff, K., Spangenberg, T., Foderaro, J. E., Jumani, R. S., Ward, G. E., & Huston, C. D. (2014). Identification of Cryptosporidium parvum active chemical series by Repurposing the open access malaria box. *Antimicrob Agents Chemother, 58*(5), 2731-2739. doi:10.1128/AAC.02641-13

Burrows, J. N., Duparc, S., Gutteridge, W. E., Hooft van Huijsduijnen, R., Kaszubska, W., Macintyre, F., . . . Wells, T. N. C. (2017). New developments in anti-malarial target candidate and product profiles. *Malaria journal, 16*(1), 26. doi:10.1186/s12936-016-1675-x

Burrows, J. N., van Huijsduijnen, R. H., Mohrle, J. J., Oeuvray, C., & Wells, T. N. (2013). Designing the next generation of medicines for malaria control and eradication. *Malaria journal, 12*, 187. doi:10.1186/1475-2875-12-187

Bushen, O. Y., Kohli, A., Pinkerton, R. C., Dupnik, K., Newman, R. D., Sears, C. L., . . . Guerrant, R. L. (2007). Heavy cryptosporidial infections in children in northeast Brazil: comparison of Cryptosporidium hominis and Cryptosporidium parvum. *Transactions of the Royal Society of Tropical Medicine and Hygiene, 101*(4), 378-384. doi:10.1016/j.trstmh.2006.06.005

Cabada, M. M., & White, A. C., Jr. (2010). Treatment of cryptosporidiosis: do we know what we think we know? *Current opinion in infectious diseases, 23*(5), 494-499. doi:10.1097/QCO.0b013e32833de052

Cacciò, S. M. (2005). Molecular epidemiology of human cryptosporidiosis. *Parassitologia, 47*(2), 185-192.

Castellanos-Gonzalez, A., White, A. C., Jr., Ojo, K. K., Vidadala, R. S., Zhang, Z., Reid, M. C., . . . Van Voorhis, W. C. (2013). A novel calcium-dependent protein kinase inhibitor as a lead compound for treating cryptosporidiosis. *J Infect Dis, 208*(8), 1342-1348. doi:10.1093/infdis/jit327

Chalmers, R. M., & Katzer, F. (2013). Looking for Cryptosporidium: the application of advances in detection and diagnosis. *Trends in parasitology, 29*(5), 237-251. doi:10.1016/j.pt.2013.03.001

Chao, A. T., Lee, B. H., Wan, K. F., Selva, J., Zou, B., Gedeck, P., . . . Manjunatha, U. H. (2018). Development of a Cytopathic Effect-Based Phenotypic Screening Assay against Cryptosporidium. *ACS Infect Dis*. doi:10.1021/acsinfecdis.7b00247

Chatelain, E. (2015). Chagas disease drug discovery: toward a new era. *Journal of biomolecular screening : the official journal of the Society for Biomolecular Screening, 20*(1), 22-35. doi:10.1177/1087057114550585

Chatelain, E., & Ioset, J. R. (2011). Drug discovery and development for neglected diseases: the DNDi model. *Drug Des Devel Ther, 5*, 175-181. doi:10.2147/DDDT.S16381

Checkley, W., White, A. C., Jr., Jaganath, D., Arrowood, M. J., Chalmers, R. M., Chen, X. M., . . . Houpt, E. R. (2015). A review of the global burden, novel diagnostics, therapeutics, and vaccine targets for cryptosporidium. *Lancet Infect Dis, 15*(1), 85-94. doi:10.1016/s1473-3099(14)70772-8

Chen, X. M., Keithly, J. S., Paya, C. V., & LaRusso, N. F. (2002). Cryptosporidiosis. *N Engl J Med, 346*(22), 1723-1731. doi:10.1056/NEJMra013170

Cryptosporidiosis: assessment of chemotherapy of males with acquired immune deficiency syndrome (AIDS). (1982). *MMWR. Morbidity and mortality weekly report, 31*(44), 589-592.

Current, W. L., & Reese, N. C. (1986). A comparison of endogenous development of three isolates of Cryptosporidium in suckling mice. *J Protozool, 33*(1), 98-108.

De Rycker, M., Hallyburton, I., Thomas, J., Campbell, L., Wyllie, S., Joshi, D., . . . Gray, D. W. (2013). Comparison of a high-throughput high-content intracellular Leishmania donovani assay with an axenic amastigote assay. *Antimicrob Agents Chemother, 57*(7), 2913-2922. doi:10.1128/aac.02398-12

Dillingham, R. A., Pinkerton, R., Leger, P., Severe, P., Guerrant, R. L., Pape, J. W., & Fitzgerald, D. W. (2009). High early mortality in patients with chronic acquired immunodeficiency syndrome diarrhea initiating antiretroviral therapy in Haiti: a case-control study. *Am J Trop Med Hyg, 80*(6), 1060-1064.

Disease, G. B. D., Injury, I., & Prevalence, C. (2016). Global, regional, and national incidence, prevalence, and years lived with disability for 310 diseases and injuries, 1990-2015: a systematic analysis for the Global Burden of Disease Study 2015. *Lancet, 388*(10053), 1545-1602. doi:10.1016/S0140-6736(16)31678-6

Duffy, S., Sykes, M. L., Jones, A. J., Shelper, T. B., Simpson, M., Lang, R., . . . Avery, V. M. (2017). Screening the Medicines for Malaria Venture Pathogen Box across Multiple Pathogens Reclassifies Starting Points for Open-Source Drug Discovery. *Antimicrob Agents Chemother, 61*(9). doi:10.1128/aac.00379-17

DuPont, H. L., Chappell, C. L., Sterling, C. R., Okhuysen, P. C., Rose, J. B., & Jakubowski, W. (1995). The Infectivity of Cryptosporidium parvum in Healthy Volunteers. *New England Journal of Medicine, 332*(13), 855-859. doi:doi:10.1056/NEJM199503303321304

Eder, J., Sedrani, R., & Wiesmann, C. (2014). The discovery of first-in-class drugs: origins and evolution. *Nat Rev Drug Discov, 13*(8), 577-587. doi:10.1038/nrd4336

Fayer, R., & Xiao, L. (2007). *Cryptosporidium and Cryptosporidiosis, Second Edition*: Taylor & Francis.

Flanigan, T., Whalen, C., Turner, J., Soave, R., Toerner, J., Havlir, D., & Kotler, D. (1992). Cryptosporidium Infection and CD4 Counts. *Annals of Internal Medicine, 116*(10), 840-842. doi:10.7326/0003-4819-116-10-840

Gamo, F. J., Sanz, L. M., Vidal, J., de Cozar, C., Alvarez, E., Lavandera, J. L., . . . Garcia-Bustos, J. F. (2010). Thousands of chemical starting points for antimalarial lead identification. *Nature, 465*(7296), 305-310. doi:10.1038/nature09107

Gorla, S. K., McNair, N. N., Yang, G., Gao, S., Hu, M., Jala, V. R., . . . Hedstrom, L. (2014). Validation of IMP dehydrogenase inhibitors in a mouse model of cryptosporidiosis. *Antimicrob Agents Chemother, 58*(3), 1603-1614. doi:10.1128/aac.02075-13

Guerrant, D. I., Moore, S. R., Lima, A. A., Patrick, P. D., Schorling, J. B., & Guerrant, R. L. (1999). Association of early childhood diarrhea and cryptosporidiosis with impaired physical fitness and cognitive function four-seven years later in a poor urban community in northeast Brazil. *Am J Trop Med Hyg, 61*(5), 707-713.

Guiguemde, W. A., Shelat, A. A., Bouck, D., Duffy, S., Crowther, G. J., Davis, P. H., . . . Guy, R. K. (2010). Chemical genetics of Plasmodium falciparum. *Nature, 465*(7296), 311-315. doi:10.1038/nature09099

Hlavsa, M. C., Roberts, V. A., Anderson, A. R., Hill, V. R., Kahler, A. M., Orr, M., . . . Yoder, J. S. (2011). Surveillance for waterborne disease outbreaks and other health events associated with recreational water --- United States, 2007--2008. *MMWR. Surveillance summaries : Morbidity and mortality weekly report. Surveillance summaries / CDC, 60*(12), 1-32.

Human cryptosporidiosis--Alabama. (1982). *MMWR. Morbidity and mortality weekly report, 31*(19), 252-254.

Hunter, P. R., Hughes, S., Woodhouse, S., Nicholas, R., Syed, Q., Chalmers, R. M., . . . Goodacre, J. (2004). Health Sequelae of Human Cryptosporidiosis in Immunocompetent Patients. *Clinical Infectious Diseases, 39*(4), 504-510. doi:10.1086/422649

Hunter, P. R., & Thompson, R. C. A. (2005). The zoonotic transmission of Giardia and Cryptosporidium. *Int J Parasitol, 35*(11–12), 1181-1190. doi:http://dx.doi.org/10.1016/j.ijpara.2005.07.009

Huston, C. D., Spangenberg, T., Burrows, J., Willis, P., Wells, T. N., & van Voorhis, W. (2015). A Proposed Target Product Profile and Developmental Cascade for New Cryptosporidiosis Treatments. *PLoS Negl Trop Dis, 9*(10), e0003987. doi:10.1371/journal.pntd.0003987

Katsuno, K., Burrows, J. N., Duncan, K., Hooft van Huijsduijnen, R., Kaneko, T., Kita, K., . . . Slingsby, B. T. (2015). Hit and lead criteria in drug discovery for infectious diseases of the developing world. *Nat Rev Drug Discov, 14*(11), 751-758. doi:10.1038/nrd4683

Khanna, I. (2012). Drug discovery in pharmaceutical industry: productivity challenges and trends. *Drug discovery today, 17*(19-20), 1088-1102. doi:10.1016/j.drudis.2012.05.007

Korpe, P. S., Haque, R., Gilchrist, C., Valencia, C., Niu, F., Lu, M., . . . Petri, W. A., Jr. (2016). Natural History of Cryptosporidiosis in a Longitudinal Study of Slum-Dwelling Bangladeshi Children: Association with Severe Malnutrition. *PLoS Negl Trop Dis, 10*(5), e0004564. doi:10.1371/journal.pntd.0004564

Kotloff, K. L., Nataro, J. P., Blackwelder, W. C., Nasrin, D., Farag, T. H., Panchalingam, S., . . . Levine, M. M. (2013). Burden and aetiology of diarrhoeal disease in infants and young children in developing countries (the Global Enteric Multicenter Study, GEMS): a prospective, case-control study. *Lancet, 382*(9888), 209-222. doi:10.1016/S0140-6736(13)60844-2

Lasser, K. H., Lewin, K. J., & Ryning, F. W. (1979). Cryptosporidial enteritis in a patient with congenital hypogammaglobulinemia. *Human pathology, 10*(2), 234-240.

Liu, J., Platts-Mills, J. A., Juma, J., Kabir, F., Nkeze, J., Okoi, C., . . . Houpt, E. R. (2016). Use of quantitative molecular diagnostic methods to identify causes of diarrhoea in children: a reanalysis of the GEMS case-control study. *Lancet, 388*(10051), 1291-1301. doi:10.1016/S0140-6736(16)31529-X

Liu, J., Platts-Mills, J. A., Juma, J., Kabir, F., Nkeze, J., Okoi, C., . . . Houpt, E. R. (2016). Use of quantitative molecular diagnostic methods to identify causes of diarrhoea in children: a reanalysis of the GEMS case-control study. *The Lancet, 388*(10051), 1291-1301. doi:10.1016/s0140-6736(16)31529-x

Love, M. S., Beasley, F. C., Jumani, R. S., Wright, T. M., Chatterjee, A. K., Huston, C. D., . . . McNamara, C. W. (2017). A high-throughput phenotypic screen identifies clofazimine as a potential treatment for cryptosporidiosis. *PLoS Negl Trop Dis, 11*(2), e0005373. doi:10.1371/journal.pntd.0005373

Mac Kenzie, W. R., Hoxie, N. J., Proctor, M. E., Gradus, M. S., Blair, K. A., Peterson, D. E., . . . Davis, J. P. (1994). A Massive Outbreak in Milwaukee of Cryptosporidium Infection Transmitted through the Public Water Supply. *New England Journal of Medicine, 331*(3), 161-167. doi:doi:10.1056/NEJM199407213310304

Macfarlane, D. E., & Horner-Bryce, J. (1987). Cryptosporidiosis in well-nourished and malnourished children. *Acta Paediatr Scand, 76*(3), 474-477.

Malebranche, R., Arnoux, E., Guerin, J. M., Pierre, G. D., Laroche, A. C., Pean-Guichard, C., . . . et al. (1983). Acquired immunodeficiency syndrome with severe gastrointestinal manifestations in Haiti. *Lancet, 2*(8355), 873-878.

Manjunatha, U. H., Chao, A. T., Leong, F. J., & Diagana, T. T. (2016). Cryptosporidiosis Drug Discovery: Opportunities and Challenges. *ACS Infect Dis, 2*(8), 530-537. doi:10.1021/acsinfecdis.6b00094

Manjunatha, U. H., Vinayak, S., Zambriski, J. A., Chao, A. T., Sy, T., Noble, C. G., . . . Diagana, T. T. (2017). A Cryptosporidium PI(4)K inhibitor is a drug candidate for cryptosporidiosis. *Nature, 546*(7658), 376-380. doi:10.1038/nature22337

Meisel, J. L., Perera, D. R., Meligro, C., & Rubin, C. E. (1976). Overwhelming watery diarrhea associated with a cryptosporidium in an immunosuppressed patient. *Gastroenterology, 70*(6), 1156-1160.

Meuten, D. J., Van Kruiningen, H. J., & Lein, D. H. (1974). Cryptosporidiosis in a calf. *Journal of the American Veterinary Medical Association, 165*(10), 914-917.

Molina, I., Gomez i Prat, J., Salvador, F., Trevino, B., Sulleiro, E., Serre, N., . . . Pahissa, A. (2014). Randomized trial of posaconazole and benznidazole for chronic Chagas' disease. *N Engl J Med, 370*(20), 1899-1908. doi:10.1056/NEJMoa1313122

Mortality, G. B. D., & Causes of Death, C. (2016). Global, regional, and national life expectancy, all-cause mortality, and cause-specific mortality for 249 causes of death, 1980-2015: a systematic analysis for the Global Burden of Disease Study 2015. *Lancet, 388*(10053), 1459-1544. doi:10.1016/S0140-6736(16)31012-1

Navin, T. R., Weber, R., Vugia, D. J., Rimland, D., Roberts, J. M., Addiss, D. G., . . . Bryan, R. T. (1999). Declining CD4+ T-lymphocyte counts are associated with increased risk of enteric parasitosis and chronic diarrhea: results of a 3-year longitudinal study. *J Acquir Immune Defic Syndr Hum Retrovirol, 20*(2), 154-159.

Ndao, M., Nath-Chowdhury, M., Sajid, M., Marcus, V., Mashiyama, S. T., Sakanari, J., . . . Caffrey, C. R. (2013). A cysteine protease inhibitor rescues mice from a lethal Cryptosporidium parvum infection. *Antimicrob Agents Chemother, 57*(12), 6063-6073. doi:10.1128/aac.00734-13

Nime, F. A., Burek, J. D., Page, D. L., Holscher, M. A., & Yardley, J. H. (1976). Acute enterocolitis in a human being infected with the protozoan Cryptosporidium. *Gastroenterology, 70*(4), 592-598.

Nwaka, S., & Hudson, A. (2006). Innovative lead discovery strategies for tropical diseases. *Nat Rev Drug Discov, 5*(11), 941-955. doi:10.1038/nrd2144

Nwaka, S., Ramirez, B., Brun, R., Maes, L., Douglas, F., & Ridley, R. (2009). Advancing drug innovation for neglected diseases-criteria for lead progression. *PLoS Negl Trop Dis, 3*(8), e440. doi:10.1371/journal.pntd.0000440

Nwaka, S., & Ridley, R. G. (2003). Virtual drug discovery and development for neglected diseases through public-private partnerships. *Nat Rev Drug Discov, 2*(11), 919-928. doi:10.1038/nrd1230

Panciera, R. J., Thomassen, R. W., & Garner, F. M. (1971). Cryptosporidial Infection in a Calf. *Veterinary Pathology Online, 8*(5-6), 479-484. doi:10.1177/030098587100800 5-00610

Pawlowic, M. C., Vinayak, S., Sateriale, A., Brooks, C. F., & Striepen, B. (2017). Generating and Maintaining Transgenic Cryptosporidium parvum Parasites. *Curr Protoc Microbiol, 46*, 20B 22 21-20B 22 32. doi:10.1002/cpmc.33

Payne, D. J., Gwynn, M. N., Holmes, D. J., & Pompliano, D. L. (2007). Drugs for bad bugs: confronting the challenges of antibacterial discovery. *Nat Rev Drug Discov, 6*(1), 29-40. doi:10.1038/nrd2201

Perkins, F. O., Barta, J. R., Clopton, R. E., Peirce, M. A., & Upton, S. J. (2000). *Phylum Apicomplexa* (2nd ed.): Society of Protozoologists.

Pham, J. S., Dawson, K. L., Jackson, K. E., Lim, E. E., Pasaje, C. F., Turner, K. E., & Ralph, S. A. (2014). Aminoacyl-tRNA synthetases as drug targets in eukaryotic parasites. *Int J Parasitol Drugs Drug Resist, 4*(1), 1-13. doi:10.1016/j.ijpddr.2013.10.001

Pink, R., Hudson, A., Mouries, M. A., & Bendig, M. (2005). Opportunities and challenges in antiparasitic drug discovery. *Nat Rev Drug Discov, 4*(9), 727-740. doi:10.1038/nrd1824

Platts-Mills, J. A., Babji, S., Bodhidatta, L., Gratz, J., Haque, R., Havt, A., . . . Investigators, M.-E. N. (2015). Pathogen-specific burdens of community diarrhoea in developing countries: a multisite birth cohort study (MAL-ED). *Lancet Glob Health, 3*(9), e564-575. doi:10.1016/S2214-109X(15)00151-5

Plouffe, D., Brinker, A., McNamara, C., Henson, K., Kato, N., Kuhen, K., . . . Winzeler, E. A. (2008). In silico activity profiling reveals the mechanism of action of antimalarials discovered in a high-throughput screen. *Proc Natl Acad Sci U S A, 105*(26), 9059-9064. doi:10.1073/pnas.0802982105

Reese, N. C., Current, W. L., Ernst, J. V., & Bailey, W. S. (1982). Cryptosporidiosis of Man and Calf: a Case Report and Results of Experimental Infections in Mice and Rats. *Am J Trop Med Hyg, 31*(2), 226-229.

Rose, J. B., Huffman, D. E., & Gennaccaro, A. (2002). Risk and control of waterborne cryptosporidiosis. *FEMS microbiology reviews, 26*(2), 113-123.

Schaefer, D. A., Betzer, D. P., Smith, K. D., Millman, Z. G., Michalski, H. C., Menchaca, S. E., . . . Riggs, M. W. (2016). Novel Bumped Kinase Inhibitors Are Safe and Effective Therapeutics in the Calf Clinical Model for Cryptosporidiosis. *J Infect Dis, 214*(12), 1856-1864. doi:10.1093/infdis/jiw488

Schuster, F. L. (2002). Cultivation of plasmodium spp. *Clin Microbiol Rev, 15*(3), 355-364.

Shirley, D. A., Moonah, S. N., & Kotloff, K. L. (2012). Burden of disease from cryptosporidiosis. *Current opinion in infectious diseases, 25*(5), 555-563. doi:10.1097/QCO.0b013e328357e569

Shoultz, D. A., de Hostos, E. L., & Choy, R. K. (2016). Addressing Cryptosporidium Infection among Young Children in Low-Income Settings: The Crucial Role of New and Existing Drugs for Reducing Morbidity and Mortality. *PLoS Negl Trop Dis, 10*(1), e0004242. doi:10.1371/journal.pntd.0004242

Slavin, D. (1955). Cryptosporidium meleagridis (sp. nov.). *J Comp Pathol, 65*(3), 262-266.

Sow, S. O., Muhsen, K., Nasrin, D., Blackwelder, W. C., Wu, Y., Farag, T. H., . . . Levine, M. M. (2016). The Burden of Cryptosporidium Diarrheal Disease among Children < 24 Months of Age in Moderate/High Mortality Regions of Sub-Saharan Africa and South Asia, Utilizing Data from the Global Enteric

Multicenter Study (GEMS). *PLoS Negl Trop Dis, 10*(5), e0004729. doi:10.1371/journal.pntd.0004729

Stebbins, E., Jumani, R. S., Klopfer, C., Barlow, J., Miller, P., Campbell, M. A., . . . Huston, C. D. (2018). Clinical and microbiologic efficacy of the piperazine-based drug lead MMV665917 in the dairy calf cryptosporidiosis model. *PLoS Negl Trop Dis, 12*(1), e0006183. doi:10.1371/journal.pntd.0006183

Swinney, D. C. (2013). Phenotypic vs. target-based drug discovery for first-in-class medicines. *Clin Pharmacol Ther, 93*(4), 299-301. doi:10.1038/clpt.2012.236

Theodos, C. M., Griffiths, J. K., D'Onfro, J., Fairfield, A., & Tzipori, S. (1998). Efficacy of nitazoxanide against Cryptosporidium parvum in cell culture and in animal models. *Antimicrob Agents Chemother, 42*(8), 1959-1965.

Trotz-Williams, L. A., Jarvie, B. D., Peregrine, A. S., Duffield, T. F., & Leslie, K. E. (2011). Efficacy of halofuginone lactate in the prevention of cryptosporidiosis in dairy calves. *Vet Rec, 168*(19), 509. doi:10.1136/vr.d1492

Trouiller, P., Olliaro, P., Torreele, E., Orbinski, J., Laing, R., & Ford, N. (2002). Drug development for neglected diseases: a deficient market and a public-health policy failure. *Lancet, 359*(9324), 2188-2194. doi:10.1016/S0140-6736(02)09096-7

Tyzzer, E. E. (1907). A sporozoan found in the peptic glands of the common mouse. *Proc. Soc. Exp. Biol. Med., 5*, 12-13.

Tyzzer, E. E. (1910). An extracellular Coccidium, Cryptosporidium Muris (Gen. Et Sp. Nov.), of the gastric Glands of the Common Mouse. *The Journal of medical research, 23*(3), 487-510 483.

U.S. Cancer Statistics Working Group, (2017). United States Cancer Statistics: 1999-2014 Incidence and Mortality Web-based Report. Atlanta: U.S. Department of Health and Human Services, Centers for Disease Control and Prevention and National Cancer Institute. Retrieved from www.cdc.gov/uscs

Van Voorhis, W. C., Adams, J. H., Adelfio, R., Ahyong, V., Akabas, M. H., Alano, P., . . . Willis, P. A. (2016). Open Source Drug Discovery with the Malaria Box Compound Collection for Neglected Diseases and Beyond. *PLoS Pathog, 12*(7), e1005763. doi:10.1371/journal.ppat.1005763

Vinayak, S., Pawlowic, M. C., Sateriale, A., Brooks, C. F., Studstill, C. J., Bar-Peled, Y., . . . Striepen, B. (2015). Genetic modification of the diarrhoeal pathogen Cryptosporidium parvum. *Nature, 523*(7561), 477-480. doi:10.1038/nature14651

Weisburger, W. R., Hutcheon, D. F., Yardley, J. H., Roche, J. C., Hillis, W. D., & Charache, P. (1979). Cryptosporidiosis in an immunosuppressed renal-transplant recipient with IgA deficiency. *American journal of clinical pathology, 72*(3), 473-478.

Zhang, J. H. (1999). A Simple Statistical Parameter for Use in Evaluation and Validation of High Throughput Screening Assays. *Journal of Biomolecular Screening, 4*(2), 67-73. doi:10.1177/108705719900400206

CHAPTER 2: A NOVEL PIPERAZINE-BASED DRUG LEAD FOR CRYPTOSPORIDIOSIS FROM THE MEDICINES FOR MALARIA VENTURE OPEN ACCESS MALARIA BOX

Jumani RS[1,2], Bessoff K[1#], Love MS[3], Miller P[1], Stebbins EE[1], Teixeira JE[1], Campbell MA[4], Meyers MJ[4], Zambriski JA[5], Nunez V[3], Woods AK[3], McNamara CW[3], Huston CD[1,2]*

[1]Dept. of Medicine, University of Vermont Larner College of Medicine, Burlington, VT

[2]Cellular, Molecular and Biomedical Sciences Graduate Program, University of Vermont, Burlington, VT

[3]California Institute for Biomedical Research, La Jolla, CA

[4]Saint Louis University School of Medicine, St. Louis, MO

[5]Paul G. Allen School for Global Animal Health, College of Veterinary Medicine, Washington State University, Pullman, WA

[#]Current address: Dept. of Surgery, Stanford University School of Medicine, Palo Alto, CA

2.1. Abstract

Cryptosporidiosis causes life-threatening diarrhea in children under age five, and prolonged diarrhea in immunodeficient people, especially AIDS patients. The standard of care, nitazoxanide, is modestly effective in children and ineffective in immunocompromised individuals. In addition to a need for new drugs, better

knowledge of drug properties that drive *in vivo* efficacy is needed to facilitate drug development. We report identification of a piperazine-based lead compound for *Cryptosporidium* drug development, MMV665917, and a new pharmacodynamic method used for its characterization. MMV665917 was identified from the Medicines for Malaria Venture Malaria Box, followed by dose response studies, *in vitro* toxicity studies, and structure activity relationship studies using commercial analogues. Potency against *C. parvum* Iowa and field isolates, and *C. hominis* was comparable. Furthermore, unlike nitazoxanide, clofazimine, and paromomycin, MMV665917 appeared to be curative in a chronic NOD SCID gamma mouse model of cryptosporidiosis. MMV665917 was also efficacious in an acute interferon-γ knockout mouse model. To determine if efficacy in this chronic mouse model might relate to whether compounds are cidal or static for *C. parvum*, we developed a novel *in vitro* parasite persistence assay. This assay suggested that MMV665917 was cidal, unlike nitazoxanide, clofazimine, and paromomycin. It also enabled determination of the compound concentration required to maximize the rate of parasite elimination. This time-kill assay can be used to prioritize early-stage *Cryptosporidium* drug leads, and may aide in planning *in vivo* efficacy experiments. Collectively, these results identify MMV665917 as a promising lead, and establish a new method for characterizing potential anticryptosporidial agents.

2.2. Introduction

Cryptosporidiosis, caused by infection of the gastrointestinal epithelium by *Cryptosporidium* parasites, is a major cause of life-threatening diarrhea in children, particularly those under 1 year of age (Kotloff et al., 2013; Liu et al., 2016; Platts-Mills et al., 2015). It is also highly associated with growth stunting and developmental delays (Bushen et al., 2007; Guerrant et al., 1999; Korpe et al., 2016; Kotloff et al., 2013). Two species, *Cryptosporidium hominis* and *Cryptosporidium parvum*, cause more than 98% of human cases (Checkley et al., 2015). While cryptosporidiosis predominantly affects children in developing countries, it is also the most important cause of waterborne diarrhea in the United States (Hlavsa et al., 2011), and a frequent cause of diarrhea in immunocompromised individuals, especially AIDS patients and transplant recipients, amongst whom the infection is typically prolonged and can be fatal (Malebranche et al., 1983; Navin et al., 1999).

Better treatments for cryptosporidiosis are badly needed. Nitazoxanide, the current standard of care, accelerates recovery in immunocompetent individuals (Beatrice Amadi et al., 2002). However, nitazoxanide is only partially effective in children, and is no better than placebo in AIDS patients (Abubakar, Aliyu, Arumugam, Hunter, & Usman, 2007; B. Amadi et al., 2009). Paromomycin, which is used as a positive control in rodent drug efficacy studies, is also ineffective in AIDS patients (Abubakar et al., 2007). Unfortunately, the reasons for nitazoxanide and paromomycin failure are not known. One possibility is that both drugs inhibit *Cryptosporidium*

growth, but do not actually kill *Cryptosporidium* (i.e. they may be "static" rather than "cidal"), depending on the host's immune system to clear the infection.

Several recent target- and phenotype-based screening efforts have resulted in the identification of multiple lead compounds with promising *in vivo* efficacy (Bessoff, Sateriale, Lee, & Huston, 2013; Bessoff et al., 2014; Castellanos-Gonzalez et al., 2013; Gollapalli et al., 2010; Gorla et al., 2014; Love et al., 2017; Manjunatha et al., 2017; Maurya et al., 2009; Murphy et al., 2010; Ndao et al., 2013; Sonzogni-Desautels et al., 2015), but there is no established pathway for the development of effective *Cryptosporidium* drugs (Huston et al., 2015). The lack of a reliably efficacious drug to serve as a benchmark and variable outcomes of existing leads in different animal models both complicate compound prioritization for further development, since the meaning of variable outcomes in different animal models and compound characteristics that predict efficacy are unknown. Thus, appropriate prioritization of such compounds for further development is poorly defined and new prioritization methods are needed.

Here, we report the discovery of a promising new piperazine-based drug lead for treatment of cryptosporidiosis by using an immunocompromised mouse model of prolonged infection in combination with a novel *in vitro* assay that is analogous to a classical bacterial time-kill curve assay. By reanalyzing our prior Medicines for Malaria Venture (MMV) Malaria Box screening data (Bessoff et al., 2014), we identified MMV665917 as a highly selective *Cryptosporidium* inhibitor with activity against multiple parasite isolates. Nitazoxanide, clofazimine, and paromomycin were not curative in chronically infected NOD SCID gamma (NSG) mice, but clofazimine

and paromomycin were effective in an acute mouse model. On the other hand, MMV665917 was effective in both chronic and acute mouse models of cryptosporidiosis. Measurement of the rate of parasite elimination following exposure to different drug concentrations enabled determination of the concentration of MMV665917 needed to maximize the rate of parasite elimination. Furthermore, the data suggested that MMV665917 was cidal against *Cryptosporidium*, while nitazoxanide, clofazimine, and paromomycin appeared to be static. We believe this parasite persistence assay has general value for *Cryptosporidium* drug development, since information from it may be useful for prioritizing early-stage drug leads, and for planning and understanding the results of *in vivo* efficacy studies.

2.3. Materials and Methods

2.3.1. Re-analysis of MMV Malaria Box screening data

Previously published screening data of the MMV Malaria Box used a screening "hit" definition of 80% inhibition to identify potential *Cryptosporidium* growth inhibitors (Bessoff et al., 2014). These data were re-analyzed to identify additional *Cryptosporidium* inhibitors, by assuming that the average compound in the collection had no effect and using a statistical approach to identify compounds that differed from the average. For this, the average number of parasites per host nuclei for all compounds was set to zero effect. Data for each compound were then normalized to this average and the difference from the population mean for each compound was plotted on a frequency distribution plot. Using GraphPad Prism version 6.01, normality

was tested with the D'Agostino-Pearson omnibus K2 test and the 95th percentile range was calculated. Inhibitors at or beyond the 95th percentile were considered hits.

2.3.2. Cell culture and parasites

Human ileocecal adenocarcinoma (HCT-8) cells (ATCC) were cultured in RPMI-1640 medium (Invitrogen) supplemented with 10% heat-inactivated fetal bovine serum (Sigma-Aldrich) and 120 U/mL penicillin and 120μg/mL streptomycin (ATCC) at 37°C and 5% CO_2. HCT-8 cells were used between passage 9 and 39 for all experiments. *C. parvum* Iowa isolate oocysts were purchased from Bunch Grass Farms, (Deary, Idaho). Oocysts were stored in phosphate buffered saline (PBS) with penicillin and streptomycin at 4°C, and were used within 5 months of shedding. *C. hominis* TU502 isolate oocysts were purchased from the Tzipori laboratory (Tufts University), and field *C. parvum* isolates were kindly provided by Jennifer Zambriski (Washington State University) and Daryl Nydam (Cornell University).

2.3.3. *Cryptosporidium* growth inhibition immunofluorescence assay

C. parvum growth inhibition was measured as previously described (Bessoff et al., 2013). Oocysts were excysted by treating with 10 mM hydrochloric acid (10 mins at 37°C), followed by exposure to 2 mM sodium taurocholate (Sigma-Aldrich) in PBS for 10 mins at 16°C. Excysted oocysts were then added to >95% confluent HCT-8 cell monolayers in 384-well plates at a concentration of 5,500 Iowa isolate oocysts per well. For *C. parvum* field isolates, the inoculum required to give an infection level similar to

that produced by 5,500 Iowa isolate oocysts per well was determined and used for subsequent assays of parasite inhibition. Compounds were added just before or 3 h after infection, and assay plates were incubated for 48 h post-infection at 37°C and 5% CO_2. Wells were then washed 3 times with PBS containing 111 mM D-galactose, fixed with 4% paraformaldehyde in PBS for 15 mins at room temperature, permeabilized with 0.25% Triton X-100 for 10 mins at 37°C, washed 3 times with PBS with 0.1% Tween 20, and blocked with 4% bovine serum albumin (BSA) in PBS for 2 h at 37°C or 4°C overnight. Parasitophorous vacuoles were stained with 1.33 µg/mL of fluorescein-labeled *Vicia villosa* lectin (Vector Laboratories) diluted in 1% BSA in PBS with 0.1% Tween 20 for 1 h at 37°C, followed by addition of Hoechst 33258 (Anaspec) at a final concentration of 0.09 mM diluted in water for another 15 mins at 37°C. Wells were then washed 5 times with PBS containing 0.1% Tween 20. A Nikon Eclipse Ti2000 epifluorescence microscope with an automated stage was programmed using NIS-Elements Advanced Research software (Nikon, USA) to focus on the center of each well and take a 3×3 composite image using an EXi blue fluorescence microscopy camera (QImaging, Canada) with a 20X objective (NA = 0.45). Nuclei and parasite images were separately exported as .tif files and analyzed using macros developed on the ImageJ platform (National Institutes of Health) (Bessoff et al., 2013). The only modification from the published macro used to count parasites was that the lower size threshold for parasites was decreased from 16.5 to 4 pixels (1 pixel = 0.65 µm). Graphs were plotted, and half maximal effective concentration (EC_{50}) and 90% effective concentration (EC_{90}) values were calculated using GraphPad Prism software version

6.01. For every *C. parvum* field isolate experiment, a dose response against the *C. parvum* Iowa isolate was performed simultaneously as a reference.

Cryptosporidium hominis growth inhibition assays were performed at the California Institute for Biomedical Research (Calibr, San Diego, CA) using a slightly modified immunofluorescence assay to enable automated compound handling and the use of 1536-well microtiter plates (Love et al., 2017). The HCT-8 culture medium was replaced with RPMI 1640 supplemented with 2% heat-inactivated horse serum, 100 U/mL penicillin, and 100 mg/mL streptomycin 24 h prior to infection with either *C. hominis* or the *C. parvum* Iowa isolate as a reference. For these assays, D-galactose was found to be unnecessary and was eliminated from the plate wash buffer. Imaging was performed using a CellInsight CX5 High Content Screening Platform (Thermo) with a 10X objective and acquisition of one microscopic field per well. Images were processed using HCS Studio Scan software, and the Selected Object Count (HCT-8 cells) and Spot Count (*C. hominis*) were analyzed in Genedata Screener (v13.0-Standard). Dose response curves and EC values were calculated using the Smart Fit function of Genedata Analyzer.

2.3.4. Parasite persistence assay

Excysted *C. parvum* oocysts were added to >90% confluent HCT-8 cells in 384-well plates. Compounds were added at EC_{50} or multiples of EC_{90} concentrations ~24 hours after infection. At ~24 h (i.e. the time of compound addition) and the indicated time intervals thereafter, parasites were washed, fixed, permeabilized, stained and

imaged as in the *C. parvum* growth assay. For the extended compound exposure experiments, the media and compound were replaced every three days. A separate 384-well plate was used for each time interval. Parasite numbers were normalized to host nuclei numbers and expressed as % parasite per nuclei. In order to fit parasite decay curves, the effect of drugs was isolated from expected changes in parasite numbers over time by expressing parasite numbers as the % of DMSO control for each time point. Exponential decay curves were fit using GraphPad Prism software version 6.01, and curve validity was assessed using the replicates test.

2.3.5. Host cell toxicity assay

Host cell toxicity was measured as previously described (Bessoff et al., 2013). HCT-8 cells were grown to >95% confluence in 384-well plates. Increasing concentrations of compounds were added and assay plates incubated at 37°C, 5% CO_2 for 48 h. The corner wells of each plate were trypsinized to remove cells and used as a blank for measuring absorbance at 490 nm. Cell proliferation was measured using the CellTiter AQ_{ueous} assay kit (Promega, USA) following the manufacturer's instructions, and was expressed as the percent of vehicle control (DMSO). GraphPad Prism software version 6.01 was used to plot graphs and calculate the concentration that inhibits 50% of host cell proliferation compared to DMSO control (TC_{50}). A selectivity index (SI) was calculated as the ratio of *C. parvum* EC_{50} to the host cell TC_{50}.

2.3.6. Pharmacokinetic measurements

Mouse single-dose plasma pharmacokinetic (PK) studies were previously performed as part of the Malaria Box program (Van Voorhis et al., 2016), and data were kindly provided by the Medicines for Malaria Venture (Geneva, Switzerland). Three overnight fasted CD-1 male mice were each given an oral suspension of 55 mg/kg of MMV665917 in 5% DMSO solution in 1% hydroxylpropyl methyl cellulose (HPMC). Blood samples were collected at 0.083, 0.25, 1, 2, 4, 6, and 9 hours post-treatment, transferred to microcentrifuge containing 1000 IU/mL of sodium heparin, and spun at 3000×*g* for 15 min at 4°C. MMV665917 levels were then measured by liquid chromatography-tandem mass spectrometry (LC/MS/MS), using an API 4000 AB Sciex Instruments mass spectrometer with a Phenomenex Kinetex C18 (2.6 µm × 2.1 × 50 mm) column (phase A: 0.1% formic acid/4.9% acetonitrile/95% water; phase B: 0.1% formic acid/4.9% water/95% acetonitrile). Compound spiked into control plasma was used as a standard.

Fecal and intestinal content MMV665917 concentrations were measured following compound extraction. Feces or intestinal contents were homogenized in PBS (0.1 g/mL) in a polypropylene tube and then further diluted prior to addition of an internal standard (enalapril) and acetonitrile protein precipitation. The supernatant was then transferred to a fresh polypropylene tube and dried using a speed vac. Samples were then resuspended and analyzed using LC/MS/MS.

2.3.7. *In vivo* efficacy

All NOD SCID gamma mouse studies were performed in compliance with animal care guidelines and were approved by the University of Vermont Institutional Animal Care and Use Committee. Normal flora NOD SCID gamma mice (NOD.Cg-*Prkdc*^{scid} *IL2rg*^{tm1Wjl}/SzJ) (Shultz et al., 2005) were purchased from Jackson laboratory (Maine, USA) and housed for at least a week for acclimatization. At 4—5 weeks of age, mice were infected with 10^5 *C. parvum* Iowa isolate oocysts. Fecal oocyst shedding is detected 6 days after infection using a qPCR assay, so treatment was started on day seven after infection. Mice (n=4 per experimental group) were treated orally (p.o.) with MMV665917 30 or 60 mg/kg BID, intraperitoneally (i.p.) with MMV665917 60 mg/kg BID, or p.o. with 1000 mg/kg BID paromomycin. MMV665917 was suspended in DMSO, sonicated for 30 secs three times to get a fine suspension, aliquoted and stored at -80°C for less than 10 days. On the day of treatment, DMSO aliquots of MMV665917 were thawed, mixed well using a vortexter and diluted with 1% HPMC and sonicated as before, three times for 30 secs each, mixed well and given to mice either p.o. or by i.p. injection. A final 5% DMSO concentration was used in 100 µL of 1% HPMC per dose. For the additional malaria box compounds and compound variants tested, the doses were prepared in the same way and specific dosages tested are included in Table S3. Mice were treated for either four or seven days as indicated, allowed to recover for a week and then sacrificed. Oocyst shedding in feces was monitored throughout by qPCR, including relapse in infection post-treatment.

All interferon-gamma (IFNγ) knockout mouse studies were performed in compliance with animal care guidelines and were approved by Explora BioLabs (San Diego, CA) Institutional Animal Care and Use Committee. Four-week old female normal flora C57BL/6 IFNγ$^{-/-}$ mice were purchased from the Jackson Laboratory and acclimated for three days prior to infection by oral gavage with 10^6 *C. parvum* Iowa isolate oocysts (Sterling Parasitology Laboratory, University of Arizona) suspended in sterile distilled water. At the indicated times post infection, mice were treated with compound vehicle alone, clofazimine (positive control), or MMV665917. As described previously, fecal parasite shedding was quantified at the indicated times post infection by isolating oocysts using a sucrose gradient centrifugation method (Arrowood & Sterling, 1987), followed by staining for immunofluorescence microscopy using a fluorescein isothiocyanate-conjugated mouse anti-*Cryptosporidium* antibody (0.25 µg per sample), and analysis with a Guava EasyCyte flow cytometer and CytoSoft Data Acquisition and Analysis software (v5.3; Guava Technologies, Inc.). Oocyst counts/mL of sample were exported to Excel (Microsoft Corp.), and normalized to counts/mg feces. Final data analysis and graphing were done using GraphPad Prism software (version 6.01).

2.4. Results

2.4.1. Re-analysis of the MMV Malaria Box *C. parvum* screen identified new inhibitors

The results from the recently screened MMV Open Access Malaria Box (Bessoff et al., 2014) were re-analyzed using a modified hit definition. The mean of parasite numbers normalized to host nuclei numbers was determined for the full library and set to zero. The results for each compound were then expressed as the distance from the mean and used to generate a frequency distribution plot, giving rise to a normal distribution (Fig. S1). Using the 95th percentile as the cutoff, 20 potential inhibitors were identified. Three of the 20 compounds also affected host nuclei numbers and were therefore excluded from further analysis. Fifteen of the remaining 17 were purchased and confirmed as selective *in vitro* inhibitors of *C. parvum* development. This re-analysis gave an overall hit rate of 3.75% (15/400), and yielded six *Cryptosporidium* inhibitors that were not identified in our previous study (Table S1) (Bessoff et al., 2014). The parent compound and/or commercially available variants for eight of the fifteen *Cryptosporidium* inhibitors were subsequently tested in an immunocompromised mouse model of chronic cryptosporidiosis (Table S2). Only MMV665917 was efficacious at the dose tested.

2.4.2. MMV665917 is a highly selective inhibitor of *Cryptosporidium*

A piperazine-containing scaffold, MMV665917 (Fig. 1A), appeared to be a particularly promising new hit, since its activity was highly selective for

Cryptosporidium and erythrocyte-stage *Plasmodium* species (Van Voorhis et al., 2016). MMV665917 was previously reported to be inactive in numerous biological assays, including assays against eleven species of bacteria (e.g. *Escherichia coli, Klebsiella pneumoniae, Salmonella typhimurium, Staphylococcus aureus,* and *Streptococcus suis*), twelve protozoa, and seven helminths (Van Voorhis et al., 2016). Based on previously reported toxicity profiling (Van Voorhis et al., 2016), MMV665917 was not toxic to zebrafish and had a selectivity index (SI) of > 20 for *C. parvum* over five mammalian cell lines. MMV665917 was also known to have modest plasma protein binding (83.3% and 88.8% for mouse and human, respectively), to have a low potential for significant drug-drug interactions based on low inhibition of five human and one mouse cytochrome P450 (CYP) isoforms (1A2, 2C9, 2C19, 2D6, 3A4-M, 3A4-T) at 10 µM, and to have a kinetic solubility of 18 µM at pH 7.4 (Van Voorhis et al., 2016). The major known liability for development was hERG inhibition, a marker for potential cardiotoxicity, by 58% at 11 µM (Van Voorhis et al., 2016).

The half maximal effective concentration (EC_{50}) of MMV665917 against asexual stages of the *C. parvum* Iowa isolate was 2.10 µM (Fig. 1B). There was no toxic effect on host HCT-8 cell proliferation at concentrations up to 100 µM (Fig. 1C), giving an SI of > 47. MMV665917 displayed a similar EC_{50} against three *C. parvum* field isolates isolated from calves, and an EC_{50} of 4.05 µM against *C. hominis* (TU502 isolate) (Fig. 1D). A preliminary structure activity relationship (SAR) study using commercially available analogues showed that changes could be made around the piperazine linker to both the R and R' groups defined in Fig. 1A without losing anti-*Cryptosporidium*

activity (Table S3; Figures S2 and S3). Addition of a second chlorine at the meta position of the urea's terminal aryl ring increased potency (Fig. 1E). Compounds with an aryl urea at the R position were generally more active than aryl carboxamides, oxyacetamides, and sulfonamides (Fig. 1E). It is worth noting that compounds with an altered substituent on the terminal aryl ring of the carboxamides and sulfonamides regained some potency (Fig. 1E, D-44 and D-79), suggesting options for further improvement of potency. More detailed preliminary SAR are shown in Supplementary Figures S2 and S3.

2.4.3. Oral MMV665917 is curative in both chronic and acute mouse models of cryptosporidiosis

Most prior *in vivo* studies of potential *Cryptosporidium* treatments have used one of several self-resolving infection models, and therefore, focused on the acute phase of infection (Campbell, Stewart, & Mead, 2002; Gorla et al., 2014; Love et al., 2017; You et al., 1998). Others have used interferon-gamma (IFNγ) knockout (KO) mice to model chronic infection (Griffiths, Theodos, Paris, & Tzipori, 1998), but the results from different research groups are variable, ranging from lethal in some cases to self-limited infection in others (Griffiths et al., 1998; Love et al., 2017; Ndao et al., 2013; Sonzogni-Desautels et al., 2015). In our hands, infection of IFNγ KO mice is self-resolving (Love et al., 2017). Therefore, to mimic chronic infection in immunocompromised people and afford the opportunity to assess relapse after treatment, we developed a new immunocompromised mouse model using NOD SCID

gamma (NSG) mice. In addition to the severe combined immunodeficiency deficiency (SCID) defect, NSG mice lack known sources of IFNγ, including the monocyte/macrophage lineage and natural killer cells (Ito et al., 2002). Our intention was to more cheaply mimic a previously reported model using SCID mice treated with an IFNγ neutralizing antibody (Tzipori, Rand, & Theodos, 1995). Much as reported in that study, infection of NSG mice was reliably established by six days following oral gavage of 4-5 week old NSG mice with ~10^5 *C. parvum* oocysts, and asymptomatic fecal shedding of oocysts continued for greater than two months (data not shown).

Paromomycin (positive control; 1,000 mg/kg oral twice daily (BID)) and MMV665917 (30 or 60 mg/kg oral BID) were compared in the NSG mouse cryptosporidiosis model with treatment of mice beginning seven days after infection. Mice treated for 7 days with paromomycin relapsed promptly upon cessation of treatment (Fig. 2A). Twice daily 30 mg/kg MMV665917 reduced oocyst shedding by > 90%, but similar to paromomycin, mice treated at this dose relapsed. Mice treated with MMV665917 60 mg/kg twice daily, on the other hand, were apparently cured, with no oocyst shedding observed at any time after stopping treatment (Fig. 2A). As with the other commonly used cryptosporidiosis mouse models, nitazoxanide did not reduce oocyst shedding in NSG mice (Fig. 2B). Clofazimine was also tested using several different vehicles, and completely lacked efficacy in the NSG mouse model (Fig. 2B and data not shown (various vehicles)). This was surprising based on its known efficacy in an acute mouse model (Love et al., 2017).

To better enable comparison of results amongst different mouse models, the efficacy of MMV665917 30 mg/kg twice daily was directly compared to that of clofazimine in an IFNγ KO mouse model. As noted above and for unknown reasons, *C. parvum* infection of IFNγ KO mice ranges from a self-resolving acute infection to lethal; in our hands, the infection is self-resolving (Love et al., 2017). MMV665917 was highly efficacious in this acute infection model (Fig. 3A and B); clofazimine efficacy was also confirmed.

2.4.4. Intraperitoneal dosing of MMV665917

In hopes of determining if MMV665917 efficacy was due to intestinal or oral exposure, we compared the efficacy of oral and i.p. MMV665917 in the NSG mouse model. MMV665917 was equally efficacious regardless of the route of administration (Fig. 4A). This suggested the possibilities that: 1) MMV665917 undergoes biliary excretion into the intestinal lumen; 2) systemic compound concentrations drive *in vivo* efficacy of MMV665917; or 3) both.

Fecal concentrations of MMV665917 were determined during treatment of cryptosporidiosis, and fecal MMV665917 levels vastly exceeded the measured EC_{90} concentration regardless of the route of administration (Fig. 4B). In fact, very high levels of MMV665917 were detected in the feces shortly after even a single 60 mg/kg i.p. dose (approximately 78× EC_{90} vs. 490× EC_{90} when given orally) (Fig. 4B). Following euthanasia on day 14 between 12 and 15 h after the final dose, the intestinal contents contained MMV665917 at many times the EC_{90} concentration regardless of

the route of administration (Fig. 4C). Serum samples from these infected NSG mice treated orally or i.p. with MMV665917 were unfortunately lost during shipping. Based on an independent PK exposure study in CD-1 male mice, MMV665917 plasma levels continued to increase for 9 hours following administration of a single oral dose of 55 mg/kg, demonstrating that in contrast to the immediately elevated fecal levels observed, MMV665917 plasma concentrations build over time (Supplemental Fig. S4). The possible interpretation of these data is limited, since the terminal time point was quite early. Collectively, however, these data demonstrated biliary excretion of MMV665917, but did not provide any insight into whether MMV665917 works via presence in the gut lumen, the tissue, or both.

2.4.5. Rate of parasite elimination

Adapted from classical anti-bacterial time-kill curves, we developed an *in vitro* parasite persistence assay to determine the concentration of compound required to achieve the maximal anti-*Cryptosporidium* response, and the rate of parasite elimination following exposure to different compound concentrations. A similar approach has been applied by the Medicines for Malaria Venture to compare anti-malaria drug candidates to benchmark compounds in immunocompromised mice (Angulo-Barturen et al., 2008; Burrows, van Huijsduijnen, Mohrle, Oeuvray, & Wells, 2013). *C. parvum* cannot be continuously cultured using simple *in vitro* methods, with growth in epithelial monolayers peaking at ~60 h post-infection. In the parasite persistence assay, we used this narrow time window to mimic treatment of an

established *in vivo* infection by allowing infection of epithelial cell monolayers to progress for 24 hours prior to addition of compounds at the EC_{50} or multiples of the EC_{90} and then sequentially quantifying parasite numbers (schematic in Fig. 5A). Predicted outcomes include continued growth of control-treated parasites, or parasite growth inhibition versus parasite elimination for potentially static (or slowly cidal) or rapidly cidal compounds, respectively (Fig. 5B). In this assay, parasites persist at the highest non-toxic concentrations of nitazoxanide, paromomycin, and clofazimine (Fig. 5C and Supplemental Fig. S5). MMV665917, on the other hand, reduced parasite numbers at concentrations higher than the EC_{90}, with a maximal rate of parasite elimination achieved at a concentration of $3\times EC_{90}$ (Fig. 5D). However, significant parasite numbers remained at 72 hours following even the highest dose treatment with MMV665917. To further assess if MMV665917 results in parasite elimination compared to paromomycin, an extended treatment experiment was performed in which the culture medium and drugs were replaced every three days for a total of 14 days (i.e. 13 days of drug exposure) (Fig. S6). As expected, parasite numbers continued to fall during treatment with the vehicle alone, reaching a low of ~6% of host cells infected by day 13. Paromomycin treatment closely mirrored the DMSO vehicle control at five days of culture and beyond, but MMV665917 treatment resulted in a progressive decline in the percent of host cells infected to nearly zero by day 13 of treatment (~0.1% of host cells positive). These data suggested that MMV665917 is cidal for *C. parvum*, while paromomycin is static.

Data from the parasite persistence assay were next used to estimate the *in vitro* rate of parasite elimination in the presence of MMV665917, nitazoxanide, paromomycin, and clofazimine. The parasite numbers for the tested highest non-toxic concentration were expressed as percent of the DMSO control for each time-point in order to isolate the anti-*Cryptosporidium* effect attributable to each drug, and one-phase exponential decay curves were fit to calculate decay constants (Fig. 5E and 5F, and Supplemental Fig. S5). Note that it was not possible to fit exponential decay curves to the data for nitazoxanide, paromomycin, or clofazimine ($p < 0.05$ for each; replicates test; GraphPad Prism), but a high-quality curve was readily generated for MMV665917. The maximal rate of parasite elimination was achieved at $3\times EC_{90}$ concentration of MMV665917, with the rate of parasite decay similar for $3\times EC_{90}$ and $12\times EC_{90}$ (decay rate constant, $r = 0.05346$ and 0.05864 for $3\times EC_{90}$ and $12\times EC_{90}$ respectively). The difference in the ability to fit decay curves for MMV665917, nitazoxanide, clofazimine, and paromomycin gave an objective indication that MMV665917 reduced parasite numbers under the conditions of the parasite persistence assay in a manner distinct from the other drugs tested.

2.5. Discussion

The most important result of this study is the identification of MMV665917 as a novel, piperazine-based lead compound for treatment of cryptosporidiosis. It is active against *C. hominis* and field isolates of *C. parvum*, shows no *in vitro* cytotoxicity at high concentrations, and consistent with previously published data on the MMV

Malaria Box (Van Voorhis et al., 2016), is highly specific for *Cryptosporidium* parasites and blood stage *Plasmodium* species. MMV665917 appears to cure established cryptosporidiosis in highly immunocompromised NSG mice, unlike paromomycin (the most commonly used positive control), nitazoxanide, and the recently identified repurposing lead clofazimine. It is also highly efficacious in an acute IFNγ KO mouse model of infection. Interestingly, MMV665917 is efficacious in NSG mice regardless of dosing by oral or i.p. routes, and accumulates rapidly in the feces following i.p. dosing, indicating that it is at least partially excreted via the biliary tract. To further understand MMV665917's *in vivo* efficacy, we developed and used a new *in vitro* PD assay to measure parasite elimination vs. time at varying concentrations of compound. Efficacy in the chronic NSG mouse model correlated with progressive parasite elimination in the presence of compound, since MMV665917 appeared to be cidal and resulted in parasite elimination over time, while nitazoxanide, paromomycin, and clofazimine all appeared to be static. These features of MMV665917 and the methods used to define them provide guidance for further development of this piperazine-based compound series to treatcryptosporidiosis. Given the lack of a clearly defined developmental pathway for anti-cryptosporidials, we believe these studies provide general guidance for *Cryptosporidium* drug development.

Since MMV665917 is active against both *C. hominis* and a variety of *C. parvum* isolates and it is relatively specific for *Cryptosporidium* (Van Voorhis et al., 2016), it is an especially promising lead. The *in vivo* efficacy studies done here, however, only used *C. parvum* and non-clinical rodent models of cryptosporidiosis. While both *C.*

parvum and *C. hominis* cause human disease, and both species are also believed to be distributed similarly within tissues, it is important to note that the majority of children with life-threatening cryptosporidiosis are actually infected with *C. hominis* (Liu et al., 2016). Thus, additional early-stage testing is needed as proof of principle for *in vivo* treatment of *C. hominis* with MMV665917. The gnotobiotic piglet model is the preferred model for such studies (Akiyoshi, Mor, & Tzipori, 2003). Similarly, MMV665917 needs to be tested in a clinical model of cryptosporidiosis in which the host develops diarrhea, such as the dairy calf model (Manjunatha et al., 2017; Schaefer et al., 2016; Zambriski et al., 2013).

Although *in vitro* cytotoxicity was not observed with MMV665917 for host cell lines and it is well tolerated in zebra fish and mice, the inhibition of hERG (58% at 11 μM) presents a potential cardiotoxicity liability. This is confounded by the modest potency of the compound versus *Cryptosporidium*, which suggests the possibility of a narrow therapeutic window in animals (Van Voorhis et al., 2016). The results of the *in vitro Cryptosporidium* time-kill curve assay should aide in design of such studies, since ignoring protein binding, a concentration of compound $3\times EC_{90}$ maximized the anti-parasitic effect. The preliminary SAR studies presented here also suggest that this hERG liability may be addressed through medicinal chemistry to significantly improve compound potency and/or reduce hERG inhibition. Of course, such a program would be aided by identification of the molecular mechanism of action of MMV665917, which remains unknown.

Since MMV665917 was present in the feces regardless of administration via the oral or i.p. route, no conclusion is possible about the PK characteristics that drive *in vivo* efficacy (i.e. intestinal vs. systemic exposure). This is a very important area of investigation for *Cryptosporidium* drug development in general, since the parasite resides in an unusual parasitophorous vacuole on the luminal surface, but enclosed within intestinal epithelial cells. The fecal levels measured only provide an indirect view of cumulative drug exposure in the intestinal mucosa, since the fecal levels include both compound being eliminated and compound that is never absorbed after oral administration. Furthermore, the day-to-day variability seen in Figure 4B may simply represent variation in drug excretion and/or fecal volumes. The important conclusion from the limited PK analysis performed here is that MMV665917 is at least partially excreted in the feces, and presumably undergoes enterohepatic recirculation. Further studies to define the PK characteristics that drive MMV665917 *in vivo* efficacy are needed, and should aide in medicinal chemistry and formulation strategies for optimization.

Variability in outcomes in different rodent models of cryptosporidiosis and lack of knowledge of the basis and significance of such variability greatly complicates *Cryptosporidium* drug development. Our approach comparing results in chronically infected NSG mice to results in an acute IFNγ KO mouse model suggests that the chronic NSG mouse model sets a more stringent standard than acute models, since MMV665917 was highly efficacious in both models, but several compounds with good efficacy in an acute IFNγ KO mouse model were ineffective in NSG mice (i.e.

clofazimine, paromomycin, and data not shown). However, it should be stressed that this conclusion is based on only a small number of compounds and, in any case, it remains unknown if such a high standard is required to achieve reliable efficacy in people. In addition, we have only included data for one chronic model and one acute model of infection, and results may differ further amongst the other available models. The best pathway for developing anti-*Cryptosporidium* drugs is still being determined, and the predictive value of *Cryptosporidium* animal models for drug efficacy within different patient populations is not known. Our data suggest that the chronic NSG mouse model is a model of greater stringency than the acute (i.e. self-curing) IFNγ KO mouse model. As noted above, in some mouse facilities, infection of IFNγ KO mice is lethal (Griffiths et al., 1998; Ndao et al., 2013; Sonzogni-Desautels et al., 2015), and may represent a similarly high-stringency model. In any case, there is likely value to prioritizing compounds in development by testing them in animal models of differing stringency. A lack of efficacy in the NSG model may not preclude high-value compounds from advancing in development (e.g. repurposing of clofazimine); however, this model may help to further differentiate and prioritize the growing number of lead compounds that have recently been discovered. It is logical that efficacy in a chronic mouse model such as the NSG model may predict drugs that will be efficacious for treatment of AIDS patients with chronic cryptosporidiosis and severely malnourished children.

The data also suggest that efficacy in NSG mice, which lack all aspects of adaptive immunity, may depend on the ability of a compound to eliminate parasites in

the absence of a competent immune system (i.e. compound parasite killing or so-called cidality) and/or the rate of parasite elimination at physiologically relevant compound concentrations. By quantifying parasite persistence vs. elimination in the presence of different drug concentrations, it is possible to determine the concentration required to maximize the effect of a compound. In the absence of a simple continuous culture system, it is not formally possible to prove cidality on a routine basis (e.g. use of the recently reported hollow-fiber culture system (Morada et al., 2016) would require a large amount of compound and be prohibitively expensive). However, this time-kill curve assay enables determination of whether a compound eliminates parasites or simply blocks further growth during the time frame of the assay, which likely indicates whether a compound is cidal or static under the conditions tested. More importantly, the method is simple, inexpensive, and requires only a small amount of compound, so this method provides the opportunity to directly compare different compounds or compound classes to aide in prioritization of early-stage drug leads. The numbers of compounds studied here are too few to enable an absolute conclusion, but based on our experience with the NSG mouse model and analogy with general principles for treatment of infections in highly immunocompromised individuals, it is likely that cidal compounds will be of the greatest value for treatment of cryptosporidiosis in the very patients for whom nitazoxanide is either ineffective (e.g. AIDS patients and/or transplant patients) or only modestly effective (e.g. malnourished children). In this regard, MMV665917 is in keeping with a recently proposed ideal product profile for an anti-cryptosporidial drug (Huston et al., 2015).

In summary, we present MMV665917 as a promising lead for further development of an anticryptosporidial drug, and new methods with general value for *Cryptosporidium* drug development. Current studies with MMV665917 include testing in a clinical model of infection in dairy calves, additional SAR studies to eliminate hERG inhibition and improve potency, and efforts for drug-target identification.

2.6. Acknowledgements

We thank Mercedes Rincon, Ph.D. and Keara McElroy-Yaggy (University of Vermont (UVM)) for helpful discussions in establishing the NSG mouse model of cryptosporidiosis. We also thank members of the Huston lab, and, although too numerous to name individually, members of the anti-*Cryptosporidium* drug development community for their thoughtful comments.

2.7. Figure Legends

Figure 1. The piperazine-based Malaria Box compound, MMV665917, is a selective inhibitor of *Cryptosporidium* growth *in vitro*. (A) Structure of MMV665917 showing a piperazine linker connecting the indicated R and R' groups. (B) Dose response curve showing inhibition of intracellular *C. parvum* growth in HCT-8 cells after 48 h of incubation. Parasite numbers were normalized to DMSO vehicle control data. Each point represents the mean and SD of 3 biological replicates with 4 technical replicates per experiment. (C) Effect of MMV665917 on proliferation of host HCT-8 cells as assessed by CellTiter AQ_{ueous} assay (Promega). Data are the mean and SD combined from 2 biological replicates with 4 technical replicates each. (D)

MMV665917 activity against *C. hominis* TU502 and 3 different bovine field isolates of *C. parvum*. The mean and SD of 2 independent experiments with 4 technical replicates per experiment are shown, except for *C. hominis* TU502 where mean of 3 replicates from 1 biological experiment is shown. (E) Preliminary structure activity relationship studies using commercially available variants on R demonstrating a preference for aryl urea (D-28) over carboxamides (D-46, D-44), oxyacetamides (D-41), and sulphonamides (D-23, D-79) (see also Fig. S2 and Table S2).

Figure 2. MMV665917 cures NOD SCID gamma mice with established cryptosporidiosis. (A) Efficacy of MMV665917 compared to paromomycin (positive control) in NOD SCID gamma (NSG) mice. NSG mice were infected by oral gavage of *C. parvum* Iowa isolate oocysts. Fecal parasite shedding is detected by qPCR on day 6, after which animals were treated with the indicated drug regimens for one week, and then monitored for relapse of infection (n = 4 mice per experimental group, except paromomycin where n = 3; data are the mean and SEM; **, $p \leq 0.01$ and ns, $p > 0.05$, by non-parametric multiple comparisons Kruskal-Wallis test for each treatment vs. vehicle control; BID = twice daily dosing regimen). (B) Short-term efficacy of nitazoxanide, paromomycin, and clofazimine in the NSG mouse model. NSG mice were infected and fecal parasite shedding was measured by qPCR as above. Beginning 7 days after infection, mice were treated with the indicated drug regimens. Fecal parasite shedding was measured just prior to initiation of treatment and the day

following completion (n = 4 mice per experimental group; data are the mean and SEM: * indicates $p \leq 0.05$ by Mann-Whitney test).

Figure 3. MMV665917 is effective in IFNγ knockout mice acutely infected with *C. parvum*. (A) Efficacy of MMV665917 and clofazimine (positive control) in the acute IFNγ knockout (KO) mouse model. IFNγ KO mice were infected by oral gavage of *C. parvum* Iowa isolate oocysts. Compounds or the indicated vehicles were dosed as indicated twice daily on days 4, 5, and 6 post-infection. Fecal parasite shedding was measured by isolation of oocysts using sucrose gradient flotation, followed by immunofluorescence staining and detection by flow cytometry. (n = 4 mice per experimental group). (A) Time course comparing MMV665917 to clofazimine (positive control). Data are the mean and SEM. Horizontal dashed line indicates reliable limit of detection. (B) Total fecal shedding for days 4-7. Each symbol indicates an individual mouse. GraphPad Prism was used to calculate the area under the fecal shedding vs. time curves. Data are the mean and SD: * indicates $p \leq 0.05$; ** indicates $p \leq 0.01$ by two-tailed student's t-test.

Figure 4. Oral vs intraperitoneal (i.p.) treatment with MMV665917. (A) Efficacy data measured by fecal qPCR following administration of MMV665917 at the indicated dose by either oral gavage or intraperitoneal (i.p.) injection. Efficacy was independent of the dosing route (data are the mean and SEM; n = 4 for oral dosing; n = 3 for i.p. dosing; ns indicates $p = 0.2$ (Mann-Whitney test)). (B) Fecal MMV665917 levels of

mice treated for 7 days orally or i.p. with 60 mg/kg twice daily (BID) from first 12 h of treatment and every 24 h thereafter. (C) Small intestinal MMV665917 levels following euthanasia 12 to 15 h after the last treatment dose. For (B) and (C) data expressed in µM of MMV665917 after considering 1g of intestinal contents or feces as equivalent to 1 mL.

Figure 5. Parasite persistence assay showing *in vitro* elimination of *C. parvum* following MMV665917 exposure vs. parasite persistence in the presence of nitazoxanide. (A) Experimental design of the parasite persistence assay. After establishing an infection for approximately 24 h, compounds are added at varying concentrations as labeled, and then parasites and host cells are enumerated at multiple time points using immunofluorescence microscopy. (B) Cartoon showing predicted outcomes for potentially cidal or static compounds compared to vehicle control (DMSO). (C, D) Data showing parasite numbers normalized to host nuclei over time with increasing concentrations of (C) nitazoxanide, or (D) MMV665917. These data shown are representative of 3 independent experiments (n = 4 per data point; mean and SD). (E) Nitazoxanide and (F)) MMV665917 one-phase exponential decay curve fit using parasite persistence assay data normalized to percent of the DMSO control for each time point. Data points are the mean and SD; n = 4; representative of 3 independent experiments. The p value is the replicates test result (note that $p \geq 0.05$ indicates a valid curve fit).

Supplementary Figure 1. Re-analysis of MMV box screening data identifies new *Cryptosporidium* inhibitors. The previously published screening data of 400 compounds of the MMV box were re-analyzed (Bessoff et al., 2014). Parasite numbers were normalized to nuclei and expressed as percent nuclei. Mean of % parasite / nuclei was determined and each individual value subtracted from the cumulative mean to determine the distance from mean. A frequency distribution plot of each compound's distance from the mean gave rise to a normal distribution. The upper 95^{th} percentile concentration was set as a cut-off to identify potential inhibitors.

Supplementary Figure 2. Preliminary structure activity relationship studies using commercially available variants on the left-hand side R position. The mean EC_{50} for 2 biological replicates is shown, as measured against *C. parvum* in HCT-8 cells.

Supplementary Figure 3. Preliminary structure activity relationship studies using commercially available variants on the right-hand side R' position. The mean EC_{50} for 2 biological replicates is shown, as measured against *C. parvum* in HCT-8 cells.

Supplementary Figure 4. Plasma pharmacokinetic information. Male CD-1 mice were administered 55 mg/kg of MMV665917 orally, after which plasma levels were measured at the indicated times (data for individual mice are shown).

Supplementary Figure 5. Clofazimine and paromomycin both appear to be static for *C. parvum*. (A and B) Parasite persistence assay data for the highest non-toxic concentrations of (A) clofazimine and (B) paromomycin. (C and D) Parasite elimination curves for (C) clofazimine and (D) paromomycin. These data were normalized to the DMSO control for each time point; GraphPad Prism was used to try to fit a single-phase exponential decay curve. For both drugs, it is not possible to fit a decay curve (replicates test; $p < 0.05$). Data are representative of 3 independent experiments (mean and SD; n = 4 per experiment).

Supplementary Figure 6. Effects of prolonged MMV665917 vs. paromomycin exposure. The parasite persistence assay was extended by replacing the media and compound every 3 days for a total of 14 days of infection (i.e. 13 days of drug exposure). (A) MMV665917 treatment. (B) Paromomycin treatment. Data points are the mean and SD (n=12).

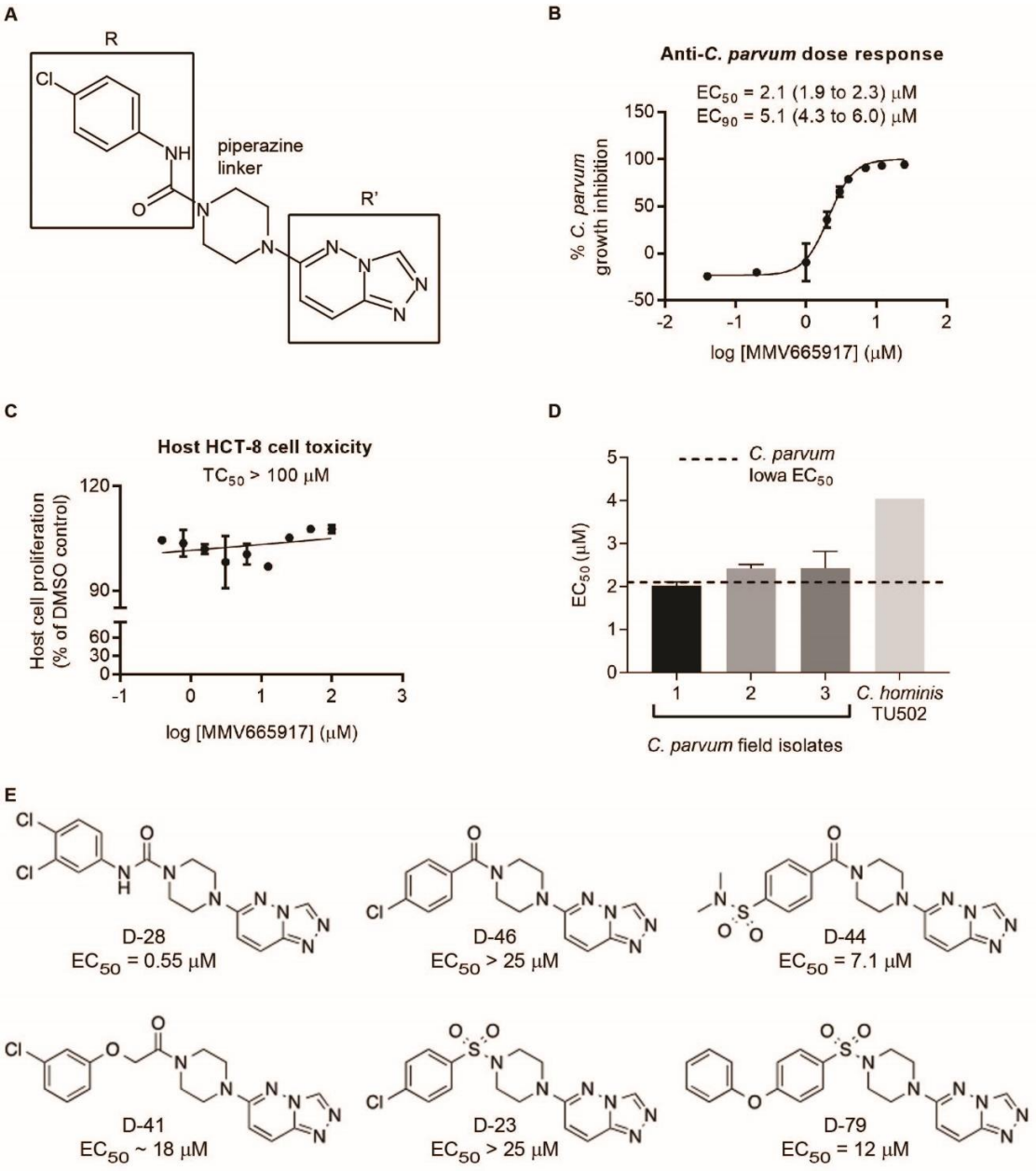

Figure 1. The piperazine-based Malaria Box compound, MMV665917, is a selective inhibitor of *Cryptosporidium* growth *in vitro*.

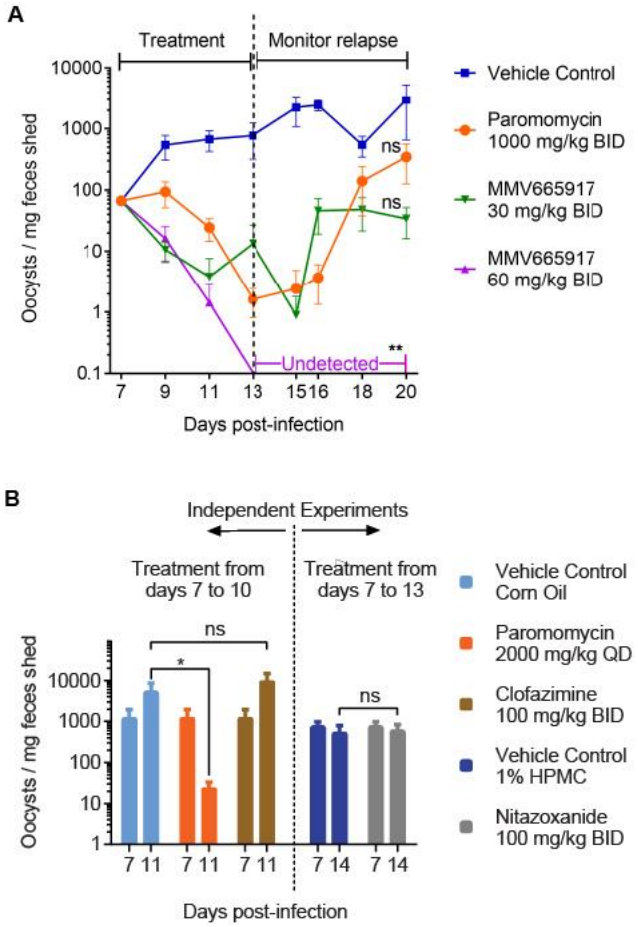

Figure 2. MMV665917 cures NOD SCID gamma mice with established cryptosporidiosis.

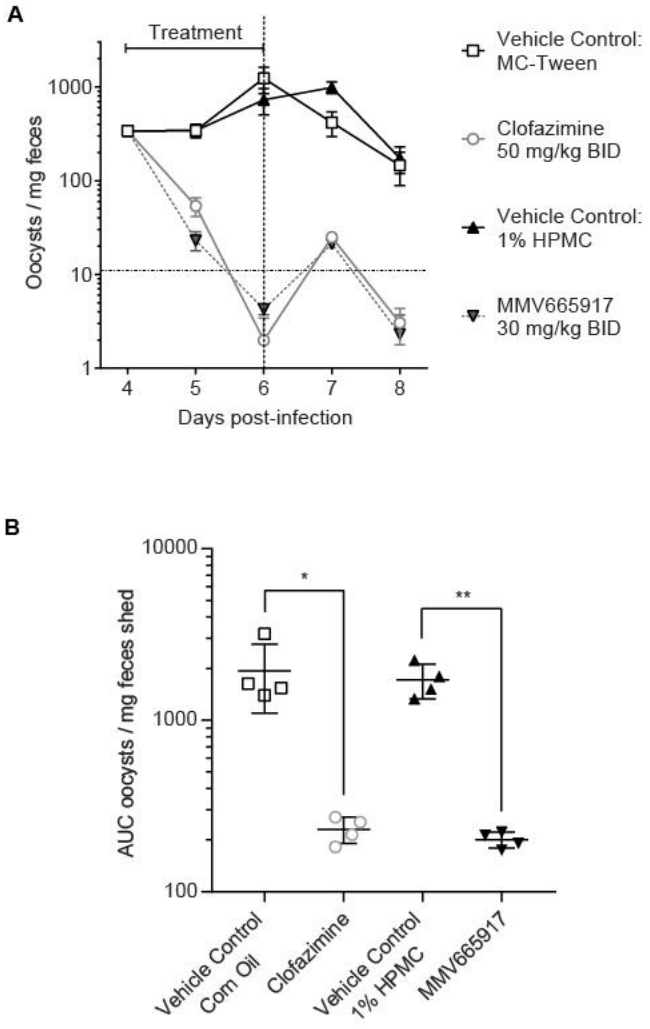

Figure 3. MMV665917 is effective in IFNγ knockout mice acutely infected with *C. parvum*.

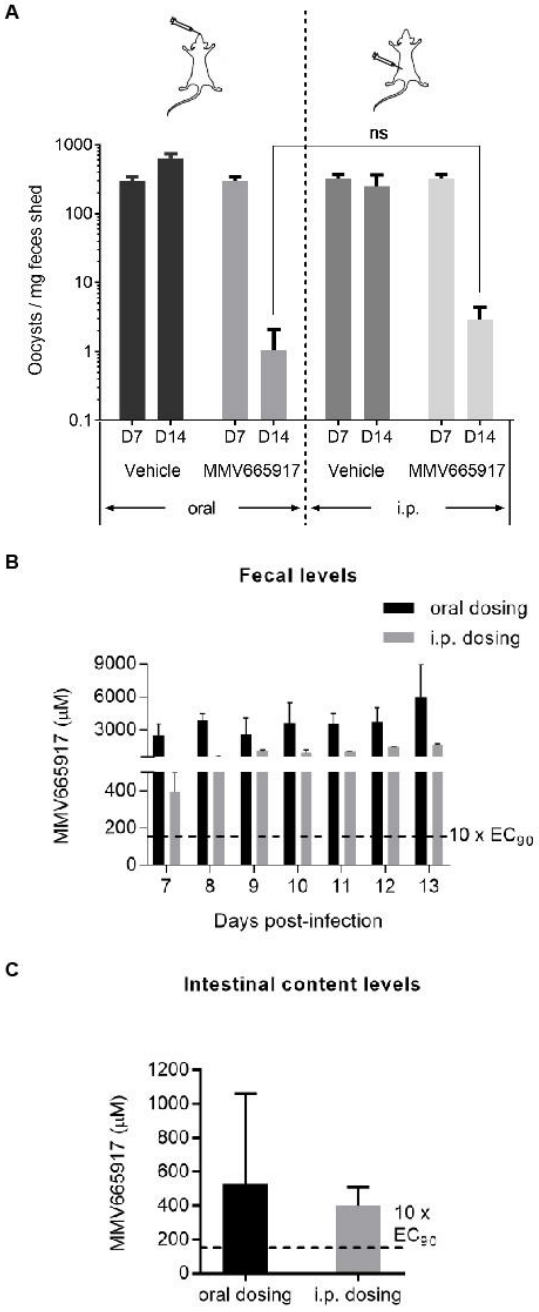

Figure 4. Oral vs intraperitoneal (i.p.) treatment with MMV665917.

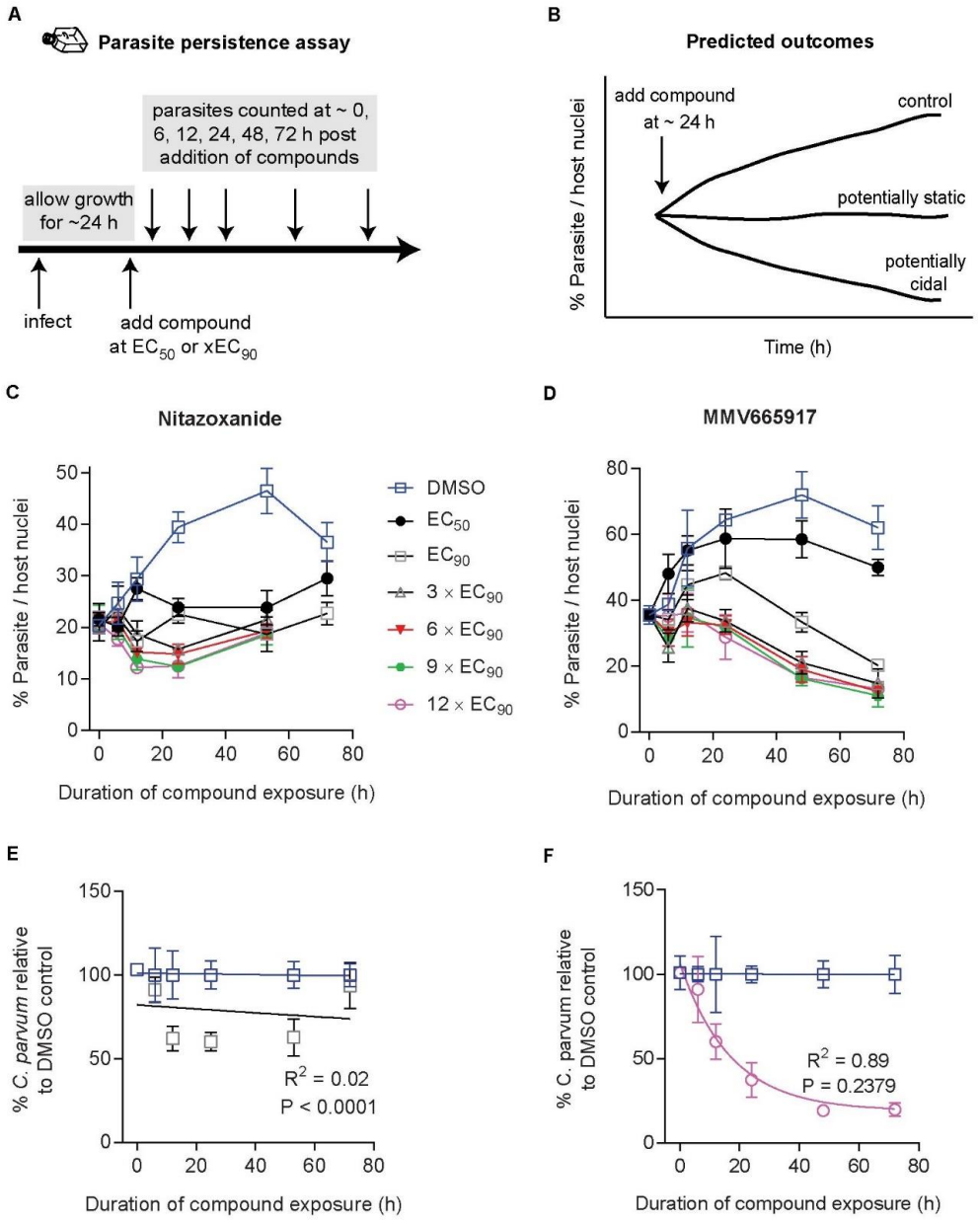

Figure 5. Parasite persistence assay showing *in vitro* elimination of *C. parvum* following MMV665917 exposure vs. parasite persistence in the presence of nitazoxanide.

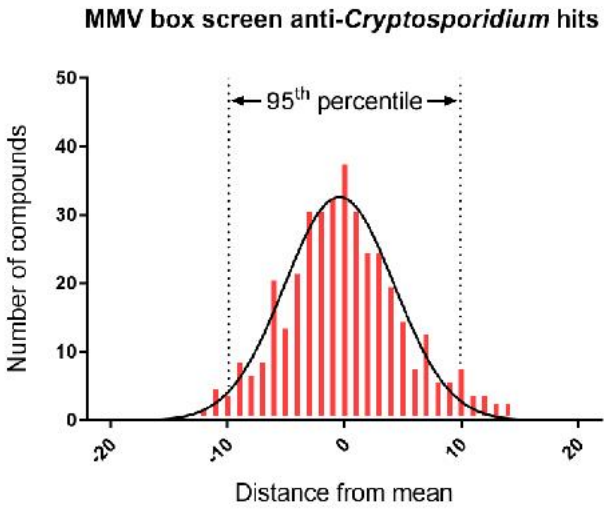

Supplementary Figure 1. Re-analysis of MMV box screening data identifies new *Cryptosporidium* inhibitors.

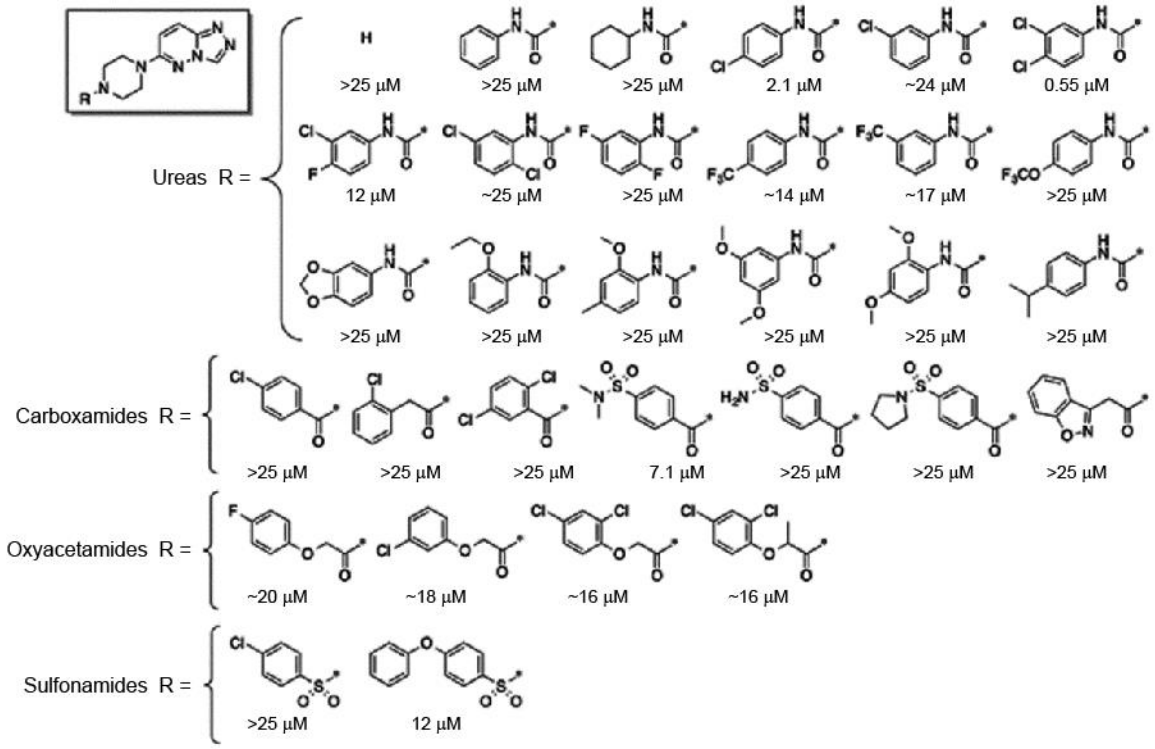

Supplementary Figure 2. Preliminary structure activity relationship studies using commercially available variants on the left-hand side R position.

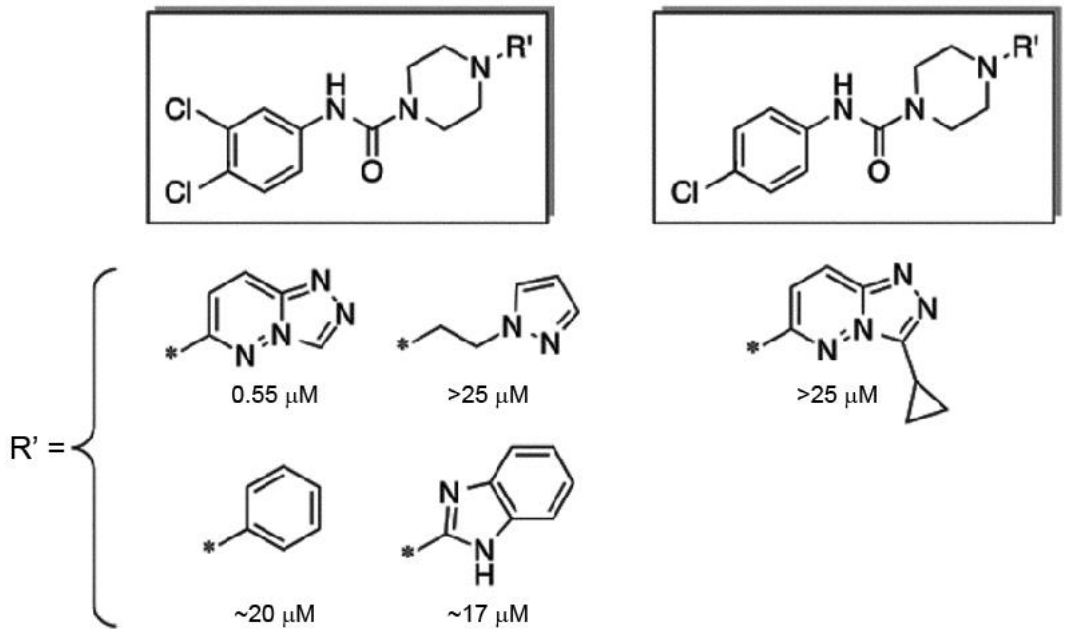

Supplementary Figure 3. Preliminary structure activity relationship studies using commercially available variants on the right-hand side R' position.

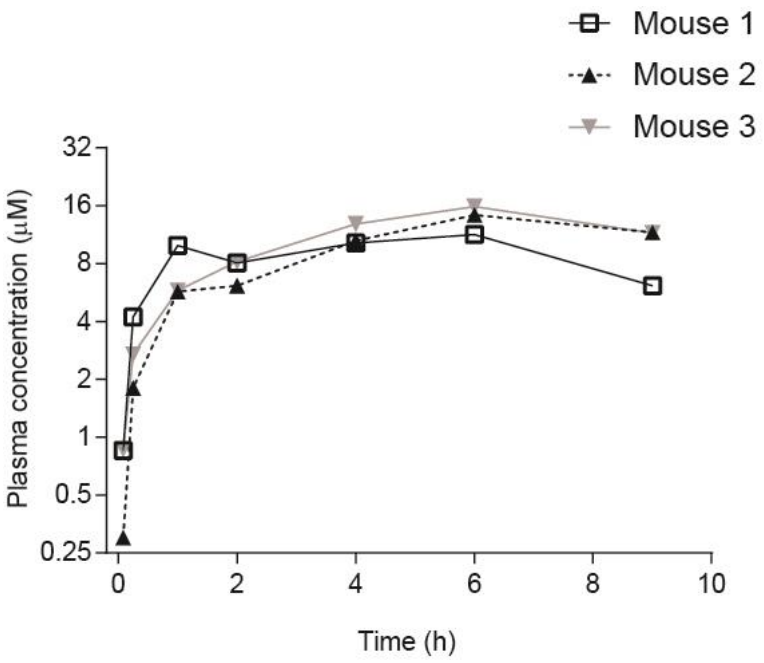

Supplementary Figure 4. Plasma pharmacokinetic information.

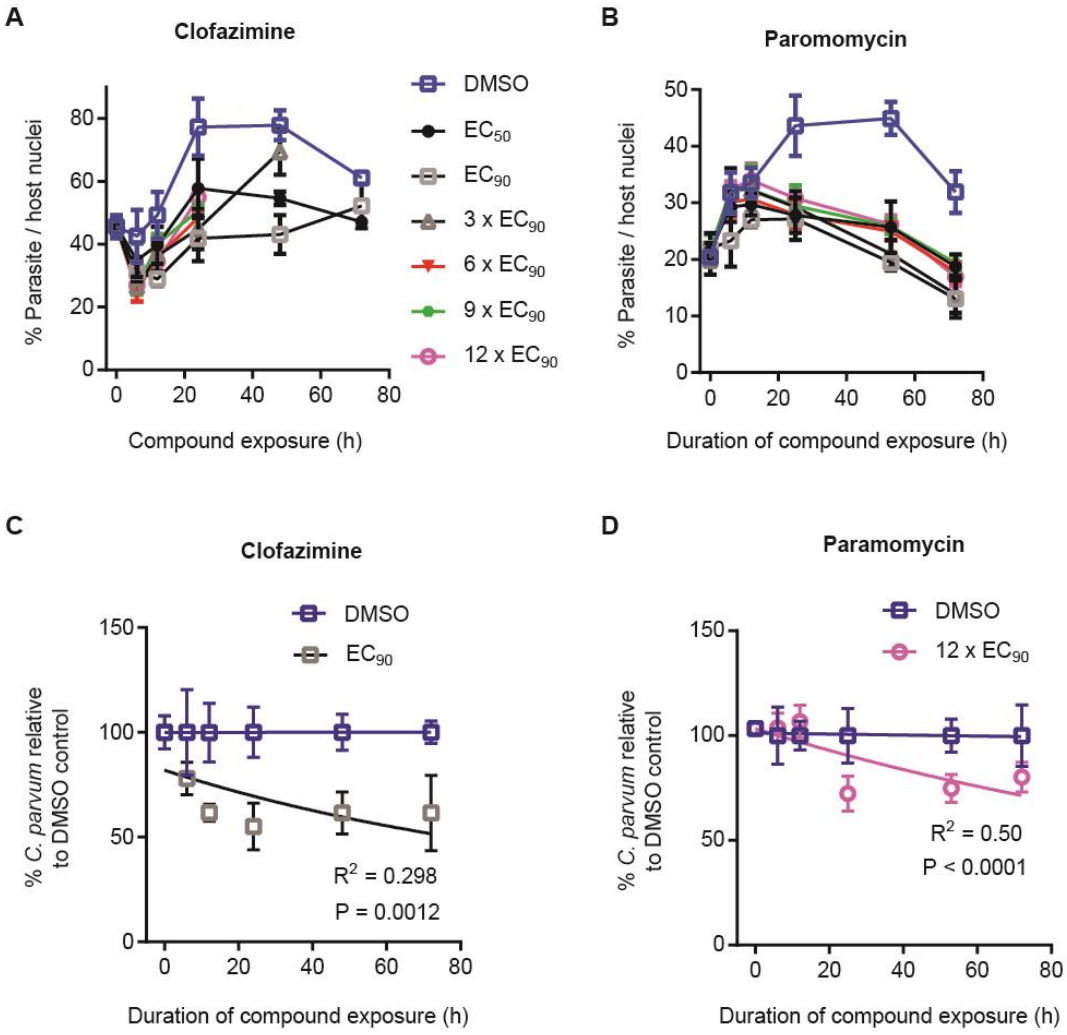

Supplementary Figure 5. Clofazimine and paromomycin both appear to be static for *C. parvum*.

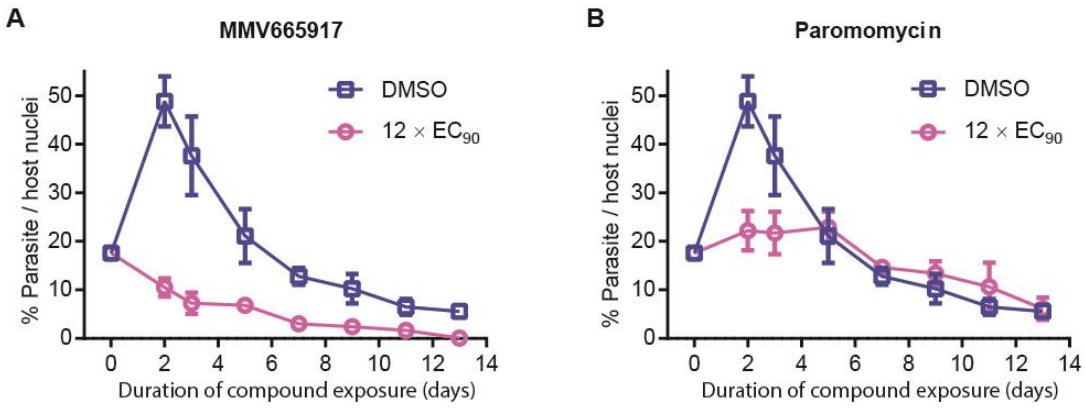

Supplementary Figure 6. Effects of prolonged MMV665917 vs. paromomycin exposure.

Table S1. Open access Malaria Box anti-*C. parvum* confirmed screening hits using new hit-definition.

Compound ID	Smiles	Repurchased source	Mol wt (g/mol)	ALogP	*C. parvum* EC_{50} (95% CI) (μM)[b]
MMV006169[a]	C(Nc1nc(Nc2ccccc2)nc3ccccc13)c4ccccc4	Biomolecules	326.39	4.28	1.5 (1.2-1.9)
MMV403679[a]	c1(c(cnn1c2cccc(C)c2)C(=O)N3)N=C3n4nc(C)cc4NC(=O)c5cc(cccc6)c6o5	SPECS	465.46	4.34	0.12 (0.10-0.14)
MMV009085	OCCCCN1C(=O)c2ccc3C(=O)N(CCCCO)C(=O)c4ccc(C1=O)c2c34	SPECS	410.42	1.01	2.6 (1.9-3.5)
MMV665852	Clc1ccc(NC(=O)Nc2ccc(Cl)c(Cl)c2)cc1Cl	SPECS	350.03	5.18	3.4 (3.1-3.7)
MMV000720[a]	Cc1ccnc(NC(c2cccc(OCc3ccccc3)c2)c4ccc5cccnc5c4O)c1	ChemDiv	447.53	6.22	0.21 (0.17-0.27)
MMV001246[a]	CSc1ccccc1C(=O)Nc2nc(cs2)c3ccccn3	ChemDiv	327.42	3.38	1.8 (1.3-2.6)
MMV665814[a]	Oc1c(ccc2cccnc12)C(Nc3ccccn3)c4cccc(Oc5ccccc5)c4	SPECS	419.47	5.73	0.59 (0.52-0.67)
MMV665917	Clc1ccc(NC(=O)N2CCN(CC2)c3ccc4nncn4n3)cc1	SPECS	357.80	1.69	2.1 (1.9-2.3)
MMV665941[a]	CN(C)c1ccc(cc1)C(O)(c2ccc(cc2)N(C)C)c3ccc(cc3)N(C)C	ChemBridge	389.53	4.76	0.83 (0.69-1.0)
MMV666054[a]	COc1ccc(cc1)C(=O)NC(c2ccc(Cl)cc2Cl)c3cc(Cl)c4cccnc4c3O	ChemBridge	487.76	6.15	0.81 (0.58-1.1)
MMV006753	CC1=CC(=O)Oc2c1ccc3oc(C(=O)c4ccccc4)c(C)c23	SPECS	318.32	4.83	0.25 (0.03-2.3)
MMV011944	n1c(NCCO)c2c(cccc2)nc1Nc3cccc(OC)c3	SPECS	310.35	2.14	3.5 (2.9-4.3)
MMV665909	Brc1ccccc1C(=O)Nc2nc(cs2)c3ccccn3	SPECS	360.23	3.59	3.3 (2.9-3.8)
MMV000760	Oc1c(CN2CCN(CC2)c3ccccc3F)cc(Br)c4cccnc14	SPECS	416.29	4.43	0.29 (0.23-0.37)
MMV665969[a]	COc1cccc(c1)C(=O)NC(c2ccc(C)cc2)c3cc(Cl)c4cccnc4c3O	ChemBridge	432.90	5.31	0.054 (0.041-0.070)

[a] Previously repurchased and confirmed hits from reference 1

[b] EC_{50}, indicates 50% inhibitory concentration

Table S2. Summary of NSG mouse efficacy experiments for Malaria Box screening hits.

Compound ID	Smiles	Supplier	Dose (mg/kg)	Interval (h)	Duration (days)	Vehicle	NSG efficacy
MMV006169 v1	C(Nc1nc(Nc2ccccc2)nc3ccccc13)c4ccccc4	Life Chemicals	50	12	4	1% HPMC[a] / 5% DMSO	No
MMV006169 v2	C1CCC(C1)Nc1nc(NCc2ccccc2)c2c(n1)cccc2	Life Chemicals	50	12	4	1% HPMC[a] / 5% DMSO	No
MMV006169 v3	COc1ccc(cc1Cl)Nc1nc(NCc2ccccc2Cl)c2c(n1)cccc2	Life Chemicals	50	12	4	1% HPMC[a] / 5% DMSO	No
MMV403679 v1	c31c(cnn1-c2cc(ccc2)C)C(=O)NC(=N3)n4c(cc(n4)C)NC(=O)c5c(cc(cc5)OC)OC	Life Chemicals	100	24	7	1% HPMC[a] / 5% DMSO	No
MMV403679 v2	c31c(cnn1-c2cc(ccc2)C)C(=O)NC(=N3)n4c(cc(n4)C)NC(=O)C5CC5	Life Chemicals	100	24	7	1% HPMC[a] / 5% DMSO	No
MMV403679 v3	c31c(cnn1-c2cc(ccc2)C)C(=O)NC(=N3)n4c(cc(n4)C)NC(=O)C5CCCC5	Life Chemicals	100	24	7	1% HPMC[a] / 5% DMSO	No
MMV403679 v4	c31c(cnn1-c2ccccc2)C(=O)NC(=N3)n4c(cc(n4)C)NC(=O)c5oc6c(c5)cccc6	Life Chemicals	100	24	7	1% HPMC[a] / 5% DMSO	No
MMV403679 v5	c31c(cnn1-c2cc(ccc2)C)C(=O)NC(=N3)n4c(cc(n4)C)N	Life Chemicals	100	24	7	1% HPMC[a] / 5% DMSO	No
MMV009085	OCCCCN1C(=O)c2ccc3C(=O)N(CCCCO)C(=O)c4ccc(C1=O)c2c34	-	-	-	-	-	ND
MMV665852	Clc1ccc(NC(=O)Nc2ccc(Cl)c(Cl)c2)cc1Cl	-	-	-	-	-	ND
MMV000720	Cc1ccnc(NC(c2cccc(OCc3ccccc3)c2)c4ccc5cccnc5c4O)c1	-	-	-	-	-	ND
MMV001246	CSc1ccccc1C(=O)Nc2nc(cs2)c3ccccn3	Enamine	50	12	4	1% HPMC[a] / 5% DMSO	No
MMV665814	Oc1c(ccc2cccnc12)C(Nc3ccccn3)c4cccc(Oc5ccccc5)c4	SPECS	50	12	4		No
MMV665917	Clc1ccc(NC(=O)N2CCN(CC2)c3ccc4nncn4n3)cc1	Life Chemicals	30	12	4	1% HPMC[a] / 5% DMSO	Yes
MMV665941	CN(C)c1ccc(cc1)C(O)(c2ccc(cc2)N(C)C)c3ccc(cc3)N(C)C	SPECS	50	12	4	1% HPMC[a] / 5% DMSO	No
MMV666054	COc1ccc(cc1)C(=O)NC(c2ccc(Cl)cc2Cl)c3cc(Cl)c4cccnc4c3O	-	-	-	-	-	ND
MMV006753	CC1=CC(=O)Oc2c1ccc3oc(C(=O)c4ccccc4)c(C)c23	-	-	-	-	-	ND
MMV011944	n1c(NCCO)c2c(cccc2)nc1Nc3cccc(OC)c3	-	-	-	-	-	ND
MMV665909	Brc1ccccc1C(=O)Nc2nc(cs2)c3ccccn3	Enamine	50	12	4	1% HPMC[a] / 5% DMSO	No
MMV000760	Oc1c(CN2CCN(CC2)c3ccccc3F)cc(Br)c4cccnc14	-	-	-	-	-	ND
MMV665969	COc1cccc(c1)C(=O)NC(c2ccc(C)cc2)c3cc(Cl)c4cccnc4c3O	SPECS	50	12	4	1% HPMC[a] / 5% DMSO	No

[a]HPMC, hydroxypropyl methyl cellulose

Table S3. Structure-activity relationship of MMV665917.

Compound_ID	Supplier	SMILES	Mol wt (g/mol)	miLogP[a]	TPSA[b] (Å^2)	*C. parvum* EC_{50} (95% CI) (μM)[c]
D-1 (MMV665917)	Life Chemicals	Clc1ccc(NC(=O)N2CCN(CC2)c3ccc4nncn4n3)cc1	357.81	2.40	78.67	2.1 (1.9-2.3)
D-2	Vitas M Labs	CN1CCN(CC1)c1ccc2n(n1)c(nn2)C(F)(F)F	286.26	1.37	49.57	>25
D-3	Vitas M Labs	FC(c1nnc2n1nc(cc2)N1CCN(CC1)Cc1ccccc1)(F)F	362.35	2.77	49.57	>25
D-4	Vitas M Labs	CCOC(=O)N1CCN(CC1)c1ccc2n(n1)c(nn2)C(F)(F)F	344.29	1.82	75.87	>25
D-9	Vitas M Labs	c1ccc(cc1)N1CCN(CC1)c1ccc2n(n1)cnn2	280.33	2.07	49.57	>25
D-12	Vitas M Labs	CC(=O)N1CCN(CC1)c1ccc2n(n1)c(nn2)C(F)(F)F	314.27	0.74	66.64	>25
D-18	Life Chemicals	O=C(N1CCN(CC1)c1ccc2n(n1)cnn2)Nc1ccccc1	323.35	1.72	78.67	>25
D-19	Life Chemicals	O=C(N1CCN(CC1)c1ccc2n(n1)cnn2)Nc1ccc2c(c1)OCO2	367.36	1.61	97.13	>25
D-20	Life Chemicals	O=C(N1CCN(CC1)c1ccc2n(n1)cnn2)NC1CCCCC1	329.40	2.48	78.67	>25
D-21	Life Chemicals	O=C(N1CCN(CC1)c1ccc2n(n1)c(C)nn2)NCc1ccccc1	351.41	2.06	78.67	>25
D-22	Life Chemicals	O=C(N1CCN(CC1)c1ccc2n(n1)c(nn2)C1CC1)NC1CCCCC1	369.46	2.94	78.67	>25
D-23	Life Chemicals	Clc1ccc(cc1)S(=O)(=O)N1CCN(CC1)c1ccc2n(n1)cnn2	378.84	1.96	83.71	>25
D-26	Life Chemicals	Fc1ccc(cc1)OCC(=O)N1CCN(CC1)c1ccc2n(n1)cnn2	356.35	1.54	75.87	20 (17-23)
D-27	Life Chemicals	O=C(N1CCN(CC1)c1ccc2n(n1)cnn2)Nc1cccc(c1)C(F)(F)F	391.35	2.59	78.67	17 (14-22)
D-28	Life Chemicals	O=C(N1CCN(CC1)c1ccc2n(n1)cnn2)Nc1ccc(c(c1)Cl)Cl	392.24	3.01	78.67	0.55 (0.46-0.65)
D-29	Life Chemicals	Fc1ccc(cc1)C(=O)N1CCN(CC1)c1ccc2n(n1)c(nn2)C1CC1	366.39	1.55	66.64	>25
D-31	Vitas M Labs	COc1ccc(cc1)N1CCN(CC1)c1ccc2n(n1)cnn2	310.35	2.13	58.80	>25
D-32	Life Chemicals	Clc1ccc(c(c1)NC(=O)N1CCN(CC1)c1ccc2n(n1)cnn2)Cl	392.24	3.01	78.67	~24.81
D-33	Life Chemicals	CCOc1ccccc1NC(=O)N1CCN(CC1)c1ccc2n(n1)cnn2	367.41	2.11	87.90	>25
D-34	Life Chemicals	COc1ccc(cc1NC(=O)N1CCN(CC1)c1ccc2n(n1)cnn2)C	367.41	2.16	87.90	>25
D-35	Life Chemicals	COc1cc(cc(c1)OC)NC(=O)N1CCN(CC1)c1ccc2n(n1)cnn2	383.40	1.76	97.13	>25
D-36	Life Chemicals	O=C(N1CCN(CC1)c1ccc2n(n1)cnn2)Nc1ccc(cc1)C(C)C	365.43	3.23	78.67	>25
D-37	Life Chemicals	Fc1ccc(c(c1)NC(=O)N1CCN(CC1)c1ccc2n(n1)cnn2)F	359.33	1.98	78.67	>25
D-38	Life Chemicals	O=C(N1CCN(CC1)c1ccc2n(n1)cnn2)Nc1ccc(c(c1)Cl)F	375.79	2.49	78.67	12 (11-14)
D-40	Life Chemicals	COc1ccc(cc1NC(=O)N1CCN(CC1)c1ccc2n(n1)cnn2)OC	383.40	1.76	97.13	>25
D-41	Life Chemicals	Clc1cccc(c1)OCC(=O)N1CCN(CC1)c1ccc2n(n1)cnn2	372.81	2.03	75.87	18 (16-21)
D-42	Life Chemicals	O=C(N1CCN(CC1)c1ccc2n(n1)cnn2)Cc1ccccc1Cl	356.81	2.13	66.64	>25
D-43	Life Chemicals	O=C(N1CCN(CC1)c1ccc2n(n1)c(nn2)C1CC1)Nc1ccc(c(c1)Cl)F	415.85	2.94	78.67	>25
D-44	Life Chemicals	O=C(c1ccc(cc1)S(=O)(=O)N(C)C)N1CCN(CC1)c1ccc2n(n1)cnn2	415.47	0.25	104.02	7.1 (5.9-8.5)
D-45	Life Chemicals	O=C(c1ccc(cc1)S(=O)(=O)N)N1CCN(CC1)c1ccc2n(n1)cnn2	387.42	-0.37	126.80	>25
D-46	Life Chemicals	Clc1ccc(cc1)C(=O)N1CCN(CC1)c1ccc2n(n1)cnn2	342.78	1.61	66.64	>25
D-47	Life Chemicals	Clc1ccc(c(c1)C(=O)N1CCN(CC1)c1ccc2n(n1)cnn2)Cl	377.23	2.22	66.64	>25
D-48	Life Chemicals	O=C(c1ccc(cc1)S(=O)(=O)N1CCCC1)N1CCN(CC1)c1ccc2n(n1)cnn2	441.51	0.65	104.02	>25
D-49	Life Chemicals	O=C(N1CCN(CC1)c1ccc2n(n1)cnn2)Cc1noc2c1cccc2	363.37	1.53	92.67	>25
D-50	Life Chemicals	Clc1ccc(c(c1)Cl)OCC(=O)N1CCN(CC1)c1ccc2n(n1)cnn2	407.25	2.66	75.87	16 (14-18)
D-51	Life Chemicals	Clc1ccc(c(c1)Cl)OC(C(=O)N1CCN(CC1)c1ccc2n(n1)cnn2)C	421.28	3.02	78.87	>25
D-53	Life Chemicals	N1CCN(CC1)c1ccc2n(n1)cnn2	204.23	-0.22	58.36	>25
D-60	Vitas M Labs	O=C(N1CCN(CC1)c1ccc2n(n1)c(C)nn2)OC(C)(C)C	318.37	1.50	75.87	>25
D-74	Sigma	O=C(Nc1ccc(Cl)c(Cl)c1)N2CCN(CC2)c3ccccc3	350.25	4.56	35.57	20 (12-32)
D-75	Life Chemicals	FC(F)(F)c1ccc(cc1)NC(=O)N2CCN(CC2)c3ccc4nncn4n3	391.36	2.62	78.67	11 (9.3-13)
D-76	Life Chemicals	FC(F)(F)Oc1ccc(cc1)NC(=O)N2CCN(CC2)c3ccc4nncn4n3	407.36	2.69	87.90	>25
D-77	Life Chemicals	Clc1cccc(c1)NC(=O)N2CCN(CC2)c3ccc4nncn4n3	357.81	2.38	78.67	~23.67
D-78	Life Chemicals	O=C(N1CCN(C2=NN3C(C=C2)=NN=C3)CC1)NC5=CC=C(Cl)C=C5	357.80	2.40	78.67	>25
D-79	Life Chemicals	O=S(N1CCN(C2=NN3C(C=C2)=NN=C3)CC1)(C4=CC=C(OC5=CC=CC=C5)C=C4)=O	436.50	3.04	92.94	12 (9.2-16)
D-80	Life Chemicals	O=C(N1CCN(C2=NC3=C(C=CC=C3)N2)CC1)NC4=CC=C(Cl)C(Cl)=C4	390.27	4.38	64.26	17 (14-20)
D-81	Life Chemicals	O=C(N1CCN(CCN2N=CC=C2)CC1)NC3=CC=C(Cl)C(Cl)=C3	368.27	2.94	53.40	>25

[a] and [b], calculated using molinspiration property engine versions v2013.09, v2014.11, and v2016.10

[c] EC_{50}, indicates half maximal effective concentration

2.8. References

Abubakar, I., Aliyu, S. H., Arumugam, C., Hunter, P. R., & Usman, N. K. (2007). Prevention and treatment of cryptosporidiosis in immunocompromised patients. *Cochrane database of systematic reviews*(1), CD004932. doi:10.1002/14651858.CD004932.pub2

Akiyoshi, D. E., Mor, S., & Tzipori, S. (2003). Rapid displacement of Cryptosporidium parvum type 1 by type 2 in mixed infections in piglets. *Infect Immun, 71*(10), 5765-5771.

Amadi, B., Mwiya, M., Musuku, J., Watuka, A., Sianongo, S., Ayoub, A., & Kelly, P. (2002). Effect of nitazoxanide on morbidity and mortality in Zambian children with cryptosporidiosis: a randomised controlled trial. *The Lancet, 360*(9343), 1375-1380. doi:10.1016/s0140-6736(02)11401-2

Amadi, B., Mwiya, M., Sianongo, S., Payne, L., Watuka, A., Katubulushi, M., & Kelly, P. (2009). High dose prolonged treatment with nitazoxanide is not effective for cryptosporidiosis in HIV positive Zambian children: a randomised controlled trial. *BMC infectious diseases, 9*, 195. doi:10.1186/1471-2334-9-195

Angulo-Barturen, I., Jimenez-Diaz, M. B., Mulet, T., Rullas, J., Herreros, E., Ferrer, S., . . . Gargallo-Viola, D. (2008). A murine model of falciparum-malaria by in vivo selection of competent strains in non-myelodepleted mice engrafted with human erythrocytes. *PLoS One, 3*(5), e2252. doi:10.1371/journal.pone.0002252

Arrowood, M. J., & Sterling, C. R. (1987). Isolation of Cryptosporidium oocysts and sporozoites using discontinuous sucrose and isopycnic Percoll gradients. *J Parasitol, 73*(2), 314-319.

Bessoff, K., Sateriale, A., Lee, K. K., & Huston, C. D. (2013). Drug Repurposing Screen Reveals FDA-Approved Inhibitors of Human HMG-CoA Reductase and Isoprenoid Synthesis that Block Cryptosporidium parvum Growth. *Antimicrobial agents and chemotherapy*. doi:10.1128/AAC.02460-12

Bessoff, K., Spangenberg, T., Foderaro, J., Jumani, R. S., Ward, G. E., & Huston, C. D. (2014). Identification of Cryptosporidium parvum active chemical series by repurposing the Open Access Malaria Box. *Antimicrob Agents Chemother*. doi:10.1128/AAC.02641-13

Burrows, J. N., van Huijsduijnen, R. H., Mohrle, J. J., Oeuvray, C., & Wells, T. N. (2013). Designing the next generation of medicines for malaria control and eradication. *Malaria journal, 12*, 187. doi:10.1186/1475-2875-12-187

Bushen, O. Y., Kohli, A., Pinkerton, R. C., Dupnik, K., Newman, R. D., Sears, C. L., . . . Guerrant, R. L. (2007). Heavy cryptosporidial infections in children in northeast Brazil: comparison of Cryptosporidium hominis and Cryptosporidium parvum. *Transactions of the Royal Society of Tropical Medicine and Hygiene, 101*(4), 378-384. doi:10.1016/j.trstmh.2006.06.005

Campbell, L. D., Stewart, J. N., & Mead, J. R. (2002). Susceptibility to Cryptosporidium parvum infections in cytokine- and chemokine-receptor

knockout mice. *J Parasitol, 88*(5), 1014-1016. doi:10.1645/0022-3395(2002)088[1014:STCPII]2.0.CO;2

Castellanos-Gonzalez, A., White, A. C., Jr., Ojo, K. K., Vidadala, R. S., Zhang, Z., Reid, M. C., . . . Van Voorhis, W. C. (2013). A novel calcium-dependent protein kinase inhibitor as a lead compound for treating cryptosporidiosis. *J Infect Dis, 208*(8), 1342-1348. doi:10.1093/infdis/jit327

Checkley, W., White, A. C., Jr., Jaganath, D., Arrowood, M. J., Chalmers, R. M., Chen, X. M., . . . Houpt, E. R. (2015). A review of the global burden, novel diagnostics, therapeutics, and vaccine targets for cryptosporidium. *Lancet Infect Dis, 15*(1), 85-94. doi:10.1016/S1473-3099(14)70772-8

Gollapalli, D. R., Macpherson, I. S., Liechti, G., Gorla, S. K., Goldberg, J. B., & Hedstrom, L. (2010). Structural determinants of inhibitor selectivity in prokaryotic IMP dehydrogenases. *Chemistry & biology, 17*(10), 1084-1091. doi:10.1016/j.chembiol.2010.07.014

Gorla, S. K., McNair, N. N., Yang, G., Gao, S., Hu, M., Jala, V. R., . . . Hedstrom, L. (2014). Validation of IMP dehydrogenase inhibitors in a mouse model of cryptosporidiosis. *Antimicrob Agents Chemother, 58*(3), 1603-1614. doi:10.1128/aac.02075-13

Griffiths, J. K., Theodos, C., Paris, M., & Tzipori, S. (1998). The gamma interferon gene knockout mouse: a highly sensitive model for evaluation of therapeutic agents against Cryptosporidium parvum. *J Clin Microbiol, 36*(9), 2503-2508.

Guerrant, D. I., Moore, S. R., Lima, A. A., Patrick, P. D., Schorling, J. B., & Guerrant, R. L. (1999). Association of early childhood diarrhea and cryptosporidiosis with impaired physical fitness and cognitive function four-seven years later in a poor urban community in northeast Brazil. *Am J Trop Med Hyg, 61*(5), 707-713.

Hlavsa, M. C., Roberts, V. A., Anderson, A. R., Hill, V. R., Kahler, A. M., Orr, M., . . . Yoder, J. S. (2011). Surveillance for waterborne disease outbreaks and other health events associated with recreational water --- United States, 2007--2008. *MMWR. Surveillance summaries : Morbidity and mortality weekly report. Surveillance summaries / CDC, 60*(12), 1-32.

Huston, C. D., Spangenberg, T., Burrows, J., Willis, P., Wells, T. N., & van Voorhis, W. (2015). A Proposed Target Product Profile and Developmental Cascade for New Cryptosporidiosis Treatments. *PLoS Negl Trop Dis, 9*(10), e0003987. doi:10.1371/journal.pntd.0003987

Ito, M., Hiramatsu, H., Kobayashi, K., Suzue, K., Kawahata, M., Hioki, K., . . . Nakahata, T. (2002). NOD/SCID/gamma(c)(null) mouse: an excellent recipient mouse model for engraftment of human cells. *Blood, 100*(9), 3175-3182. doi:10.1182/blood-2001-12-0207

Korpe, P. S., Haque, R., Gilchrist, C., Valencia, C., Niu, F., Lu, M., . . . Petri, W. A., Jr. (2016). Natural History of Cryptosporidiosis in a Longitudinal Study of Slum-Dwelling Bangladeshi Children: Association with Severe Malnutrition. *PLoS Negl Trop Dis, 10*(5), e0004564. doi:10.1371/journal.pntd.0004564

Kotloff, K. L., Nataro, J. P., Blackwelder, W. C., Nasrin, D., Farag, T. H., Panchalingam, S., . . . Levine, M. M. (2013). Burden and aetiology of diarrhoeal

disease in infants and young children in developing countries (the Global Enteric Multicenter Study, GEMS): a prospective, case-control study. *The Lancet, 382*(9888), 209-222. doi:http://dx.doi.org/10.1016/S0140-6736(13)60844-2

Liu, J., Platts-Mills, J. A., Juma, J., Kabir, F., Nkeze, J., Okoi, C., . . . Houpt, E. R. (2016). Use of quantitative molecular diagnostic methods to identify causes of diarrhoea in children: a reanalysis of the GEMS case-control study. *Lancet, 388*(10051), 1291-1301. doi:10.1016/S0140-6736(16)31529-X

Love, M. S., Beasley, F. C., Jumani, R. S., Wright, T. M., Chatterjee, A. K., Huston, C. D., . . . McNamara, C. W. (2017). A high-throughput phenotypic screen identifies clofazimine as a potential treatment for cryptosporidiosis. *PLoS Negl Trop Dis, 11*(2), e0005373. doi:10.1371/journal.pntd.0005373

Malebranche, R., Arnoux, E., Guerin, J. M., Pierre, G. D., Laroche, A. C., Pean-Guichard, C., . . . et al. (1983). Acquired immunodeficiency syndrome with severe gastrointestinal manifestations in Haiti. *Lancet, 2*(8355), 873-878.

Manjunatha, U. H., Vinayak, S., Zambriski, J. A., Chao, A. T., Sy, T., Noble, C. G., . . . Diagana, T. T. (2017). A Cryptosporidium PI(4)K inhibitor is a drug candidate for cryptosporidiosis. *Nature, 546*(7658), 376-380. doi:10.1038/nature22337

Maurya, S. K., Gollapalli, D. R., Kirubakaran, S., Zhang, M., Johnson, C. R., Benjamin, N. N., . . . Cuny, G. D. (2009). Triazole inhibitors of Cryptosporidium parvum inosine 5'-monophosphate dehydrogenase. *J Med Chem, 52*(15), 4623-4630. doi:10.1021/jm900410u

Morada, M., Lee, S., Gunther-Cummins, L., Weiss, L. M., Widmer, G., Tzipori, S., & Yarlett, N. (2016). Continuous culture of Cryptosporidium parvum using hollow fiber technology. *Int J Parasitol, 46*(1), 21-29. doi:10.1016/j.ijpara.2015.07.006

Murphy, R. C., Ojo, K. K., Larson, E. T., Castellanos-Gonzalez, A., Perera, B. G., Keyloun, K. R., . . . Maly, D. J. (2010). Discovery of Potent and Selective Inhibitors of Calcium-Dependent Protein Kinase 1 (CDPK1) from C. parvum and T. gondii. *ACS Med Chem Lett, 1*(7), 331-335. doi:10.1021/ml100096t

Navin, T. R., Weber, R., Vugia, D. J., Rimland, D., Roberts, J. M., Addiss, D. G., . . . Bryan, R. T. (1999). Declining CD4+ T-lymphocyte counts are associated with increased risk of enteric parasitosis and chronic diarrhea: results of a 3-year longitudinal study. *J Acquir Immune Defic Syndr Hum Retrovirol, 20*(2), 154-159.

Ndao, M., Nath-Chowdhury, M., Sajid, M., Marcus, V., Mashiyama, S. T., Sakanari, J., . . . Caffrey, C. R. (2013). A cysteine protease inhibitor rescues mice from a lethal Cryptosporidium parvum infection. *Antimicrob Agents Chemother, 57*(12), 6063-6073. doi:10.1128/aac.00734-13

Platts-Mills, J. A., Babji, S., Bodhidatta, L., Gratz, J., Haque, R., Havt, A., . . . Investigators, M.-E. N. (2015). Pathogen-specific burdens of community diarrhoea in developing countries: a multisite birth cohort study (MAL-ED). *Lancet Glob Health, 3*(9), e564-575. doi:10.1016/S2214-109X(15)00151-5

Schaefer, D. A., Betzer, D. P., Smith, K. D., Millman, Z. G., Michalski, H. C., Menchaca, S. E., . . . Riggs, M. W. (2016). Novel Bumped Kinase Inhibitors

Are Safe and Effective Therapeutics in the Calf Clinical Model for Cryptosporidiosis. *J Infect Dis, 214*(12), 1856-1864. doi:10.1093/infdis/jiw488

Shultz, L. D., Lyons, B. L., Burzenski, L. M., Gott, B., Chen, X., Chaleff, S., . . . Handgretinger, R. (2005). Human lymphoid and myeloid cell development in NOD/LtSz-scid IL2R gamma null mice engrafted with mobilized human hemopoietic stem cells. *J Immunol, 174*(10), 6477-6489.

Sonzogni-Desautels, K., Renteria, A. E., Camargo, F. V., Di Lenardo, T. Z., Mikhail, A., Arrowood, M. J., . . . Ndao, M. (2015). Oleylphosphocholine (OlPC) arrests Cryptosporidium parvum growth in vitro and prevents lethal infection in interferon gamma receptor knock-out mice. *Front Microbiol, 6*, 973. doi:10.3389/fmicb.2015.00973

Tzipori, S., Rand, W., & Theodos, C. (1995). Evaluation of a two-phase scid mouse model preconditioned with anti-interferon-gamma monoclonal antibody for drug testing against Cryptosporidium parvum. *J Infect Dis, 172*(4), 1160-1164.

Van Voorhis, W. C., Adams, J. H., Adelfio, R., Ahyong, V., Akabas, M. H., Alano, P., . . . Willis, P. A. (2016). Open Source Drug Discovery with the Malaria Box Compound Collection for Neglected Diseases and Beyond. *PLoS Pathog, 12*(7), e1005763. doi:10.1371/journal.ppat.1005763

You, X., Schinazi, R. F., Arrowood, M. J., Lejkowski, M., Juodawlkis, A. S., & Mead, J. R. (1998). In-vitro activities of paromomycin and lasalocid evaluated in combination against Cryptosporidium parvum. *J Antimicrob Chemother, 41*(2), 293-296.

Zambriski, J. A., Nydam, D. V., Bowman, D. D., Bellosa, M. L., Burton, A. J., Linden, T. C., . . . Mohammed, H. O. (2013). Description of fecal shedding of Cryptosporidium parvum oocysts in experimentally challenged dairy calves. *Parasitol Res, 112*(3), 1247-1254. doi:10.1007/s00436-012-3258-2

CHAPTER 3: LIFE STAGE ASSAYS TO PRIORITIZE ANTI-*CRYPTOSPORIDIUM* HITS BASED ON DIVERSITY

Jumani RS[1,2], Stebbins EE[1], Hasan MM[1,2], Liam[1], Miller P[1], Klopfer C[1], Bessoff K[1#], Teixeira JE[1], Love MS[3], McNamara CW[3], Huston CD[1,2]*

[1]Dept. of Medicine, University of Vermont Larner College of Medicine, Burlington, VT

[2]Cellular, Molecular and Biomedical Sciences Graduate Program, University of Vermont, Burlington, VT

[3]California Institute for Biomedical Research, La Jolla, CA

[#]Current address: Dept. of Surgery, Stanford University School of Medicine, Palo Alto, CA

3.1. Abstract

Cryptosporidiosis, is a diarrheal disease due to intestinal infection with one of several *Cryptosporidium* species. It is a leading cause of life-threatening diarrhea in young children and causes prolonged disease in malnourished children and immunocompromised people like AIDS patients. Nitazoxanide, the only approved drug, is not very effective in these populations. Large-scale phenotypic screens are ongoing to identify anti-*Cryptosporidium* growth inhibitors (hits). In the absence of a gold standard drug, the *in vitro* and *in vivo* properties to guide prioritization of hits are not known. With a goal to prioritize a diverse set of hits without knowledge about the

actual mechanism of action, we developed a range of medium-throughput life stage assays, including an assay for asexual to sexual conversion that can be used to quickly screen a large number of the phenotypic hits. Fifty-five hits and leads from several collaborators in the Bill and Melinda Gates' Foundations' *Cryptosporidium* Consortium were tested in all these assays and data was used to cluster compounds. The compounds segregated into seven different clusters with related chemical classes and compounds with similar mechanism action grouping together. Furthermore, compounds from different clusters were active in the chronic NOD SCID gamma mouse model of cryptosporidiosis, suggesting the assays could be used to obtain and maintain diversity in *Cryptosporidium* drug development pipeline.

3.2. Introduction

Diarrhea still causes ~8% of all deaths globally in children under five years of age (Disease, Injury, & Prevalence, 2016). Amongst infectious etiologies, cryptosporidiosis recently garnered increased interest when the Global Enteric Multicenter Study (GEMS) reported it as a leading cause of life-threatening childhood diarrhea in Africa and the Indian subcontinent (Kotloff et al., 2013; Liu et al., 2016). Cryptosporidiosis was also strongly associated with malnutrition and mortality. Infection of the intestinal epithelium by apicomplexan *Cryptosporidium* parasites causes cryptosporidiosis, and, although over twenty species of *Cryptosporidium* have been reported, *Cryptosporidium parvum* and *Cryptosporidium hominis* account for almost all human cases (Checkley et al., 2015). Despite numerous earlier studies that

suggested the importance of *Cryptosporidium* parasites in young children (Shirley, Moonah, & Kotloff, 2012), cryptosporidiosis was previously known best as a cause of prolonged diarrhea in immunocompromised people, especially AIDS patients in whom it is reported to cause as much as 50% of cases (Malebranche et al., 1983; Navin et al., 1999). Unfortunately, treatment options for cryptosporidiosis are very limited (Checkley et al., 2015). The only approved drug, nitazoxanide, is equivalent to a placebo in AIDS patients (Abubakar, Aliyu, Arumugam, Hunter, & Usman, 2007). And its efficacy in young children is modest, with improvement after one week of treatment in just over half of children studied compared to spontaneous improvement of approximately one quarter of untreated children (Amadi et al., 2009). Thus, there is a clear public health need for improved drugs to treat children and immunocompromised people with cryptosporidiosis.

Given that there is no highly effective treatment for cryptosporidiosis in the most affected populations, it follows that there is no well-validated developmental pathway for anti-*Cryptosporidium* drugs (Huston et al., 2015; Manjunatha, Chao, Leong, & Diagana, 2016). Ideally, early-stage investments should be made in compounds with a diverse set of molecular mechanisms, since there is currently no means to judge which will succeed and which will fail (Katsuno et al., 2015). The situation is further complicated by both economic and technical issues. First, the potential market for anti-*Cryptosporidium* drugs is small, since the disease predominantly affects people in low and middle income countries. Second, despite successful use of CRISPR/Cas9 for genome manipulation, genetic studies must

presently be carried out in a mouse, which limits the ability to validate potential drug targets (Pawlowic, Vinayak, Sateriale, Brooks, & Striepen, 2017; Vinayak et al., 2015). These financial and technical limitations generally favor phenotypic screening approaches to identify potential starting points for drug development, since cell-based methods typically result in a shorter time to market (i.e. reduced cost of development) and do not restrict potential chemical starting points to those that affect a small number of previously validated drug targets (Nwaka & Hudson, 2006). Accordingly, several phenotypic cell-based screening methods have now been used successfully to identify *Cryptosporidium* growth inhibitors, and there is a growing number of compounds in the developmental pipeline (Bessoff, Sateriale, Lee, & Huston, 2013; Bessoff et al., 2014; Chao et al., 2018; Love et al., 2017). However, without drug target identification, which is difficult even in the most developed experimental systems, the current approach forfeits the many advantages of target-based drug development for compounds for which knowledge from other systems provides no likely mechanism of action. One key disadvantage of a developmental pipeline that is wholly dependent on cell-based screening for a single phenotype, is that there is no means to ensure that the chemical starting points in development work by a variety of molecular mechanisms.

In this study, we hypothesized that additional phenotypic assays might provide a means to group compounds that correlates with molecular mechanism, even if the molecular mechanism of a class of compounds is not known. Such a collection of assays with adequate throughput to be applied to a large number of *in vitro* inhibitors would provide important information for prioritizing early-stage inhibitors by aiding in

maintenance of a diverse portfolio of compounds in the pipeline. The Medicines for Malaria Venture (MMV) employs a similar approach for maintenance of the malaria drug pipeline (Burrows et al., 2017). Here, we present new moderate-throughput assays assessing compound effects on different life-cycle stages in a *C. parvum* tissue culture infection model, including assays for host cell invasion, intracellular DNA replication, parasite egress and reinvasion, and sexual differentiation. The methods were employed on a diverse set of compounds, and using the results from this panel of assays, we show that compounds are accurately clustered into different chemical and/or mechanistic groups. These data confirm that the approach enables maintenance of mechanistic diversity within the *Cryptosporidium* drug development portfolio. We also show that compounds targeting different life-cycle stages are active in a highly immunocompromised mouse model, which further supports the value of a diverse portfolio.

3.3. Results

Our overall strategy to determine if life-stage specific phenotypic assays enable classification of compounds according to chemical class/mechanism of action was to develop a panel of suitable assays and then use them to test a panel of "learning" compounds, which enabled subsequent clustering of compounds based on phenotype. The learning compounds used were from a variety of sources. For assay development and initial validation, publically available drug screening hits and anti-*Cryptosporidium* compounds disclosed in the literature were tested (e.g. from the Medicines for Malaria

Venture Open Access Box and the National Institutes of Health (NIH) Clinical Collection) (Bessoff et al., 2013; Bessoff et al., 2014; Jumani et al., 2018). To subsequently enlarge the database and determine if grouping compounds according to phenotype results in segregation of compounds by chemical class and/or mechanism of action, we also utilized proprietary compounds provided by collaborators within the Bill and Melinda Gates Foundation *Cryptosporidium* Drug Accelerator consortium. In most cases, these compounds were identified as *C. parvum* inhibitors by screening libraries of compounds partially developed for other indications (e.g. treatment of malaria, trypanosomiasis, tuberculosis, etc.), and many of these compounds had the advantage for purposes of our study that their likely molecular mechanisms of action are known (Castellanos-Gonzalez et al., 2013; Gorla et al., 2012; Jain et al., 2017; Kato et al., 2016; Love et al., 2017; Shibata et al., 2011).

As a first step in developing specific *Cryptosporidium* life-stage assays, we conducted a series of light microscopy time-lapse and transmission electron microscopy (TEM) timecourse experiments in order to precisely define *C. parvum* development in our hands in the HCT-8 cell culture system. Consistent with previously published studies, all life-cycle stages were observed, including development of type II meronts, macro- and micro-gametocytes, and rarely, even fertilization (Fig. 1). Although *Cryptosporidium* parasites in the HCT-8 cell culture system were not fully synchronized, initial excystation and cell invasion occured within an ~2.5 hour window, resulting in a roughly synchronized infection. This knowledge was exploited to modify a previously developed high-content microscopy assay to focus on major

life-stage events observed in the HCT-8 culture system; assays for host cell invasion, intracellular replication, host cell egress and establishment of new parasitophorous vacuoles, and sexual differentiation were developed (see light microscopy images or transmission electron micrographs (TEMs) in each assay figure) with the goal of enabling classification of multiple compounds to assist with drug development.

3.3.1. Host cell invasion assay

The first step in infection is host cell invasion and involves a complex phenotype encompassing oocyst excystation, parasite motility, adhesion, and ultimately parasitophorous vacuole formation (Fig. 2A). Our strategy to assay for invasion inhibitors was simply to expose *C. parvum* to compounds immediately after triggering excystation and throughout the invasion process, but with enumeration prior to allowing intracellular parasites to replicate (summarized in Fig. 2B). The resultant assay method was the same as a high-content microscopy assay method for *C. parvum* development that we published previously (Bessoff et al., 2013), except for the time points of compound addition and monolayer fixation. Like the prior method, this method has medium-throughput, and it has a Z' score of ≥ 0.2.

Neural Wiskott Aldrich syndrome protein (N-WASP) and Cdc42 pathway are important for the initial host cell actin remodeling required for *Cryptosporidium* parasitophorous vacuole formation (Chen et al., 2004), and the small molecule wiskostatin has been shown to inhibit purified N-WASP at 10 µM, including competitive inhibition of its activation by Cdc42 (Peterson et al., 2004). Therefore,

wiskostatin was used as a positive control for initial assay validation and optimization of the *C. parvum* invasion assay. Wiskostatin was active in the 48 hour *C. parvum* development assay with a 90% effective concentration (EC_{90}) of 11.3 µM. Wiskostatin also inhibited parasitophorous vacuole formation at this EC_{90} concentration, giving results similar to those obtained using heat-killed oocysts or fixed HCT-8 cells (Fig. 2C and 2D). As further proof-of-concept, confirmed *C. parvum* inhibitors from the MMV Malaria Box and commercially available chemical analogues of each (Supplementary Table 1) were tested at the EC_{90} concentration measured previously for each using the 48 hour *C. parvum* development assay (Fig. 2D). The anti-*C. parvum* 2,4-diaminoquinazolines inhibited host cell invasion, while allopurinol-, quinolinol-, and piperazine-based anti-*C. parvum* compounds had no effect on parasitophorous vacuole formation. The approved drug nitazoxanide and paromomycin, which is often used as a positive control in *Cryptosporidium* mouse models, also had no significant effect (Fig. 2D).

3.3.2. DNA replication assay

Following cell invasion, *Cryptosporidium* trophozoites grow and multiply to give rise to multinucleated type I meronts (Fig. 3A). The thymidine analog 5-ethynyl-2´-deoxyuridine (EdU) is efficiently incorporated into newly synthesized DNA, and can be readily detected using click chemistry (Salic & Mitchison, 2008). We therefore used EdU to measure parasite intracellular DNA synthesis, which is a surrogate for the more complex phenotype of intracellular growth and division. The approach for

differentially labeling newly synthesized parasite DNA compared to host cell DNA was to take advantage of the fact that *C. parvum* replicates more quickly than the nearly confluent host cells. Thus, by adding EdU for a short time period shortly before egress, it was possible to preferentially label replicating parasites (Fig. 3B and C). In contrast, DNA staining with Hoechst labelled all of the host and parasite DNA, making it challenging to visualize and quantify parasite DNA due to excessive host DNA. A simple DNA stain would also not distinguish pre-existing DNA from newly synthesized DNA (Fig. 3C). In contrast, EdU labeling only occurs with incorporation into newly synthesized DNA. Incorporated EdU was then easily stained for immunofluorescence and labeled parasites were quantified using high-content microscopy and an NIH ImageJ macro (Fig. 3C, DMSO condition). The thymidine analogue hydroxyurea (10 mM), a known inhibitor of DNA replication, was used as a positive control for assay validation. As expected, hydroxyurea at this concentration blocked both parasite and HCT-8 cell DNA replication (Fig. 3C). The MMV Malaria Box quinolinol series, compounds previously identified as selective *C. parvum* inhibitors, appeared to selectively block *C. parvum* replication (Fig. 3C and D). The 2,4-diaminoquinazolines (parent MMV006169), which all inhibited host cell invasion, had no effect on intracellular replication. Results for the other compounds tested were also consistent within chemical groups: the allopurinol-based chemical scaffold MMV403679 blocked *C. parvum* replication, while the piperazine-based scaffold (MMV665917) and paromomycin had no effect on EdU incorporation (Fig. 3D). As noted above, compounds with activity in this assay cannot be concluded to be DNA synthesis

inhibitors; rather, they affect at least one of the many things that DNA synthesis requires. Also, as is evident from the images, it would be feasible to enumerate the number of nuclei present in each vacuole to obtain subtler information; however, for the purpose of classifying compounds, we found that a readout based simply on *C. parvum* EdU counts normalized to total parasite numbers was readily automated using NIH ImageJ and worked well (Fig. 3D).

3.3.3. Parasite egress and host cell reinvasion assay

Type I meronts release motile merozoites that infect new HCT-8 cells and repeat the asexual replication cycle. We performed live microscopy on infected cells to visualize and better understand these processes in the *in vitro* assay system. There was modest experiment-to-experiment variation in the timing of events, with egress sometimes beginning as early as 12 h post infection and observed as late as 18 h post infection; within each experiment, the cultures were more synchronized with all egress occurring within an ~ 2.5 h time window. Individual *C. parvum* egress and reinvasion events were rapid, with parasitophorous vacuole rupture, merozoite release and re-attachment completed within 10 minutes. Re-infection was inefficient, and each parasitophorous vacuole egress event only produced ~ 2-3 new vacuoles (Fig. 4A, and Supplementary Video 1).

To identify a suitable positive control compound to aid in development of a quantitative assay, we reasoned that compounds active in the DNA replication assay would also inhibit this subsequent stage of parasite development. Thus, we used time-

lapse light microscopy to assess inhibition of cell egress by the allopurinol-based scaffold MMV403679 (C-1), which was active in the DNA replication assay. As anticipated, C-1 at the 2 × EC_{90} (1.3 μM total) inhibited parasite egress during live microscopy (Fig. 4B, and Supplementary Videos 2 and 3). Furthermore, based on the time-lapse observations, it was clear that in this crudely synchronized culture system parasite vacuole numbers did not increase smoothly; rather, vacuole numbers increased by ratcheting up by two to three-fold during the window of egress and infection of new host cells. This observation was confirmed by comparing parasite numbers in the presence of C-1 vs. the vehicle control at time points approaching and just following the approximate time of cell egress and reinvasion (Fig. 4C).

This observation suggested a less labor intensive method to estimate the effect of compounds on parasite egress and establishment of new parasitophorous vacuoles simply by measuring the ratio of the number of parasite vacuoles following and before the egress/reinvasion life-cycle stage (Fig. 4D). Time points of 19.5 h post-infection and 6 h post-infection were selected empirically. As seen in the timecourse experiment with the DMSO vehicle, the ratio of parasites at 19.5 hours to parasites at 6 hours ranged from 2.5 to 3-fold (Fig. 4C and 4E). Compounds acting at all stages up to and including parasite egress and reinvasion would be expected to reduce this ratio; furthermore, rapidly cidal compounds that act early, or compounds that permit egress but block subsequent reinvasion would result in a ratio below 1.

Given the complexity of this phenotype and the need to interpret the results in the context of the results of assays of earlier life-stages, it is not surprising that the

learner compounds tested resulted in a range of ratios. Wiskostatin, which here was added at three hours post-infection, following the invasion step, resulted in a ratio of almost precisely one. The allopurinol-based and quinolinol compounds consistently displayed ratios that were reduced but under 1, whereas the piperazines, 2,4-diaminoquinazolines, nitazoxanide and paromomycin all displayed ratios above 1. As with the other assays, the results were similar for all compounds within each chemical group. And, as expected, compounds acting at earlier stages showed at least some reduction in the ratio of vacuoles at 19.5 hours to vacuoles at 6 hours (Fig. 4E and Supplemental Table 2). This was especially evident for compounds such as the quinolinols and allopurinol-based compounds that blocked intracellular development, and likely occurred simply because no merozoites matured for egress.

3.3.4. Sexual differentiation assay

Unlike malaria parasites for which only a small fraction of blood stage parasites undergo sexual differentiation, *Cryptosporidium* is believed to undergo sexual differentiation in an obligate manner after only three to four rounds of asexual replication. Furthermore, a single host serves as the site of both asexual and sexual reproduction (i.e. is both the intermediate and definitive host) (Current & Reese, 1986). Therefore, although all of the early-stage drug leads studied to date for cryptosporidiosis were identified using assays that measure only effects on asexual development, it is theoretically possible to target sexual development for treatment of

cryptosporidiosis. Based on this logic, we sought a method to quantify *C. parvum* sexual differentiation.

3.3.4.1. Identification of DMC1 (cgd7_1690) as a marker for sexual stages

Based on the accepted *Cryptosporidium* life-cycle, *C. parvum* is haploid at all stages except for just after fertilization, at which time the diploid zygote quickly undergoes meiosis to give rise to haploid spores within thick and thin-walled oocysts that are either passed in the feces or excyst to perpetuate the infection (Current & Reese, 1986). Since meiosis only occurs following fertilization, we reasoned that genes encoding proteins specifically involved in meiosis might only be expressed in sexual forms of the parasite, including either the zygote or gamonts. Using gene expression data publically available via CryptoDB (http://cryptodb.org) (Mauzy, Enomoto, Lancto, Abrahamsen, & Rutherford, 2012), we selected the *DNA Meiotic Recombinase 1* gene, *DMC1 (cgd7_1690)*, as a likely candidate for use as a *C. parvum* sexual stage marker, since this gene increases in expression dramatically following ~48 of culture in HCT-8 cells and is also specific to *Plasmodium* sexual differentiation (Mlambo, Coppens, & Kumar, 2012). The predicted *C. parvum* DMC1 protein sequence is 99% identical to the predicted orthologous *C. hominis* (Chro.70199) protein, and the *C. parvum* protein sequence is 65% identical to the orthologue in *Plasmodium berghei* (PBANKA_0714000).

3.3.4.2. Validation of DMC1 in vitro

Real-time PCR (qRT-PCR) and transmission electron microscopy (TEM) were used to determine if *DMC1* expression correlated with the appearance of sexual-stage parasites in the HCT-8 culture system. To avoid slight variations in growth kinetics that occur between experiments, samples from neighboring wells of the same infection were analyzed, focusing on finer time-points around 48 h post-infection when gamonts were first expected to appear. *DMC1* expression was first detected at 42 h post-infection, simultaneously with the first appearance of gamonts seen by TEM (Fig 5A and 5B). DMC1 mRNA levels increased by > 100-fold between 36 hours and 72 hours of culture, and DMC1 mRNA was not detected in sporozoites or oocysts. Interestingly, *DMC1* expression decreased after peaking at 72 h post-infection.

An anti-*C. parvum* DMC1 mouse monoclonal antibody was produced in order to determine if DMC1 protein expression also correlated with the life-stages present in culture, and to generate a potential reagent to assay *C. parvum* sexual development by high-content immunofluorescence microscopy. A clear subset of parasite vacuoles stained positive for DMC1 at 72 hours post-infection, confirming the specificity of the reagent (Fig. 5C). DMC1 was detected exclusively in vacuoles that were not multi-nucleated, suggesting that it may be specifically expressed in macrogametocytes and/or fertilized zygotes. Immunogold staining and TEM with the anti-DMC1 antibody was unsuccessful, however, so the specific life-stage stained could not be determined with certainty. The timing of protein expression was similar to that of mRNA expression, with DMC1 positive parasites first detected at 42 h post-infection, peaking at 72 h post-

infection and then decreasing in number (Fig 5D). At peak expression levels, ~55 % of the lectin-positive parasites expressed DMC1.

3.3.4.3. Assay to identify inhibitors of asexual to sexual stage conversion

Based on the results above, we utilized DMC1 as a marker of *C. parvum* sexual development, and used the anti-DMC1 monoclonal antibody to develop a moderate-throughput high-content microscopy assay for characterizing anti-*Cryptosporidium* compounds (Fig. 6A). Since the percent of DMC1 positive parasites began to increase just prior to 48 hours after infection in the HCT-8 cell system, the strategy was to test the specific effect of compounds on sexual development simply by delaying addition of compounds until 48 hours post-infection and then monitoring the effect on the number of DMC1 positive parasites at 72 hours. Compounds with equal efficacy on the asexual and sexual stages would be expected to have equal potency both before and after 48 hours. The piperazine-based compound D1 (MMV665917) was such a compound (Fig. 6B). On the other hand, the 2,4-diaminoquinazoline B1 (MMV006169) was far less potent when used during the sexual phases of development (Fig. 6B), suggesting that it is relatively specific for asexual development. In practice, many compounds gave an intermediate phenotype with partial inhibition of DMC1 expression when added at 48 hours. Therefore, in order to enable numerical comparison of the ability of compounds to block sexual development with moderate throughput, we adopted a strategy of reporting the percent inhibition of DMC1 expression by the previously determined EC_{90} in the standard/asexual development assay (Fig. 6C and Supplementary Table 3).

3.3.5. Identification of hit diversity based on life-stage activity

A major goal of our study was to determine if compounds could be grouped by chemical class/mechanism of action using these phenotypic assays, in which case they could be used to maintain mechanistic diversity in the *Cryptosporidium* drug development pipeline even in the absence of knowledge of the molecular mechanisms of phenotypic screening hits. To test this idea, the panel of phenotypic assays described above was used to characterize a panel of fifty-five compounds, and the data were analyzed using a clustering algorithm based on the Ward error of sum of squares hierarchical clustering method with a distance matrix generated using Euclidean distances calculated for each compound with respect to another. Specific phenotypic assay data for each compound are given in Supplementary Table 3. The method separated the compounds into distinct clusters, grouping compounds based on the same chemical scaffold (i.e. presumed to have the same molecular MOA) and compounds known to work via the same/highly similar MOAs (e.g. compounds effecting a variety of tRNA-sythetases) (Fig. 7).

3.3.6. Correlation between *in vitro* assay activity and *in vivo* efficacy

It is feasible that *Cryptosporidium* is most susceptible to drug treatments that target a specific life cycle stage (e.g. the relatively prolonged intracellular growth and replication stage). Therefore, for the strategy of ensuring mechanistic diversity in the *Cryptosporidium* drug development pipeline based on activity against different life cycle stages, it was critical to determine if compounds belonging to different

phenotypic clusters (as in Fig. 7) could have *in vivo* efficacy. For this, a variety of compounds were tested in a mouse model of chronic *C. parvum* infection.

The factors that drive compound efficacy in a mouse model of cryptosporidiosis are not known. This is particularly complicated by the fact that, although drugs are obviously needed at the intestinal site of the infection, the precise pharmacokinetic properties desired for an effective drug are not certain and might vary based on the mechanism of action of different drugs. Furthermore, different animal models with varying stringency (e.g. self-resolving vs. chronic infection models) have been used for lead identification (Castellanos-Gonzalez et al., 2013; Gorla et al., 2014; Jumani et al., 2018; Love et al., 2017; Manjunatha et al., 2017; Ndao et al., 2013). To directly compare *in vivo* efficacy of compounds, we tested most of these compounds in the highly immunocompromised NOD SCID gamma (NSG) mouse model of established *C. parvum* infection. The *in vitro* and *in vivo* data provide a rich source to identify correlations between *in vitro* activity in these assays and *in vivo* efficacy in the NSG mouse model. Along with the above life cycle assays, we also tested all of the compounds in the previously reported *in vitro* parasite persistence assay to determine rate of parasite elimination *in vitro* (Jumani et al., 2018). While screening a larger number of compounds, we found the earlier definition of static versus cidal too simplistic. Compounds behaving like nitazoxanide were still classified as static, whereas compounds with an fast rate of parasite decay like in the case of MMV665917 were categorized as exponential inhibitors and compounds with a slow rate of parasite elimination similar to paromomycin were categorized as linear inhibitors

(Supplementary Table 3). There was no specific asexual stage assay that alone correlated with *in vivo* efficacy, and all of the compounds with *in vivo* activity had at least a partial activity in the asexual to sexual conversion assay. None of the static compounds were active in the NSG mouse model (Supplementary Table 3).

3.4. Discussion

We report a range of inexpensive medium-throughput *C. parvum* life stage assays that can be used to classify compounds quickly and obtain a diverse set, which can aid in prioritization of hits and leads for further drug development. We found a good correlation between variants within a chemical series, and for compounds with several putative mechanisms of action, including ATG-8 inhibitors, CDPK-1 inhibitors, and four different classes of tRNA synthetase inhibitors. And importantly, compounds belonging to numerous mechanistic clusters were effective in the NSG mouse model.

Currently, large-scale phenotypic screening efforts are ongoing to identify hits against *Cryptosporidium* (Chao et al., 2018; Love et al., 2017). There are no established methods to help prioritize these hits. In malaria drug development, stage specific assays have been used for prioritization of compounds, with distinct target candidate profiles based on rate of parasite elimination and stage specific activity (Burrows et al., 2017; Burrows, van Huijsduijnen, Mohrle, Oeuvray, & Wells, 2013; Delves et al., 2012). This strategy helps maintain diversity in the pipeline drug development pipeline and increases the chances of delivering quality preclinical candidates. This is particularly important in the case of malaria where drug resistance

is a major issue. We have already reported an *in vitro* parasite persistence assay to determine the rate of *C. parvum* elimination following compound exposure (Jumani et al., 2018). We believe these specific life stage assays are a quick, relatively inexpensive way to prioritize anti-*Cryptosporidium* hits in a manner similar to that used for malaria drug development. Genetic studies can then be done on a smaller set of promising leads to identify the targets (Pawlowic et al., 2017).

The set of 55 compounds used here is relatively small to draw correlations between *in vitro* assays and *in vivo* efficacy, especially without considering the PK properties of the compounds. However, this is the first report of directly comparing *in vivo* efficacy with *in vitro* assays for such a large number of anti-*Cryptosporidium* hits. These data can be used to understand factors critical for *in vivo* efficacy in the absence of an effective benchmark drug. These correlations can be better understood with an increase in the number of compounds, and with human and calf model clinical efficacy data. Apart from the life stage assays, pharmacodynamic parasite persistence assay and PK considerations, several other factors like an effect on microbiome could drive *in vivo* efficacy and should be measured (Gorla et al., 2014). These assays are not an exhaustive list, but rather should be used as a starting point.

To directly compare all compounds irrespective of potency, the EC_{90} concentration from our standard asexual inhibition assay was used in all life stage assays. A single EC_{90} concentration was chosen to determine the predominant effect of the compound on parasite life stage with a goal to directly compare compounds to attain diversity in a relatively quick and inexpensive manner using small quantities of

compounds. It is possible that at higher concentrations, compounds would be active against more than one stage. For compounds of high interest, it may be worth following up with dose response curves for all life stage assays.

With the idea to develop a medium-throughput assay along with the technical difficulties involved, the invasion assay protocol exposes sporozoites directly to compounds for a fleeting time. The design of the assay makes it easier to identify compounds that inhibit invasion by acting on host cells and this should be kept in mind when interpreting this assay's results. Interestingly, none of the compounds active in the invasion assay were efficacious in the NSG mouse model. This could be due to a small sample size of compounds tested and should not be interpreted as evidence that invasion inhibitors are inactive *in vivo* against cryptosporidiosis.

Compounds with activity against any process post-invasion and not just replication inhibitors are expected to be active in the DNA synthesis assay. Hence, one potential reason that all the aminoacyl tRNA synthetase inhibitors were potent in this assay could be that they are all lethal to the parasite before it incorporates EdU. N-WASP and host actin re-modeling are important for intracellular *Cryptosporidium*, in addition to their role in host cell invasion (Elliott et al., 2001). It is not surprising, therefore, that wiskostatin was active in both the DNA synthesis assay and the invasion assay.

Interestingly, all compounds had some activity, but to varying extents in the egress, merozoite motility and reinvasion assay. A ratio of less than one would signify disintegration of existing vacuoles without egress and/or egress without formation of

new vacuoles. The 2,4-diaminoquinazolines were potent sporozoite invasion inhibitors but had a ratio of greater than 1, suggesting that they do not affect merozoite invasion as efficiently. Using the parasitophorous vacuole number ratio was useful to classify compounds based in a higher throughput manner. Nonetheless, these data can be used to further investigate specific mechanisms. For example, a sub-set of compounds could be used in the live egress assay set-up to identify if egress or merozoite release, motility or reinvasion is specifically affected.

We have shown that *in vitro C. parvum DMC1* mRNA and protein expression coincides with appearance of sexual gamont stages in HCT-8 cells. Although a strong correlation between appearance of gamonts and DMC1 has been demonstrated, it is only correlative. Since immunogold staining with this antibody failed, and there are no other tools to label *C. parvum* gamonts, we cannot determine the specific parasitic stage wherein DMC1 appears. Our data show that at 72 h, when 80 % of the parasites were gamonts by TEM, ~55 % of parasites were DMC1 positive by immunofluorescence. Added on, DMC1 is not expressed in multinucleated cells. Microgamonts are multinucleated due to multiple microgametes per vacuole. Assuming microgamont nuclei get stained with Hoechst, DMC1 is not expressed in microgamonts, leaving the only possibility being fertilized or non-fertilized macrogamonts. The fertilization of a macrogamont is considered a rapid process, as only the macrogamonts or early oocysts can be predominantly imaged by TEM with an intermediate containing a distinguishable macrogamete nucleus very rarely seen. Hence, the *C. parvum* DMC1 could be expressed in a fertilized or non-fertilized macrogamont. Given the role of the

conserved DMC1 during meiosis in other organisms, it is possible that DMC1 expression comes up after fertilization and fusion of the macrogamete nucleus with the macrogamont nucleus, making DMC1 a marker for fertilization. On the other hand, DMC1 could be pre-expressed in macrogamonts to facilitate rapid fertilization and oocyst formation, giving the parasite an advantage for rapid turnover and re-infection. Either way, these raise very interesting possibilities about the biology of *Cryptosporidium*. The identification of DMC1 as a marker for the appearance of gamonts makes it more feasible to explore the sexual stage biology of *Cryptosporidium*. Until now there has only been a screening assay to predominantly look at asexual stage inhibitors, but with the DMC1 antibody a high-throughput screening assay can be developed for the first time to identify potential sexual stage inhibitors. Apart from drug candidates, the results can potentially yield invaluable tool compounds to explore *Cryptosporidium* biology.

This is a first report of dose response curves against asexual to sexual stage conversion. It was interesting to find compounds with similar potency against the asexual stages and DMC1 assay. Partial inhibitors are more difficult to interpret, as the *C. parvum in vitro* growth assay is a mixed and asynchronized culture with a combination of asexual and sexual stages present. The DMC1 assay was designed such that compounds were added after about 20% gamonts were already formed. Therefore, compounds with pan activity against both stages are expected to completely inhibit DMC1, whereas fast acting compounds with activity against asexual stage parasites still present at 48 h might appear to partially affect sexual development. Furthermore, it is

not clear if a drug needs to be active against the asexual and sexual stages of the parasite, or if activity against any one stage is sufficient. It was interesting to note that all the compounds that were active *in vivo* in the NSG mice had some activity in the DMC1 assay. It would be interesting to identify pure inhibitors of sexual development and test if they would be active in the NSG mouse model.

In summary, we report and validate a range of medium-throughput *in vitro* life stage assays, including an asexual to sexual stage conversion assay. This panel of assays can form the basis to directly compare compounds, thereby obtaining diversity and aiding prioritization at an early stage of *Cryptosporidium* drug development.

3.5. Methods

3.5.1. Cell culture and *C. parvum* excystation and infection

HCT-8 cells were purchased from ATCC and cultured in ATCC modified RPMI-1640 medium (Invitrogen), supplemented with 10% heat-inactivated fetal bovine serum (Sigma-Aldrich) and 120 U/mL penicillin and 120 µg/mL streptomycin (ATCC) (culture media). For dose response assays using DMC1, amphotericin B at 0.5 µg/mL was included in the culture media. For all experiments, HCT-8 cells between passages 9 and 39 were used. *C. parvum* oocysts were purchased from Bunchgrass Farms, stored at 4°C and used within 5 months of being shed. Oocyst excystation was performed as described previously (Bessoff et al., 2013). Briefly, oocysts were first treated with 10 mM hydrochloric acid for 10 min at 37°C, spun at 14000 g for 4:30 min at room

temperature, then treated with 2 mM sodium taurocholate for 10 min at 16°C, spun as before and resuspended in culture media for infection.

3.5.2. Invasion assay

C. parvum invasion inhibition was measured by modifying a previously described immunofluorescence assay (Bessoff et al., 2013). HCT-8 cells at >99% confluence in 384-well plates were pre-treated with 2 × EC_{90} concentration of compounds for 1 h before infection with parasites. In the meantime, Iowa strain oocysts were excysted. To each well, 49500 oocysts triggered for excystation were added to HCT-8 cell monolayers containing DMSO or compounds diluted to a final concentration of EC_{90} with the addition of oocysts. Plates were incubated at 37°C and 5% CO_2 for 3 h. Wells were then washed 3 times with PBS containing 111 mM D-galactose (PBS-D-gal), fixed with 4% paraformaldehyde (PFA) in PBS for 15 mins at room temperature, permeabilized with 0.25% Triton X-100 for 10 mins at 37°C, washed 3 times with PBS with 0.1% Tween 20, and blocked with 4% bovine serum albumin (BSA) in PBS for 2 h at 37°C or 4°C overnight. Parasitophorous vacuoles were stained with 1.33 µg/mL of fluorescein-labeled *Vicia villosa* lectin (Vector Laboratories) diluted in 1% BSA in PBS with 0.1% Tween 20 for 1 h at 37°C, followed by addition of Hoechst 33258 (Anaspec) at 0.09 mM diluted in water for another 15 mins at 37°C. Wells were then washed 5 times with PBS containing 0.1% Tween 20. A Nikon Eclipse Ti2000 epifluorescence microscope with an automated stage was programmed using NIS-Elements Advanced Research software (Nikon, USA) to focus

on the center of each well and take a 3×3 or 6×6 composite image using an EXi blue fluorescence microscopy camera (QImaging, Canada) with a 20X objective (NA = 0.45). Nuclei and parasite images were separately exported as .tif files and analyzed using macros developed on the ImageJ platform (National Institutes of Health) (Bessoff et al., 2013). The only modification from the published macro used to count parasites was that the lower size threshold for parasites was decreased from 16.5 to 4 pixel (1 pixel = 0.65 µm). The same microscope, camera and softwares were used for all immunofluorescence assays.

3.5.3. DNA synthesis assay

Glass bottom 96 or 384 well plates were coated with 50 µg/mL fibronectin (BD Pharmingen) as per manufacturers protocol. HCT-8 cells were grown to greater than 90% confluence in the coated glass bottom plates. Oocysts at a concentration of 55000 per well were triggered for excystation and added to cells. After allowing 3 h for invasion, cells were treated with EC90 concentration of compounds for 6 h followed by addition of 10 mM 5-ethynyl-2´-deoxyuridine (EdU). After incubation of cells with EdU for 2 h, cells were washed 3 times with PBS-D-gal and then fixed with PBS containing 4% PFA. Cells were then permeabilized and stained for EdU using the Click-iT® assay kit (Thermo Fisher Scientific) as per manufacturers indication. Cells were then imaged using a 40X air objective (0.7 NA) and EdU and lectin numbers quantified using ImageJ software and developed macros (Supplementary Method 1).

3.5.4. Time-lapse light microscopy for visualizing live *C. parvum* egress

Glass bottom 60 mm MatTek dishes (MatTek) were first coated with 50 µg/mL fibronectin (BD Pharmingen) as per manufacturer's protocol and then HCT-8 cells were grown to >95% confluence before infecting each MatTek dish with 48×10^4 oocysts that had been triggered for excystation. Cells were then imaged live with 5 min intervals using a DIC phase and a 60X oil objective (1.4 NA). For effect of compound C-1 on egress using live microscopy, 16 well polystyrene dishes (Greiner Bio-One™) were similarly coated with 50 µg/mL fibronectin (BD Pharmingen). HCT-8 cells were grown to >95% confluence before infection with 15×10^4 oocysts triggered for excystation. After 3 h cells were gently washed with warm complete media to remove oocysts shells before compound or DMSO addition. Large 2×2 images were taken live with 20 min intervals using a 40X air objective (0.7 NA) to visualize live egress.

3.5.5. Egress, motility, reinvasion assay

For quantification of parasitophorous vacuoles for timecourse experiment and ratio experiment, HCT-8 cells were grown to greater than 90% confluence in 384 well plates and infected with 11000 oocysts after they were triggered for excystation. Compounds at EC_{90} concentration were added to cells 3 h after infection and cells were washed, stained and imaged at different time points using the same protocol as mentioned in the invasion assay.

3.5.6. *C. parvum DMC1 (cgd7_1690)* identification

The predicted protein sequence of *Plasmodium berghei DMC1* was obtained from PlasmoDB (plasmodb.org), the free online *Plasmodium* genome database, and a protein BLAST against *C. parvum* genome was perfromed using the default settings in the free online *Cryptosporidium* genome database, CryptoDB (http:cryptodb.org).

3.5.7. Quantitative Real-time PCR

HCT-8 cells were seeded into 12 well culture plates (Corning) and grown to greater than 90 % confluence. Oocysts at a concentration of 1.92×10^5 oocysts per well were excysted and added to cells. Infected HCT- 8 cells were then incubated for varying lengths of time post-infection until RNA extraction was performed.

At given time points, infected cells were trypsinized, pelleted and RNA extracted as previously described (Hobbs et al., 2014). Briefly, infected cell pellets were homogenized with TRIzol™ (Invitrogen), treated with chloroform, and then RNA precipitated with ethanol. RNA was purified using RNeasy kit (Qiagen) according to manufacturer's protocol, and quantitated using NanoDrop. Superscript III First-Strand Synthesis System for RT-PCR (Invitrogen) was used to convert 730ng of RNA per sample into cDNA following the manufacturer's protocol. To amplify cDNA samples, a BIO-RAD CFX96 real-time PCR machine was used with iTaq™ Universal SYBR® Green Supermix (BIO-RAD) following the manufacturer's protocols including melting curve analysis. Real-time PCR primers were designed for *DMC1* (*cgd7_1690*) using IDT's real-time primer design tool, and the sequences used are as follows: forward

sequence- GTTGATGGGCGGATTTGAAAG, reverse sequence- AACAGACTTTCCCATTACCTCC. The expression of the *DMC1* (*cgd7_1690*) gene was normalized to *C. parvum* 18s rRNA using the delta CT method (Rider et al., 2005).

3.5.8. Transmission electron microscopy

HCT-8 cells were grown and infected with *C. parvum* oocysts as mentioned above for real-time PCR. Infected cells were harvested at specific time points using trypsin, pelleted and fixed in preparation for electron microscopy as previously described, with minor modifications, including substitution of 0.1 M cacodylate buffer for millonig phosphate buffer. In short, pelleted cells were fixed for 1 h at 4°C using half-strength Karnovsky's fixative (1% Paraformaldehyde, 2.5% Glutaraldehyde in 0.1 M cacodylate buffer (pH 7.2)), embedded in 2 % agarose, crosslinked with Karnovsky's fixative, and post-fixed with 1 % Osmium tetraoxide (Barkhuff et al., 2011). Samples were then dehydrated with increasing amounts of ethanol, followed by propylene oxide (PO), and then infiltrated gradually from PO into Spurr's resin, embedded and polymerized. Semi-thin sections (1 mm2) were cut with glass knives on a Reichert Ultracut microtome. Ultra-thin sections (60-80 nm) were cut with a diamond knife, retrieved onto 200 mesh copper grids, contrasted with uranyl acetate (2% in 50% ethanol) and lead citrate, and examined with a JEM 1400 transmission electron microscope (JEOL USA, Inc, Peabody, Mass) operating at 80 kV.

3.5.9. DMC1 Immunofluorescence microscopy

Monoclonal antibody production in mice was contracted out to GenScript who generated antibodies using recombinant *C. parvum* DMC1. Several monoclonal antibodies were screend by immunofluorescence microscopy with clone 1H10G7 giving the best signal.

Greater than 90 % confluent HCT-8 cells grown in fibronectin coated 60 mm glass bottom dishes (MatTek) were infected with excysted oocysts for specified amounts of time. Oocysts at 1e6 oocysts per dish were taken for excystation. At given time points post-infection, infected cells were washed 3 times with PBS containing 111 mM of D-galactose, fixed for 15 min at room temperature with 4 % paraformaldehyde in PBS, and permeabilized with 0.25 % triton X-100 in PBS for 10 min at 37°C. Cells were then washed 3 times with PBS and blocked at least overnight at 4°C with 1 % BSA in PBS (block). Cells were stained with monoclonal antibody (1H10G7), either neat culture supernatant or 12.8 µg/mL of purified protein in block for 1 h at 37°C, followed by 2 washes with PBS. Cells were then co-stained with goat anti-mouse Alexa fluor 568 (Invitrogen) and 1.33 µg/mL fluorescein labeled *Vicia villosa* lectin (Vector Laboratories) diluted in block for 1 h at 37°C. Stains were then removed and 0.09 mM Hoechst 33258 (Anaspec) also diluted in block added for another 15 min at 37°C, followed by 2 PBS washes and imaging on Nikon Eclipse Ti2000 epifluorescence microscope run with NIS-Elements Advanced Research software (Nikon, USA) and equipped with EXi blue fluorescent microscopy camera (QImaging, Canada). For counting, large 2 × 2 images with 15 % overlap were taken using a 40X

air objective (0.7 NA), and for finer details Z stack images taken using a 60X oil objective (1.4 NA). Lectin positive cells in focus were first counted, followed by DMC1.

For compound dose response studies, assays with similar protocol were performed in 384 well plates and imaged using a 20X air objective (NA = 0.45) with 4 × 4 binning, and large 4 × 4 to 6 × 6 images were taken using an automated stage. Images were analyzed using ImageJ software and the macro developed (Supplementary Method 2).

3.5.10. Clustering analysis

Life stage assay results were compiled into a data frame of continuous variables (see Supplemental Table 3). For each assay, data was scaled about the mean for that particular assay. Scaled data was then used to find the Euclidean distances of each compound from other compounds and generate a distance matrix for the entire data frame. The distance matrix was then used to generate a dendrogram using the Ward error sum of squares hierarchical clustering method as defined by Ward in 1963 (Ward Jr, 1963) and improved upon by Murtagh and Legendre (Murtagh, 2014). A code was developed and run using R studio (Supplementary Method 3). Label coloring is only included for identification purposes, and has no influence on cluster composition in the generated dendrogram.

3.5.11. Mouse model of chronic *C. parvum* infection

The animal care guidelines were strictly followed for all animal studies, and were performed only after obtaining approval by the University of Vermont Institutional Animal Care and Use Committee.

NOD SCID gamma mice studies were performed as previously described (Jumani et al., 2018). Mice that were 3 weeks (± 3 days) of age were purchased from Jackson Laboratories, allowed to acclimatize for one week, and then infected with 100000 oocysts per mouse. Oocyst shedding in feces was monitored by qPCR for 18s rRNA. DNA was extracted by the Omega bio-tek's E.Z.N.A. stool DNA kit per the manufacturer's protocol, with a modification of initialy using 6 flash freeze and thaw cycles in liquid nitrogen to disrupt oocysts. Different amounts of oocysts were spiked in feces, followed by DNA extraction and qPCR to generate a standard curve, which was run each time and used to calculate oocyst shed per mg feces. Mice consistently started shedding detectable oocysts in feces by qPCR 6 days after infection. Hence, mice were treated twice daily with 50 mg/kg of compounds by oral gavage from 7^{th} day after infection for 4 days, and oocysts shedding in feces was monitored every day after onset of treatment. Relapse was tested for 7 days after cessation of treatment. Based on power calculations using Statistical Solutions, LCC's software, 4 mice per group were used to obtain at least 50% reduction in parasite infections with a power of 80%.

3.6. Supplementary Methods

3.6.1. Supplementary Method 1. ImageJ macro for quantification of DNA synthesis assay.

```
Title = getTitle();
Title = replace(Title, ".tif", "");
run("Stack to Images");
rename ("lectin-"+Title);
selectWindow(Title+"-0001");
rename ("edu-"+Title);
run("Enhance Local Contrast (CLAHE)", "blocksize=9 histogram=256 maximum=3
mask=*None*");
run("Enhance Local Contrast (CLAHE)", "blocksize=9 histogram=256 maximum=3
mask=*None*");
run("Subtract Background...", "rolling=1");
setAutoThreshold("Default dark");
//run("Threshold...");
setThreshold(3000, 65535);
run("Convert to Mask");
selectWindow("lectin-"+Title);
run("Subtract Background...", "rolling=15");
setAutoThreshold("Default dark");
//run("Threshold...");
setThreshold(400, 65535);
run("Convert to Mask");
run("Fill Holes");
run("Watershed");
run("Analyze Particles...", "size=50-Infinity circularity=0.50-1.00 show=[Count
Masks] display clear summarize in_situ");
setAutoThreshold("Default dark");
//run("Threshold...");
setThreshold(0, 0);
run("Create Selection");
selectWindow("edu-"+Title);
run("Restore Selection");
run("Clear", "slice");
run("Select None");
run("Analyze Particles...", "size=3-Infinity circularity=0-1.00 show=Outlines display
clear summarize in_situ");
```

3.6.2. Supplementary Method 2. ImageJ macro for quantification of DMC1 in the asexual to sexual conversion assay.

```
Title = getTitle();
Title = replace(Title, ".tif", "");
run("Stack to Images");
rename ("nuc-"+Title);
run("Subtract Background...", "rolling=15");
run("Unsharp Mask...", "radius=3 mask=0.70");
//run("Threshold...");
setAutoThreshold("Huang dark");
run("Convert to Mask");
run("Watershed");
run("Analyze Particles...", "size=40-Infinity show=Outlines display clear summarize
in_situ");
selectWindow(Title+"-0002");
rename ("lectin-"+Title);
selectWindow(Title+"-0001");
rename ("dmc1-"+Title);
run("Subtract Background...", "rolling=1");
setAutoThreshold("Huang dark");
//run("Threshold...");
setThreshold(373, 16383);
run("Convert to Mask");
run("Fill Holes");
run("Watershed");
selectWindow("lectin-"+Title);
run("Subtract Background...", "rolling=1");
setAutoThreshold("Huang dark");
//run("Threshold...");
setThreshold(1300, 16383);
run("Convert to Mask");
run("Fill Holes");
run("Watershed");
run("Analyze Particles...", "size=2-50 circularity=0.06-1.00 show=[Count Masks]
display clear summarize in_situ");
setAutoThreshold("Huang dark");
//run("Threshold...");
setThreshold(0, 0);
run("Create Selection");
selectWindow("dmc1-"+Title);
run("Restore Selection");
run("Clear", "slice");
```

```
run("Select None");
run("Analyze Particles...", "size=0-Infinity circularity=0.5-1.00 show=Outlines display
clear summarize in_situ");
run("Images to Stack", "name=[] title=[] use");
```

3.6.3. Supplementary Method 3. Code used for clustering analysis using R studio.

```
#For generating Dendrograms

setwd("WORKING DIRECTORY HERE") #working directory
library(xlsx)           #Importing relevant libraries
library(ggplot2)
library(magrittr)
library(cluster)
library(graphics)
library(fpc)
library(RColorBrewer)
library(pvclust)


##### Data Import ######

comp_df<-data.frame(read.xlsx("FILE NAME.xlsx",
                        sheetName = "SHEET NAME", header = TRUE, rowIndex =
c(4:59),  colIndex = c(2:9)))



names(comp_df)<-c("Name","Lab Code", "Mechanism", "ID", "Invasion", "DNAsyn",
"Motility", "SexDiff")

##### Data Cleaning ######


##Preparing Data for Dendrograms

char_list<-vector(mode = "integer", length = 33)  #Empty vector to hold count values
letter_list<-c("A","B","C","D","E","F","G","H","I","J","K",
            "L","M","N","O","P","Q","R","S","T","U","V",
            "W", "X", "Y", "Z", "AA", "AB", "AC", "AD",
```

```
            "AE", "AF", "AG") #Possible Groups, this needs additions if more groups
emerge
for(x in comp_df[,3]){  #Counting group ID occurances
  char_list[which(x == letter_list)] <- char_list[which(x == letter_list)] + 1
}

repeated_values<- letter_list[which(char_list > 1)] #List of repeated groups

i<-1
for(y in comp_df[,3]){  #IDs compounds belonging to a group

  if (y %in% repeated_values){
    comp_df[i,9]<-which(as.character(repeated_values) == as.character(y))
  }else{
    comp_df[i,9]<-0
  }
  i <- i + 1
}

### Graphs Generation ###

labelColors = c("#0000FF", "#FF3030", "#228B22", "#D15FEE", "#00CED1",
"#8B7355", "#E67732", "#AD00FA", "#FEFF0E" ) #blue, red, green, orchid, turquoise,
brown, purple, bright yellow

colLab <<- function(n) {      #Function for coloring labels and assigning compund
names as labels
  if(is.leaf(n)) {
    a <- attributes(n)
    attr(n, "nodePar") <-c(a$nodePar, list(lab.col = labelColors[which(repeated_values
== as.character(comp_df[a$label,3]))], lab.font = 2))
    attr(n, "label") <- as.character(comp_df[a$label,1])
  }
  n
}

cluster_counts<- c(2,3,4,5,6,7) #Number of Clusters

clust_df=dist(comp_df[,c(5:8)], method = "euclidean") #distance matrix with euclidean
values

dendro_df<-hclust(clust_df,method = "ward.D2")%>% as.dendrogram()

##### Scaling Data Frames #####
```

```
comp_mean<-apply(na.omit(comp_df[5:8]), 2, mean)
comp_sd<-apply(na.omit(comp_df[5:8]), 2, sd)
comp_max<-apply(na.omit(comp_df[5:8]), 2, max)
comp_min<-apply(na.omit(comp_df[5:8]), 2, min)
comp_mad<-apply(na.omit(comp_df[5:8]), 2, mad)

comp_df_scaled<-data.frame(scale(na.omit(comp_df[5:8]), center = comp_mean, scale
= comp_sd))
comp_df_scaled<-cbind(na.omit(comp_df[which(!is.na(comp_df$DNAsyn)),1]),
comp_df_scaled)

clust_scaled_dist<-dist(comp_df_scaled, method = "euclidean")

dendro_scaled_dist<-hclust(clust_scaled_dist, method = "ward.D2") %>%
as.dendrogram()


##### Dendrograms #############

par(mar = c(8, 4, 5, 17))  #margins

plot(dendrapply(dendro_scaled_dist, colLab), horiz = TRUE,
    main = "Using Numerical Data Scaled about the mean\n Euclidean Distances
\nWard Method\nEgress Ratio",
    xlab = "Distance Between Clusters")
```

3.7. Acknowledgements

Although too many to name individually, we thank all our collaborators for sharing their hits and leads for testing in our assays and members of the Bill and Melinda Gates *Cryptosporidium* consortium for their helpful discussions. This work was funded by grants from PATH, Bill and Melinda Gates Foundation and R21 from NIH. We also thank the University of Vermont's microscopy core facility for all their help with electron microscopy experiments.

3.8. Figure Legends

Figure 1. Transmission electron microscopy timecourse showing *C. parvum* life cycle stages present in the HCT-8 cell culture system. *C. parvum* Iowa oocysts purified from calf feces were artificially excysted in vitro and used to infect HCT-8 monolayer. Parasite was allowed to grow and at different time points from 12 h to 96 h post-infection, cells were analyzed by transmission electron microscopy (TEM) to visualize different stages of the parasite life cycle observed in our culture system.

Figure 2. Invasion Assay. (A) Demonstration of the parasite stage investigated during the invasion assay using representative TEM images of *C. parvum* Iowa oocysts and infected HCT-8 cells (Scale = 500 nm for oocysts image and 2 µm for image with infected cell). (B) Schematic of experimental design. Confluent HCT-8 monolayers were treated with 2 × EC_{90} of compounds for 1 h followed by infection with oocysts triggered for excystation. Oocysts were allowed to excyst to release sporozoites for invasion of HCT-8 cells to form parasitophorous vacuoles for 3 h in presence of EC_{90} concentration of compounds, following which cells were washed, fixed, stained, imaged and counted. (C) Representative images of invaded parasites stained with *Vicia villosa* lectin (green) and host cell nuclei (blue) after treatment with DMSO control or EC_{90} concentration (11.34 µM) of wiskostatin. Scale = 10 µm. (D) Quantified results for various controls and compounds identifying 2,4-diaminoquinazoline series from MMV Malaria Box to be potent inhibitors of invasion. Each point represents the mean and SD of at least 2 biological replicates with 4 technical replicates per experiment.

Figure 3. DNA Synthesis Assay. (A) TEM images of *C. parvum* infected HCT-8 cells demonstrating parasite processes measured by the DNA synthesis assay (Scale = 500 nm). (B) Overview of the experimental methodology. Confluent HCT-8 cell in glass bottom plates were infected with *C. parvum*, and following invasion compounds were added at EC_{90} concentration. At 9 h post-infection, 10 µM EdU was added for another 2 h and then cells were washed, fixed, stained and imaged. (C) Representative 40X air images of parasitophorous vacuoles (green), nuclei (blue) and EdU (magenta) after treatment with DMSO, EC_{90} concentration (1.33 µM) of quinolinol A-6, or 10 mM hydroxyurea. Scale = 5 µm. (D) EdU incorporation was quantified demonstrating quinolinols and allopurinol-based series effect process that lead to inhibition of DNA synthesis. Data are mean and SD of at least 2 independent experiments, except for paromomycin, 2,4-diaminoquinazolines and D-44 wherein data represents mean from one experiment. ND represents data not determined.

Figure 4. Assay to measure parasitophorous vacuole (PV) egress, merozoite motility and reinvasion to form new parasitophorous vacuole. (A) Live microscopy DIC images taken using 60X oil objective displaying rapid events of parasitophorous vacuole (PV) egress to release motile merozoites that re-invade neighboring HCT-8 cells to form a new infection. Scale = 5 µm. (B) Live microscopy 40X air DIC timecourse images of *C. parvum* parasitophorous vacuoles in presence of allopurinol-based C-1 scaffold at 2 × EC_{90} concentration (1.3 µM) or matched DMSO

control. Scale = 10 µm. (C) Timecourse infection experiment in the presence of DMSO or allopurinol-based scaffold C-1 at EC_{90} or 2 × EC_{90} concentration measuring parasitophorous vacuole numbers over time by immunofluorescence microscopy. Data points are mean and SD, n=4, representative of 3 independent experiments. (D) Outline of the experimental design. Infected HCT-8 cells were treated with EC_{90} concentration of compound 3 h after infection and parasitophorous vacuole numbers counted before egress at 6 h (count 1), and after egress at 19.5 h after infection (count 2) by immunofluorescence microscopy and ImageJ macro. Parasitophorous vacuole ratio of count 2 by count 1 taken for all compounds as a read out for the assay. (E) Quantification of ratio of parasitophorous vacuole numbers showing all compounds inhibited parasite numbers compared to DMSO, but to varying degrees with good correlation observed within chemical series. Data combined from at least 2 independent experiments with 4 technical replicates each, mean and SD shown.

Figure 5. *DMC1* (*cgd_1690*) mRNA and protein expression correlates with appearance of sexual stages. Confluent HCT-8 cells grown in 12 well plates were infected with excysted *C. parvum* oocysts for different amounts of time before harvesting cells for (A) isolation of RNA followed by quantitative reverse transcription PCR (qRT-PCR) to quantify expression of *C. parvum DMC1* (*cgd7_1690*) relative to 18s RNA, and (B) transmission electron microscopy (TEM) to visualize stages of parasitic vacuoles at given times. To get a more specific time-frame correlation, both (A) and (B) were analyzed from the same experiment, and the data are representative of

2 independent experiments. Scale bar = 500nm. Mouse monoclonal antibodies were raised against recombinant *C. parvum* DMC1 and used for immunofluorescence staining in in (C) and (D). (B) and (C) Infected HCT-8 monolayers were harvested at different time points, fixed and stained for total parasitic vacuoles with *Vicia villosa* lectin (green), for nuclei with Hoechst (blue), and DMC1 (red). (B) Higher resolution images taken with a 60X oil immersion objective showing representative vacuoles with DMC1 (red) expression absent in multi-nucleate parasitic vacuoles at 72 h post-infection. Scale bar = 5 μm. (C) Large 2 × 2 images were taken using a 40X air objective as described in materials and methods for counting total and DMC1 positive parasitic vacuoles. Data combined from 2 biological experiments with at least 127 (except 14 h, where n=92) lectin positive vacuoles per experiment were considered for counting DMC1 positive parasites per time point.

Figure 6. Assay to Measure Asexual to Sexual Stage Conversion. (A) Schematic demonstrating experimental overview for compound dose response studies against asexual to sexual stage conversion as measured by DMC1. HCT-8 cells were infected for 48 h, followed by addition of compound for another 24 h. Cells were then washed, fixed, stained, imaged and parasites counted. (B) Dose repose curves against the asexual stage as measured by the regular 48 h infection assay using *V. villosa* lectin, compared with DMC1 inhibition in the asexual to sexual stage conversion assay for piperazine, D-1 and 2,4-diaminoquinazoline, B-1. The mean and SD from at least 2 biological replicates with 4 technical replicates per experiment are shown.

Figure 7. Clustering Analysis of Life Stage Assay Results for 55 Anti-*Cryptosporidium* hits. Results from the life stage assays were used to calculate a distance matrix using Euclidean distances followed by clustering to generate a dendorgram using the Ward error sum of squares hierarchical clustering method as described in the methods section. Compound classes are shown in colors, whereas single compounds with no related variants are shown in black.

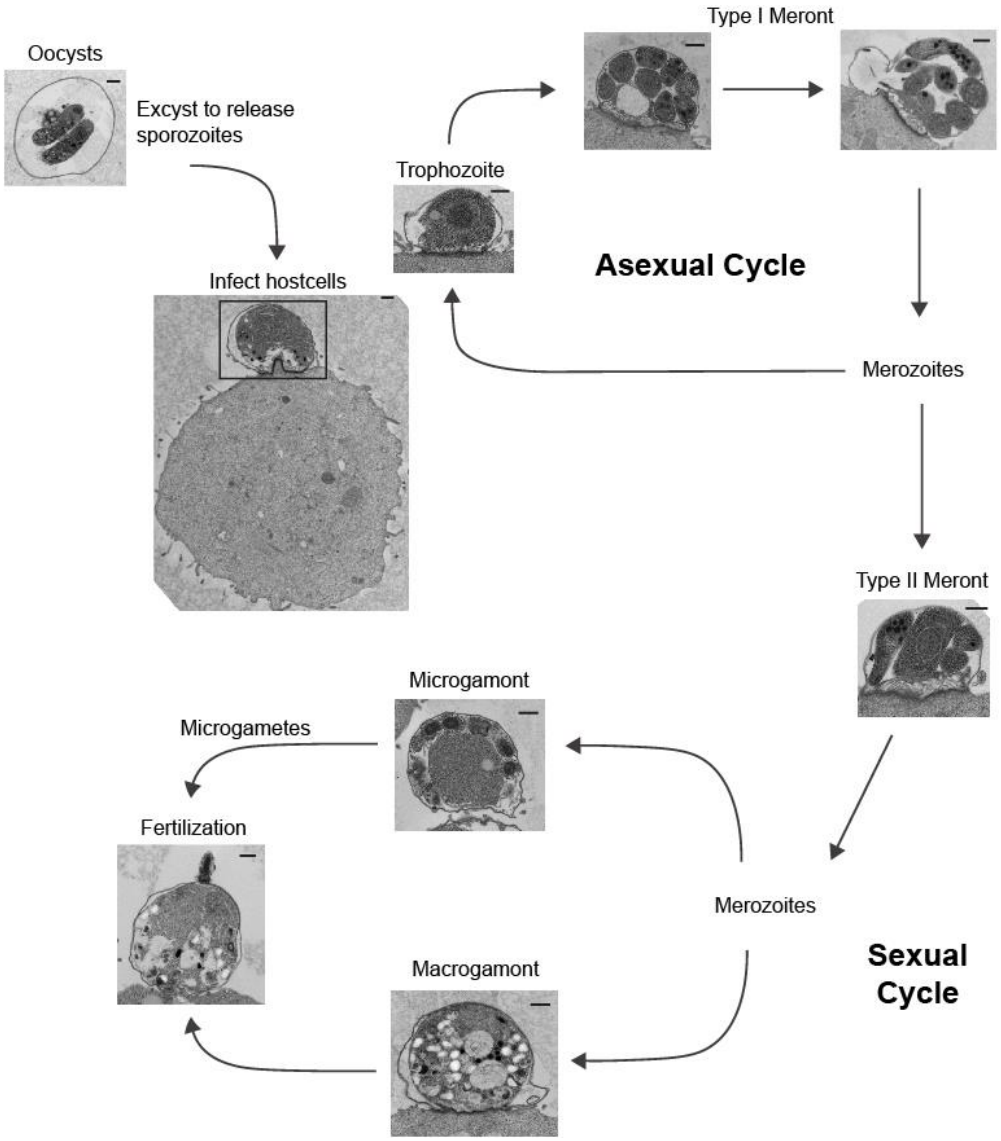

Figure 1. Transmission electron microscopy timecourse showing *C. parvum* life cycle stages present in the HCT-8 cell culture system.

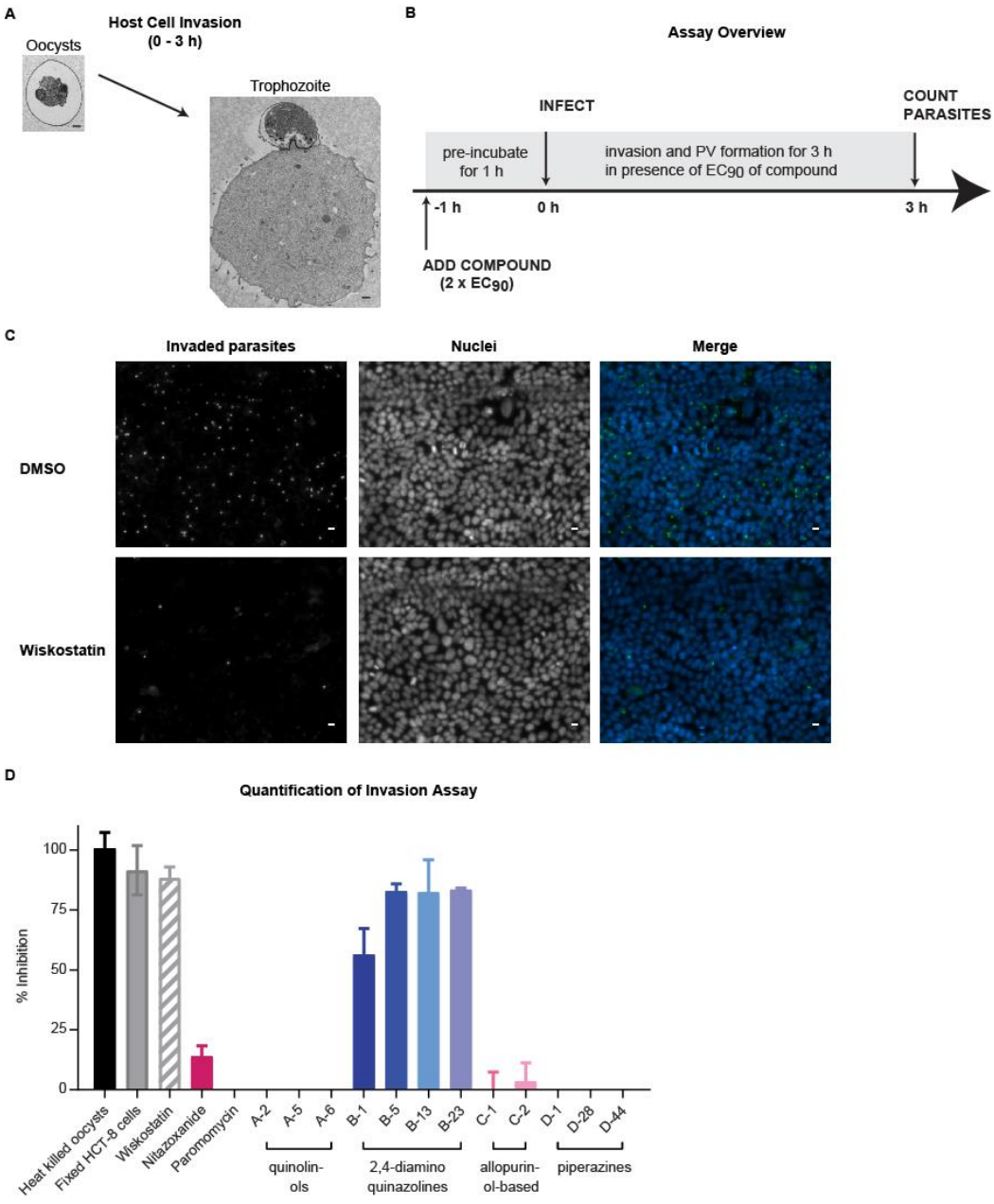

Figure 2. Invasion Assay.

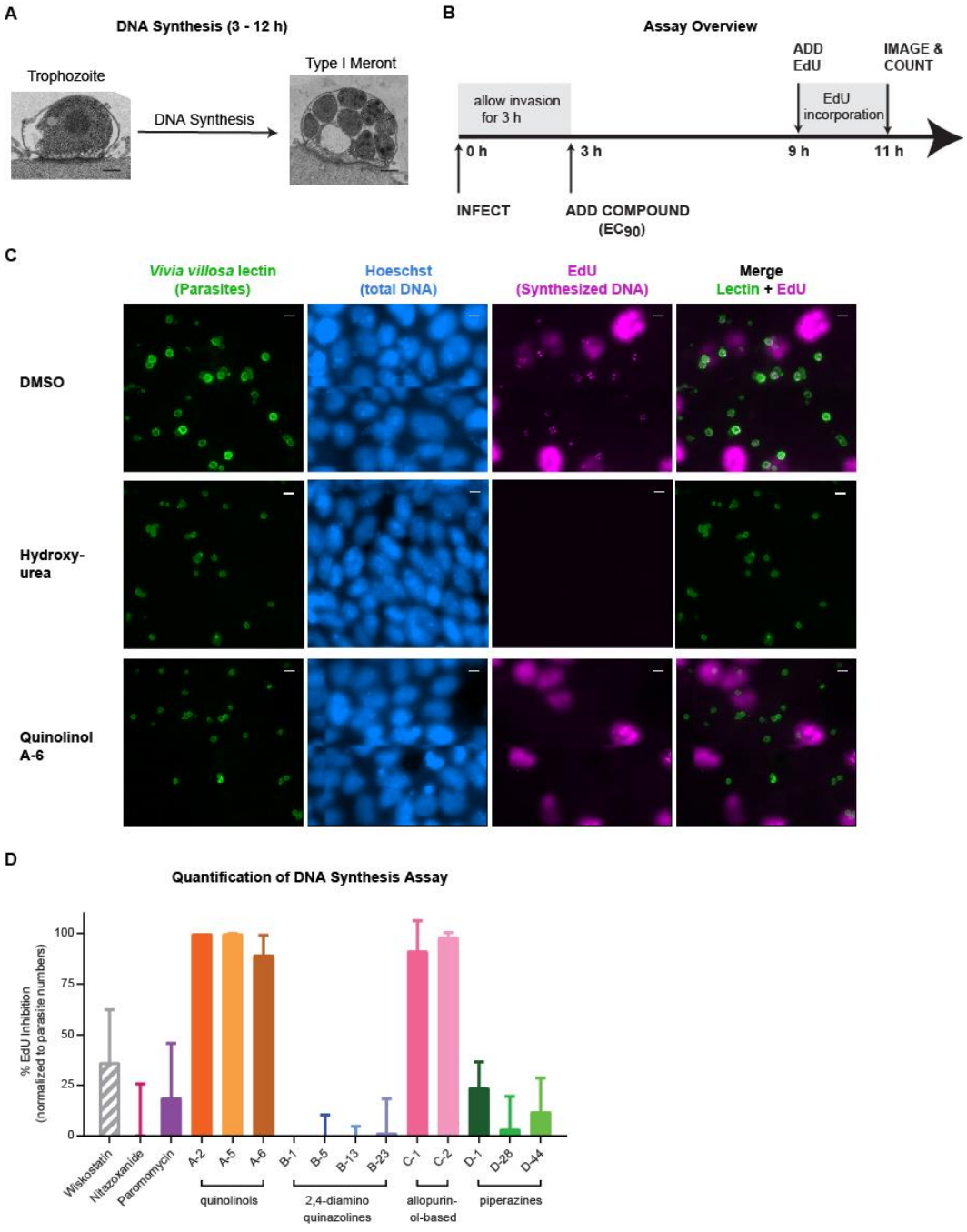

Figure 3. DNA Synthesis Assay.

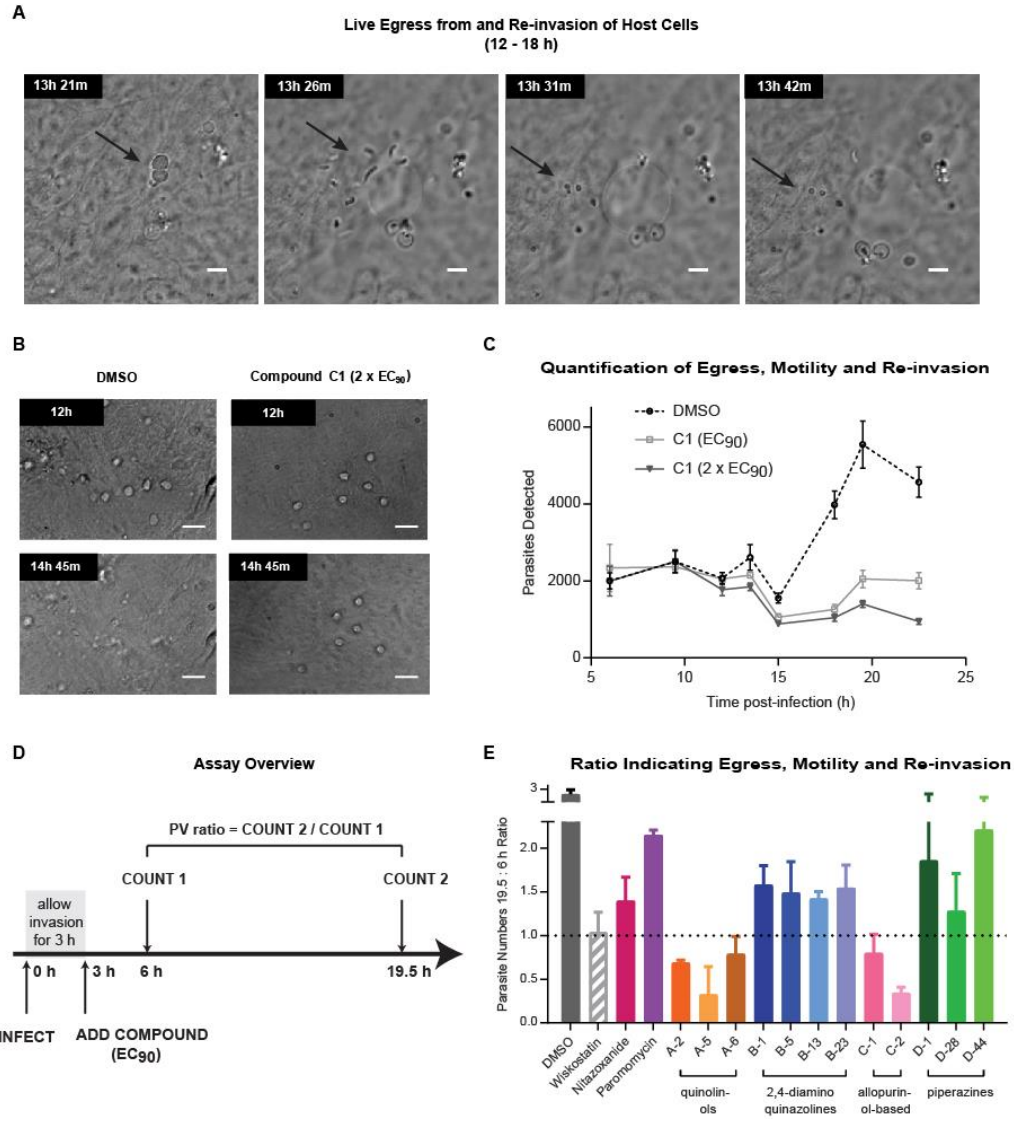

Figure 4. Assay to measure parasitophorous vacuole (PV) egress, merozoite motility and reinvasion to form new parasitophorous vacuole.

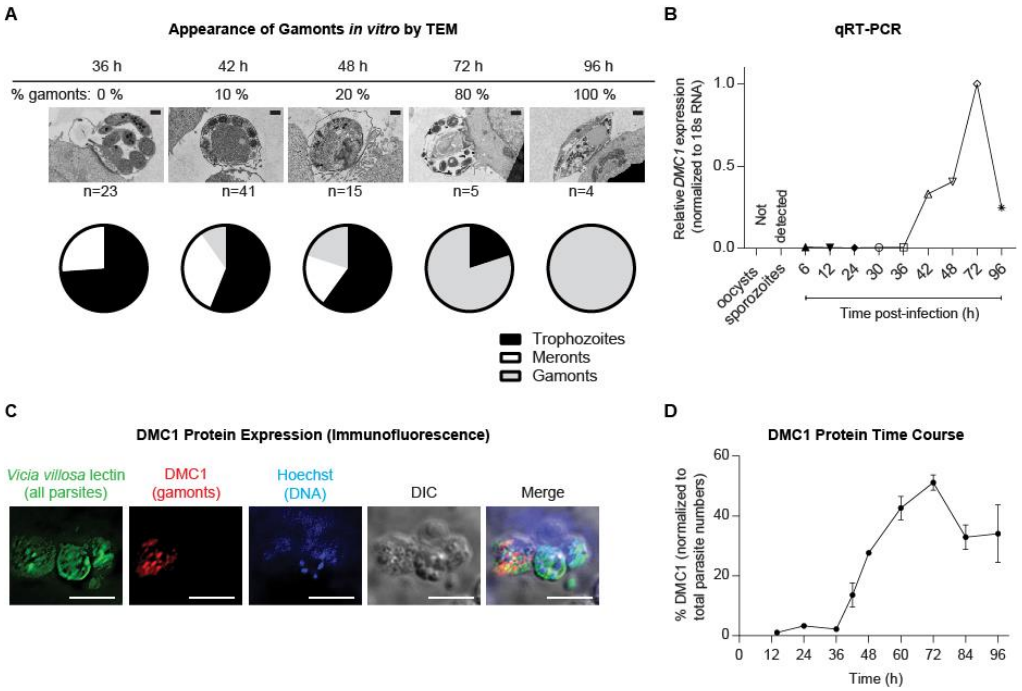

Figure 5. *DMC1* (*cgd_1690*) mRNA and protein expression correlates with appearance of sexual stages.

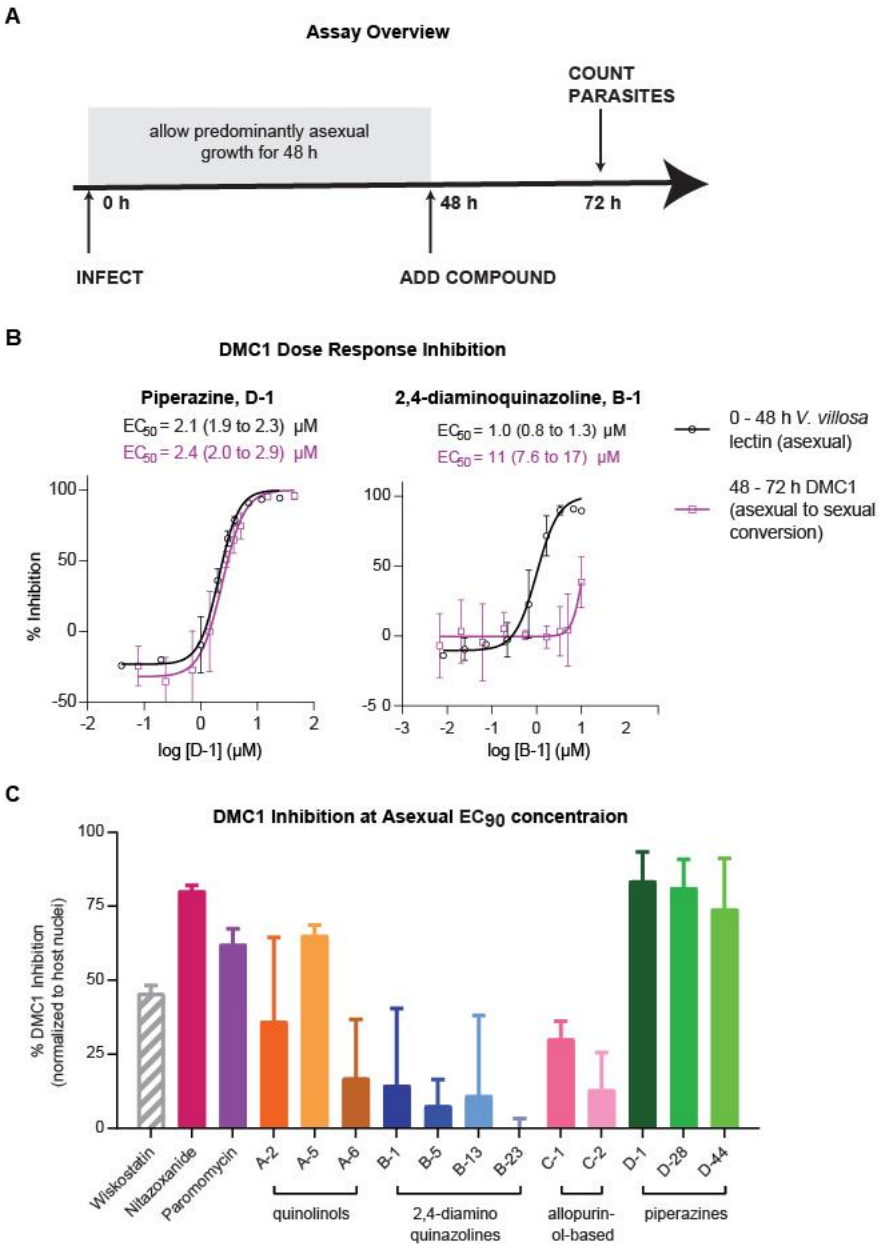

Figure 6. Assay to Measure Asexual to Sexual Stage Conversion.

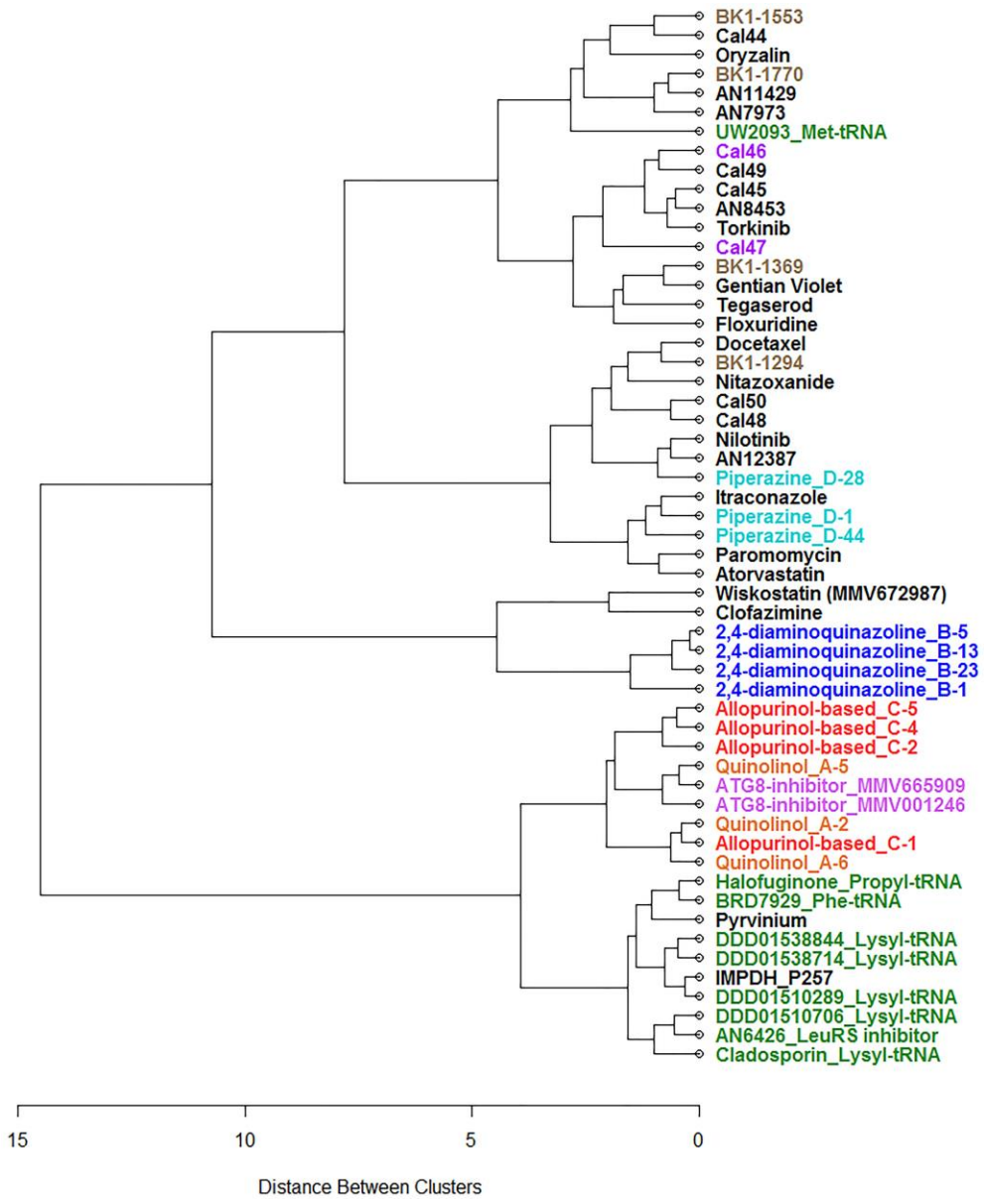

Figure 7. Clustering Analysis of Life Stage Assay Results for 55 Anti-*Cryptosporidium* hits.

Supplementary Table 1. Compounds from the Medicine for Malaria Venture Open Access Malaria Box and their variants used in the life stage assays.

Compound ID	Huston lab ID	SMILES	Structure	*C. parvum* EC_{90} (µM)
MMV665814	A-2	Oc1c(ccc2cccnc12)C(NC(=O)c3ccccc3)c4ccccc4	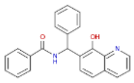	1.34
MMV666080	A-5	Oc1c(ccc2cccnc12)C(NC(=O)c3ccccc3)c4ccccc4	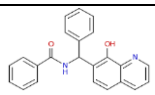	4.35
MMV000760	A-6	Oc1c(CN2CCN(CC2)c3ccccc3F)cc(Br)c4cccnc14	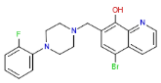	1.33
MMV006169	B-1	C(Nc1nc(Nc2ccccc2)nc3ccccc13)c4ccccc4	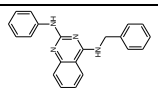	2.27
OSSL_324399	B-5	C1CCC(C1)Nc1nc(NCc2ccccc2)c2c(n1)cccc2		7.22
OSSL_723641	B-13	COc1ccc(cc1Cl)Nc1nc(NCc2ccccc2Cl)c2c(n1)cccc2	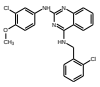	1.39
OSSL_324373 / DBeQ	B-23	c1ccc(cc1)CNc1nc(NCc2ccccc2)c2c(n1)cccc2		10.9
MMV403679	C-1	c1(c(cnn1c2cccc(C)c2)C(=O)N3)N=C3n4nc(C)cc4NC(=O)c5cc(cccc6)c6o5	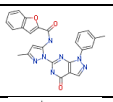	0.65
F2135-0883	C-2	c31c(cnn1-c2cc(ccc2)C)C(=O)NC(=N3)n4c(cc(n4)C)NC(=O)c5c(cc(cc5)OC)OC	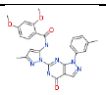	0.65
MMV665917	D-1	Clc1ccc(NC(=O)N2CCN(CC2)c3ccc4nncn4n3)cc1	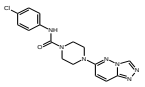	2.1
F5123-0135	D-28	O=C(N1CCN(CC1)c1ccc2n(n1)cnn2)Nc1ccc(c(c1)Cl)Cl	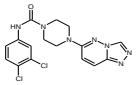	1.5
F5313-0562	D-44	O=C(c1ccc(cc1)S(=O)(=O)N(CC)C)N1CCN(CC1)c1ccc2n(n1)cnn2	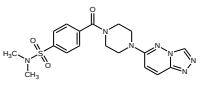	11.6
MMV001246		CSC1=CC=CC=C1C(=O)NC2=NC(=CS2)C3=CC=CC=N3	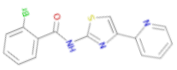	5.39
MMV665909		Brc1ccccc1C(=O)Nc2nc(cs2)c3ccccn3	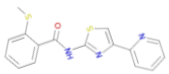	6.84

Supplementary Table 2. Grouping of select inhibitors based on the asexual life stage assays.

Scaffold class	Compound ID	Sporozoite invasion	DNA synthesis	Egress/motility/ re-invasion
2,4-diamino quinazolines	B-1	yes	no	1.58
	B-5	yes	no	1.49
	B-13	yes	no	1.42
	B-23	yes	no	1.55
Quinolinols	A-2	no	yes	0.69
	A-5	no	yes	0.32
	A-6	no	yes	0.79
	Floxuridine	no	no	0.74
	Tegaserod	no	no	1.01

Supplementary Table 3. Compiled *in vitro* life stage assays, parasite persistence assay and *in vivo* NSG efficacy data for 55 anti-*Cryptosporidium* hits.

Compound ID	Huston Lab Code	Putative mechanism/chemical relatedness	Sporozoite invasion (% inhibition)	DNA synthesis	Egress/motility/re-invasion (ratio)	Asexual to sexual differentiation (% inhibition)	Parasite persistence assay	*In vivo* activity (NSG-inhibition)	*In vivo* cure (NSG)
Nitazoxanide			13.83	-9.16	1.40	73.48	static	no	
Gentian Violet			-6.62	47.40	1.37	8.16	exponential	no	
Pyrvinium			25.69	88.30	0.61	68.07	static	no	
2,4-diaminoquinazoline_B-13	B-13	2,4-diaminoquinazoline	82.51	-3.46	1.42	11.26	exponential	no	
AN11429			-2.64	25.22	1.57	-51.37	exponential	yes	
Torkinib			-21.41	-16.16	1.61	11.19	linear	no	
2,4-diaminoquinazoline_B-23	B-23	2,4-diaminoquinazoline	83.80	1.59	1.55	-6.40	static		
Tegaserod			13.93	-6.72	1.01	12.05	linear	no	
Allopurinol-based_C-1	C-1	Allopurinol-based	-10.80	91.44	0.80	30.35	exponential	no	
AN6426_LeuRS inhibitor		tRNA Synthetase inhibitor	-16.44	86.81	0.93	62.47		no	
DDD01510706_Lysyl-tRNA		tRNA Synthetase inhibitor	-7.33	85.17	0.83	75.98	exponential	yes	
ATG8-inhibitor_MMV001246		ATG-8 inhibitor	-7.41	72.11	0.43	45.66	exponential	no	
Floxuridine		Pyrimidine analog	-28.03	20.42	0.74	-7.53	linear	no	
Piperazine_D-1 (MMV665917)	D-1	Piperazine	-25.16	23.98	1.86	79.37	exponential	yes	yes
AN8453			-19.64	5.29	1.42	2.66		no	
BK1-1294			-6.64	-5.73	1.49	45.56		no	
DDD01510289_Lysyl-tRNA		tRNA Synthetase inhibitor	7.92	86.82	0.90	75.58	exponential	yes	
BRD7929_Phe-tRNA		tRNA Synthetase inhibitor	0.40	93.39	0.72	63.11	exponential	yes	yes
Cladosporin_Lysyl-tRNA		tRNA Synthetase inhibitor	-6.64	93.15	0.68	94.16	exponential		
Piperazine_D-28	D-28	Piperazine	-13.23	3.38	1.28	81.40	exponential	yes	yes
Clofazimine			66.45	88.58	0.77	89.18	linear	no	
ATG8-inhibitor_MMV665909		ATG-8 inhibitor	-12.01	90.80	0.41	53.05	exponential	no	
Quinolinol_A-6	A-6	Quinolinol	-20.21	89.49	0.79	17.22	exponential		
Itraconazole			-29.72	-4.89	1.77	63.93	linear	no	
Atorvastatin		HMG-CoA reductase inhibitor	-38.43	-4.60	1.88	36.34	linear	no	
Piperazine_D-44	D-44	Piperazine	-11.48	12.07	2.21	74.35			
Quinolinol_A-5	A-5	Quinolinol	-13.46	99.95	0.32	65.35		no	
AN7973			-21.37	23.10	1.70	-52.26	exponential	yes	
UW2093_Met-tRNA		tRNA Synthetase inhibitor	-9.92	83.14	1.99	7.79	exponential	yes	
2,4-diaminoquinazoline_B-1	B-1	2,4-diaminoquinazoline	56.43	-31.43	1.58	14.70	linear	no	
Wiskostatin (MMV672987)		N-WASP inhibitor	88.58	36.39	1.04	45.76	exponential	no	
Quinolinol_A-2	A-2	Quinolinol	-15.19	100.00	0.69	36.33		no	
AN12387			-12.29	31.06	1.21	58.22		yes	
Paromomycin			-28.42	18.81	2.15	43.80	linear	yes	no
2,4-diaminoquinazoline_B-5	B-5	2,4-diaminoquinazoline	82.99	-9.25	1.49	7.84	static	no	
DDD01538714_Lysyl-tRNA		tRNA Synthetase inhibitor	14.15	89.96	0.95	86.44	exponential	yes	
Cal44			9.83	-18.41	2.16	-5.22	linear		
Halofuginone_Propyl-tRNA		tRNA Synthetase inhibitor	6.92	88.20	0.69	51.29			
Oryzalin		Plant Microtubule agent	1.23	12.01	2.39	-62.75			
Cal49			-5.39	-27.43	1.51	-4.71	linear		
Allopurinol-based_C-4	C-4	Allopurinol-based	9.11	99.18	0.48	41.59	exponential	no	
Docetaxel		Human Microtubule agent	-8.63	16.66	1.76	34.13			
Cal48			-22.39	-45.18	1.63	50.94			
Cal46			-0.21	-17.33	1.72	21.47	linear	yes	no
Allopurinol-based_C-5	C-5	Allopurinol-based	13.07	98.17	0.31	30.15	exponential	no	
DDD01538844_Lysyl-tRNA		tRNA Synthetase inhibitor	4.99	81.67	0.89	94.82	exponential	yes	yes
BK1-1553		CDPK1 inhibitor	-3.92	9.91	1.94	-13.81		yes	no
Cal50			-27.90	-25.65	1.44	49.26	exponential	no	
Allopurinol-based_C-2	C-2	Allopurinol-based	3.65	98.27	0.34	13.19	exponential	no	
Cal45			-18.17	-16.81	1.35	1.98	exponential		
Nilotinib			-21.88	22.05	1.05	70.96	static	no	
Cal47			-10.53	-61.28	1.44	-36.14	linear	yes	no
BK1-1770		CDPK1 inhibitor	-2.21	4.28	1.44	-37.39			
BK1-1369		CDPK1 inhibitor	-7.94	16.97	1.41	-4.30		yes	no
IMPDH_P257		IMPDH inhibitor	9.88	97.76	0.84	70.52	linear	no	

3.8. References

Abubakar, I., Aliyu, S. H., Arumugam, C., Hunter, P. R., & Usman, N. K. (2007). Prevention and treatment of cryptosporidiosis in immunocompromised patients. *Cochrane Database Syst Rev*(1), CD004932. doi:10.1002/14651858.CD004932.pub2

Amadi, B., Mwiya, M., Sianongo, S., Payne, L., Watuka, A., Katubulushi, M., & Kelly, P. (2009). High dose prolonged treatment with nitazoxanide is not effective for cryptosporidiosis in HIV positive Zambian children: a randomised controlled trial. *BMC infectious diseases, 9*, 195. doi:10.1186/1471-2334-9-195

Barkhuff, W. D., Gilk, S. D., Whitmarsh, R., Tilley, L. D., Hunter, C., & Ward, G. E. (2011). Targeted disruption of TgPhIL1 in Toxoplasma gondii results in altered parasite morphology and fitness. *PLoS One, 6*(8), e23977. doi:10.1371/journal.pone.0023977

Bessoff, K., Sateriale, A., Lee, K. K., & Huston, C. D. (2013). Drug Repurposing Screen Reveals FDA-Approved Inhibitors of Human HMG-CoA Reductase and Isoprenoid Synthesis that Block Cryptosporidium parvum Growth. *Antimicrobial agents and chemotherapy*. doi:10.1128/AAC.02460-12

Bessoff, K., Spangenberg, T., Foderaro, J. E., Jumani, R. S., Ward, G. E., & Huston, C. D. (2014). Identification of Cryptosporidium parvum active chemical series by Repurposing the open access malaria box. *Antimicrob Agents Chemother, 58*(5), 2731-2739. doi:10.1128/AAC.02641-13

Burrows, J. N., Duparc, S., Gutteridge, W. E., Hooft van Huijsduijnen, R., Kaszubska, W., Macintyre, F., . . . Wells, T. N. C. (2017). New developments in anti-malarial target candidate and product profiles. *Malaria journal, 16*(1), 26. doi:10.1186/s12936-016-1675-x

Burrows, J. N., van Huijsduijnen, R. H., Mohrle, J. J., Oeuvray, C., & Wells, T. N. (2013). Designing the next generation of medicines for malaria control and eradication. *Malaria journal, 12*, 187. doi:10.1186/1475-2875-12-187

Castellanos-Gonzalez, A., White, A. C., Jr., Ojo, K. K., Vidadala, R. S., Zhang, Z., Reid, M. C., . . . Van Voorhis, W. C. (2013). A novel calcium-dependent protein kinase inhibitor as a lead compound for treating cryptosporidiosis. *J Infect Dis, 208*(8), 1342-1348. doi:10.1093/infdis/jit327

Chao, A. T., Lee, B. H., Wan, K. F., Selva, J., Zou, B., Gedeck, P., . . . Manjunatha, U. H. (2018). Development of a Cytopathic Effect-Based Phenotypic Screening Assay against Cryptosporidium. *ACS Infect Dis*. doi:10.1021/acsinfecdis.7b00247

Checkley, W., White, A. C., Jr., Jaganath, D., Arrowood, M. J., Chalmers, R. M., Chen, X. M., . . . Houpt, E. R. (2015). A review of the global burden, novel diagnostics, therapeutics, and vaccine targets for cryptosporidium. *Lancet Infect Dis, 15*(1), 85-94. doi:10.1016/s1473-3099(14)70772-8

Chen, X. M., Huang, B. Q., Splinter, P. L., Orth, J. D., Billadeau, D. D., McNiven, M. A., & LaRusso, N. F. (2004). Cdc42 and the actin-related protein/neural

Wiskott-Aldrich syndrome protein network mediate cellular invasion by Cryptosporidium parvum. *Infect Immun, 72*(5), 3011-3021.

Current, W. L., & Reese, N. C. (1986). A comparison of endogenous development of three isolates of Cryptosporidium in suckling mice. *J Protozool, 33*(1), 98-108.

Delves, M., Plouffe, D., Scheurer, C., Meister, S., Wittlin, S., Winzeler, E. A., . . . Leroy, D. (2012). The activities of current antimalarial drugs on the life cycle stages of Plasmodium: a comparative study with human and rodent parasites. *PLoS Med, 9*(2), e1001169. doi:10.1371/journal.pmed.1001169

Disease, G. B. D., Injury, I., & Prevalence, C. (2016). Global, regional, and national incidence, prevalence, and years lived with disability for 310 diseases and injuries, 1990-2015: a systematic analysis for the Global Burden of Disease Study 2015. *Lancet, 388*(10053), 1545-1602. doi:10.1016/S0140-6736(16)31678-6

Elliott, D. A., Coleman, D. J., Lane, M. A., May, R. C., Machesky, L. M., & Clark, D. P. (2001). Cryptosporidium parvum infection requires host cell actin polymerization. *Infect Immun, 69*(9), 5940-5942.

Gorla, S. K., Kavitha, M., Zhang, M., Liu, X., Sharling, L., Gollapalli, D. R., . . . Cuny, G. D. (2012). Selective and potent urea inhibitors of cryptosporidium parvum inosine 5'-monophosphate dehydrogenase. *Journal of medicinal chemistry, 55*(17), 7759-7771. doi:10.1021/jm3007917

Gorla, S. K., McNair, N. N., Yang, G., Gao, S., Hu, M., Jala, V. R., . . . Hedstrom, L. (2014). Validation of IMP dehydrogenase inhibitors in a mouse model of cryptosporidiosis. *Antimicrob Agents Chemother, 58*(3), 1603-1614. doi:10.1128/aac.02075-13

Hobbs, C. V., Neal, J., Conteh, S., Donnelly, L., Chen, J., Marsh, K., . . . Duffy, P. E. (2014). HIV treatments reduce malaria liver stage burden in a non-human primate model of malaria infection at clinically relevant concentrations in vivo. *PLoS One, 9*(7), e100138. doi:10.1371/journal.pone.0100138

Huston, C. D., Spangenberg, T., Burrows, J., Willis, P., Wells, T. N., & van Voorhis, W. (2015). A Proposed Target Product Profile and Developmental Cascade for New Cryptosporidiosis Treatments. *PLoS Negl Trop Dis, 9*(10), e0003987. doi:10.1371/journal.pntd.0003987

Jain, V., Yogavel, M., Kikuchi, H., Oshima, Y., Hariguchi, N., Matsumoto, M., . . . Sharma, A. (2017). Targeting Prolyl-tRNA Synthetase to Accelerate Drug Discovery against Malaria, Leishmaniasis, Toxoplasmosis, Cryptosporidiosis, and Coccidiosis. *Structure, 25*(10), 1495-1505.e1496. doi:10.1016/j.str.2017.07.015

Jumani, R. S., Bessoff, K., Love, M. S., Miller, P., Stebbins, E. E., Teixeira, J. E., . . . Huston, C. D. (2018). A Novel Piperazine-Based Drug Lead for Cryptosporidiosis from the Medicines for Malaria Venture Open Access Malaria Box. *Antimicrob Agents Chemother*. doi:10.1128/aac.01505-17

Kato, N., Comer, E., Sakata-Kato, T., Sharma, A., Sharma, M., Maetani, M., . . . Schreiber, S. L. (2016). Diversity-oriented synthesis yields novel multistage antimalarial inhibitors. *Nature, 538*(7625), 344-349. doi:10.1038/nature19804

Katsuno, K., Burrows, J. N., Duncan, K., Hooft van Huijsduijnen, R., Kaneko, T., Kita, K., . . . Slingsby, B. T. (2015). Hit and lead criteria in drug discovery for infectious diseases of the developing world. *Nat Rev Drug Discov, 14*(11), 751-758. doi:10.1038/nrd4683

Kotloff, K. L., Nataro, J. P., Blackwelder, W. C., Nasrin, D., Farag, T. H., Panchalingam, S., . . . Levine, M. M. (2013). Burden and aetiology of diarrhoeal disease in infants and young children in developing countries (the Global Enteric Multicenter Study, GEMS): a prospective, case-control study. *Lancet, 382*(9888), 209-222. doi:10.1016/S0140-6736(13)60844-2

Liu, J., Platts-Mills, J. A., Juma, J., Kabir, F., Nkeze, J., Okoi, C., . . . Houpt, E. R. (2016). Use of quantitative molecular diagnostic methods to identify causes of diarrhoea in children: a reanalysis of the GEMS case-control study. *Lancet, 388*(10051), 1291-1301. doi:10.1016/S0140-6736(16)31529-X

Love, M. S., Beasley, F. C., Jumani, R. S., Wright, T. M., Chatterjee, A. K., Huston, C. D., . . . McNamara, C. W. (2017). A high-throughput phenotypic screen identifies clofazimine as a potential treatment for cryptosporidiosis. *PLoS Negl Trop Dis, 11*(2), e0005373. doi:10.1371/journal.pntd.0005373

Malebranche, R., Arnoux, E., Guerin, J. M., Pierre, G. D., Laroche, A. C., Pean-Guichard, C., . . . et al. (1983). Acquired immunodeficiency syndrome with severe gastrointestinal manifestations in Haiti. *Lancet, 2*(8355), 873-878.

Manjunatha, U. H., Chao, A. T., Leong, F. J., & Diagana, T. T. (2016). Cryptosporidiosis Drug Discovery: Opportunities and Challenges. *ACS Infect Dis, 2*(8), 530-537. doi:10.1021/acsinfecdis.6b00094

Manjunatha, U. H., Vinayak, S., Zambriski, J. A., Chao, A. T., Sy, T., Noble, C. G., . . . Diagana, T. T. (2017). A Cryptosporidium PI(4)K inhibitor is a drug candidate for cryptosporidiosis. *Nature, 546*(7658), 376-380. doi:10.1038/nature22337

Mauzy, M. J., Enomoto, S., Lancto, C. A., Abrahamsen, M. S., & Rutherford, M. S. (2012). The Cryptosporidium parvum transcriptome during in vitro development. *PLoS One, 7*(3), e31715. doi:10.1371/journal.pone.0031715

Mlambo, G., Coppens, I., & Kumar, N. (2012). Aberrant sporogonic development of Dmc1 (a meiotic recombinase) deficient Plasmodium berghei parasites. *PLoS One, 7*(12), e52480. doi:10.1371/journal.pone.0052480

Murtagh, F., & Legendre, P. (2014). Ward's Hierarchical Agglomerative Clustering Method: Which Algorithms Implement Ward's Criterion? . *Journal of Classification, 31*(3), 274-295.

Navin, T. R., Weber, R., Vugia, D. J., Rimland, D., Roberts, J. M., Addiss, D. G., . . . Bryan, R. T. (1999). Declining CD4+ T-lymphocyte counts are associated with increased risk of enteric parasitosis and chronic diarrhea: results of a 3-year longitudinal study. *J Acquir Immune Defic Syndr Hum Retrovirol, 20*(2), 154-159.

Ndao, M., Nath-Chowdhury, M., Sajid, M., Marcus, V., Mashiyama, S. T., Sakanari, J., . . . Caffrey, C. R. (2013). A cysteine protease inhibitor rescues mice from a lethal Cryptosporidium parvum infection. *Antimicrob Agents Chemother, 57*(12), 6063-6073. doi:10.1128/aac.00734-13

Nwaka, S., & Hudson, A. (2006). Innovative lead discovery strategies for tropical diseases. *Nat Rev Drug Discov, 5*(11), 941-955. doi:10.1038/nrd2144

Pawlowic, M. C., Vinayak, S., Sateriale, A., Brooks, C. F., & Striepen, B. (2017). Generating and Maintaining Transgenic Cryptosporidium parvum Parasites. *Curr Protoc Microbiol, 46*, 20B 22 21-20B 22 32. doi:10.1002/cpmc.33

Peterson, J. R., Bickford, L. C., Morgan, D., Kim, A. S., Ouerfelli, O., Kirschner, M. W., & Rosen, M. K. (2004). Chemical inhibition of N-WASP by stabilization of a native autoinhibited conformation. *Nature structural & molecular biology, 11*(8), 747-755. doi:10.1038/nsmb796

Rider, S. D., Jr., Cai, X., Sullivan, W. J., Jr., Smith, A. T., Radke, J., White, M., & Zhu, G. (2005). The protozoan parasite Cryptosporidium parvum possesses two functionally and evolutionarily divergent replication protein A large subunits. *J Biol Chem, 280*(36), 31460-31469. doi:10.1074/jbc.M504466200

Salic, A., & Mitchison, T. J. (2008). A chemical method for fast and sensitive detection of DNA synthesis in vivo. *Proc Natl Acad Sci U S A, 105*(7), 2415-2420. doi:10.1073/pnas.0712168105

Shibata, S., Gillespie, J. R., Kelley, A. M., Napuli, A. J., Zhang, Z., Kovzun, K. V., . . . Buckner, F. S. (2011). Selective inhibitors of methionyl-tRNA synthetase have potent activity against Trypanosoma brucei Infection in Mice. *Antimicrob Agents Chemother, 55*(5), 1982-1989. doi:10.1128/aac.01796-10

Shirley, D. A., Moonah, S. N., & Kotloff, K. L. (2012). Burden of disease from cryptosporidiosis. *Current opinion in infectious diseases, 25*(5), 555-563. doi:10.1097/QCO.0b013e328357e569

Vinayak, S., Pawlowic, M. C., Sateriale, A., Brooks, C. F., Studstill, C. J., Bar-Peled, Y., . . . Striepen, B. (2015). Genetic modification of the diarrhoeal pathogen Cryptosporidium parvum. *Nature, 523*(7561), 477-480. doi:10.1038/nature14651

Ward Jr, J. H. (1963). Hierarchical grouping to optimize an objective function. *Journal of the American statistical association, 58*(301), 236-244.

CHAPTER 4: DISCUSSION AND FUTURE DIRECTIONS

This chapter will briefly summarize the results from chapters 2 and 3, provide an update on developments that have occurred most recently in this rapidly changing field, and then discuss strategies for further development of MMV665917 and additional needs to establish a *Cryptosporidium* drug development pipeline.

We have identified a highly promising piperazine-based lead, MMV665917 from the Medicines for Malaria Venture Open Access Malaria Box that was active against *C. hominis* and *C. parvum* Iowa strain and field isolates *in vitro,* was efficacious in the acute interferon-γ (IFN-γ) mouse model, as well as appeared to cure the chronic NOD SCID gamma (NSG) mouse model of cryptosporidiosis (Chapter 2). On the other hand, paromomycin and clofazimine were effective in the IFN-γ mouse model, but did not cure the disease in NSG mice. Since the NSG mice are highly immunocompromised, we hypothesized that the compounds need to be cidal to cure the disease in the NSG mouse model. To aid general *in vivo* efficacy studies, we developed an *in vitro* pharmacodynamic (PD) parasite persistence assay to determine potentially static versus cidal compounds and identify the concentration of compound required to maximize the rate of parasite elimination (Chapter 2). MMV665917 appeared cidal in the parasite persistence assay, whereas, nitazoxanide, paromomycin and clofazimine seemed potentially static (Jumani et al., 2018).

Currently, there are several large phenotypic screening efforts underway to identify anti-*Cryptosporidium* compounds, with thousands of hits expected soon (Bessoff, Sateriale, Lee, & Huston, 2013; Bessoff et al., 2014; Chao et al., 2018; Love

et al., 2017). In the absence of a reliable drug, the *in vitro* and *in vivo* characteristics desired for prioritization are not known. A strategy to obtain diverse hits with different mechanisms of action has been used to prioritize hits for parasitic drug development (Burrows et al., 2017; Burrows, van Huijsduijnen, Mohrle, Oeuvray, & Wells, 2013; Katsuno et al., 2015). With a goal to obtain diversity among anti-*Cryptosporidium* hits, we developed a range of life-stage specific assays and screened a set of 34 "learner" hits that had activity against the asexual stage of *C. parvum*. Interestingly, several compounds behaved differently in the life-stage assays, forming distinct groups, but structural variants and multiple different tRNA synthetase inhibitors grouped together (Chapter 3).

Anti-*Cryptosporidium* drug development efforts have been growing at an extremely fast pace and large developments have been made since the start of this thesis. In fact, significant updates have occurred in the past few months during the writing of this thesis. MMV665917 has been shown to be highly efficacious in the clinical calf model, reducing parasite shedding as well as alleviating the symptoms of diarrhea (Stebbins et al., 2018). The compound also abrogated parasite shedding in gnotobiotic piglets infected with the *C. hominis* TU502 strain, but surprisingly, the compound alone induced diarrhea in this model, unlike in calves wherein it reduced *C. parvum* induced diarrhea (personal communication with Dr. Saul Tzipori, Tufts University). Interestingly, MMV665917 has shown the best anti-*C. hominis* efficacy to date in the gnotobiotic piglet model of cryptosporidiosis. The most potent variant of MMV665917 identified, D-28, also cured cryptosporidiosis in the NSG mouse model.

After a four-day treatment with twice-daily dose of 60 mg/kg of MMV665917 or D-28 variant, mice did not shed any detectable parasites in feces for up to 26 days after cessation of treatment (Huston lab, unpublished data). Since MMV665917 is active against *P. falciparum* blood stages and these cultures can be continuously maintained *in vitro*, resistance studies were performed in this system. More than 20 different MMV665917 resistant strains with varying degrees of resistance with a 1.3 to > 36 fold decrease in potency have been obtained (personal communication with Dr. Audrey R. Odom, Washington University School of Medicine). These resistant strains can be sequenced and can potentially provide the likely target of the drug. Large-scale screening has been performed using DMC1 as a marker to identify asexual and sexual stage specific and pan stage inhibitors (Huston lab, unpublished data). Genetic strains of *Cryptosporidium* with the inosine-5′-monophosphate dehydrogenase (*IMPDH*) knockout have been created and were viable *in vivo*, ending the IMPDH drug development program (Dr. Boris Striepen's talk at Bill and Melinda Gates Foundation's 2nd Annual *Cryptosporidium* Drug Discovery Program Meeting, Tres Cantos, Spain, June 2017). The IMPDH inhibitors had been earlier identified using target-based screens and were shown to be active in the acute IL-12 knockout mouse model of cryptosporidiosis (Gorla et al., 2012; Gorla et al., 2014).

4.1. MMV665917 Lead Optimization and Pharmacokinetic Considerations

MMV665917 is a promising lead compound with impressive activity in several animal models, something which has not been seen with any other anti-*Cryptosporidium* compound to date. The compound is quite safe *in vitro*, except for

potential hERG liabilities at higher concentrations and drug-drug interaction issues, which are compounded by a modest anti-*Cryptosporidium in vitro* potency. The other initial concern is the compound-induced diarrhea in gnotobiotic piglets during initial studies. Since the compound was highly efficacious, a more comprehensive dose-response study with a lower dose needs to be tested to abrogate compound induced diarrhea. Preliminary structure-activity relationship (SAR) studies appear promising, lending credence to addressing these issues using a medicinal chemistry program. The success of the medicinal chemistry program would depend on understanding the pharmacokinetic parameters (PK) of MMV665917 that drive *in vivo* efficacy. The first step would be to perform a thorough PK study with 30 and 60 mg/kg of MMV665917 in mice and model these data to design further *in vivo* experiments to determine minimal dose(s) required to achieve efficacy. A comparison of the PK parameters of the variant, D-28, with those of the parent could provide helpful insights about PK parameters that drive *in vivo* efficacy. A comprehensive medicinal chemistry program can not only aid in identifying compounds with improved potency, but also variants with different PK properties, which can then be used as tools to understand PK properties that drive *in vivo* efficacy.

The ideal PK parameters for anti-*Cryptosporidium* drugs have been a major unanswered question in *Cryptosporidium* drug development in general. There have been reports with Bumped Kinase inhibitors (BKI) and IMPDH inhibitors suggesting that intestinal exposure is important for efficacy (Arnold et al., 2017; Gorla et al., 2014). Using structural variants of BRD7929 (a validated *Cryptosporidium* Phe-tRNA

synthetase inhibitor (Kato et al., 2016)) with different PK properties, it is clear that systemic exposure is critical for activity of this series in the NSG mouse model. Hence, we believe the optimal PK parameters could vary depending on the compound class. Added on, there is a possibility that the PK parameters could depend on the mouse model used as well, as different mouse models have been used in the above studies. As in immunocompromised patients, the biliary tree gets infected in the NSG mice (data not shown) and it is possible that this site acts as a reservoir of infection, with systemic or enterohepatic recirculation of drugs required to cure the disease from these animals. Paromomycin is a poorly absorbed drug that reduces oocyst shedding in the NSG mice, but the infection relapses on cessation of treatment (Jumani et al., 2018). Paromomycin's inability to cure the biliary tree infection in these mice could be one among several reasons why paromomycin-treated mice relapse. To address variability between mouse models of infection, we have tested the BKI and IMPDH inhibitors in the NSG mouse model, but they were ineffective. The results are inconclusive, as the inactivity could be due to several reasons apart from PK parameters. Interestingly, clofazimine was active in the IFN-γ mouse model but not in the NSG model, whereas, MMV665917 was active in both models. Thus, an understanding of MMV665917 PK parameters would shed some light on understanding if the PK parameters desired for various mouse models are different. Confidence in these studies can be added by comparing several leads across the different mouse models of cryptosporidiosis.

An *in vitro* transmembrane assay could be potentially used to predict the PK properties desired (see Appendix II). This would involve developing a polarized

monolayer of intestinal cells using a transmembrane chamber and testing efficacy of compounds when added to the apical or basolateral side of the polarized monolayer. This assumes the apical side represents the intestinal lumen, while the basolateral side represents systemic exposure. The major challenge for the assay is to measure and correct for transport of compounds across the polarized monolayer.

4.2. Target of MMV665917

A knowledge of the target of MM665917 is not mandatory for drug development but would have several advantages. A knowledge of the target would be extremely helpful in the medicinal chemistry program and would help in increasing selectivity for the parasite over the unwanted host toxicity. There is a possibility that MMV665917 might fail as a drug candidate due to PK, selectivity issues, cost, or other reasons, but the target can potentially be a validated drugable candidate, especially as MMV665917 works remarkably well in several animal models. Thus, identification of the target would be an invaluable resource that can be helpful in developing new classes of compounds against cryptosporidiosis using a target-based screening strategy.

Since MMV665917 was identified from a whole cell screening assay where the parasite growth is dependent on the host, the target of the drug could be in the parasite or host cell pathway that is essential for parasitic growth. Since the drug is active against the related Apicomplexan parasite *Plasmodium* blood stages as well, we hypothesize that the drug potentially targets the parasite and not the host and that the target is conserved between the 2 parasites. The resistant *P. falciparum* strains recently

generated serve as a promising tool to identify a target. We are also collaborating with GlaxoSmithKline (GSK) to use their thermal proteome shift technology to identify a potential proteome target (Savitski et al., 2014). One of the partially active variants, D-74, is closely related to a kinase inhibitor identified in a patent application which was found using the chemical structure search function of the Chemical Abstracts Service (CAS) SciFinder database (https://scifinder.cas.org/). Using a similar strategy, our collaborator Dr. Marv Meyers found *C. parvum* Cyclin Dependent Kinase 8 to be a potential target for MMV665917 and is using medicinal chemistry strategies to test the same. Our collaborator Dr. Ray Hui at the University of Toronto has expressed several *C. parvum* kinases and is currently screening MMV665917 and its select variants against the kinases. These different strategies could yield a potential target, which can be confirmed in *C. parvum* by performing over-expression and mutation studies using the recently developed CRISPR/Cas9 genetics system (Pawlowic, Vinayak, Sateriale, Brooks, & Striepen, 2017; Vinayak et al., 2015).

4.3. Compare Mouse Models and *in vitro* Assays

Numerous mouse models and *in vitro* assays are currently in use for *Cryptosporidium* drug development (Castellanos-Gonzalez et al., 2013; Gorla et al., 2014; Jumani et al., 2018; Love et al., 2017; Manjunatha et al., 2017; Ndao et al., 2013). The *in vitro* and *in vivo* data reported in this thesis are the first direct comparison of a large number of promising anti-*Cryptosporidium* hits and leads from various groups in the same *in vitro* assays and *in vivo* mouse model (Bessoff et al.,

2013; Bessoff et al., 2014; Castellanos-Gonzalez et al., 2013; Downey, Chong, Graczyk, & Sullivan, 2008; Gorla et al., 2012; Jumani et al., 2018; Kato et al., 2016; Love et al., 2017; Shibata et al., 2011). This has been extremely helpful in directly comparing compounds and characterizing them. It is interesting to note that many of the compounds that were active in the acute mouse models were not active in the NSG mouse model of cryptosporidiosis. This includes the IMPDH inhibitors whose target has been shown to be non-essential for *Cryptosporidium*. The failure of IMPDH inhibitors serve as a classical example for drawbacks of target-based drug development for poorly studied neglected disease where target validation is extremely difficult. This also raises questions about the validity of the acute IL-12 knockout mouse model for *Cryptosporidium* drug development. BKI-1294 was also inactive in NSG mice, but has shown efficacy in the clinical calf model when given prophylactically. It is interesting to note that MMV665917 and AN7973 had activity in the NSG mice, and when dosed after onset of infection in calves worked much better than prophylactic administration of BKI-1294 (Huston lab, unpublished data). These preliminary correlations are interesting to note, but too small in number to draw any significant conclusions. The only other compound (apart from MMV665917 and AN7979) tested with good activity in the calf model is a phosphatidylinositol-4-OH kinase (PI(4)K) inhibitor, KDU731, from Novartis (Manjunatha et al., 2017). This compound is the only other promising lead that has not been tested in our *in vitro* assay or NSG mouse model. A variant of the KDU731 is on course to be tested in these models for a direct comparison and could yield meaningful results. KDU731 was tested in the chronic IFN-γ mouse model using

a mouse adapted nano-luciferase (Nluc) expressing *C. parvum* (Manjunatha et al., 2017). The lysine-tRNA synthetase inhibitors from Dundee have been tested in this chronic IFN-γ mouse model as well as the NSG mouse model with good efficacy correlation between the two mouse models. Hence, we expect the KDU731 to have similar activity in our NSG mouse model as well.

With many compounds inactive in the NSG mice but active in the other acute mouse models, there was a growing concern in the drug development community that the bar is very high to achieve activity in the NSG mice, which might eliminate most of the hits. This has not been the case, as after testing 29 different scaffolds in the NSG mice, we have found 9 different scaffolds (~31% hit rate) with activity in the NSG mouse model. There is a chance that screening in the NSG mouse model alone might eliminate interesting hits. Since there is no gold standard drug, the only way to know that activity in mouse models correlates with clinical efficacy is by identifying a drug that works in humans. For now, it could be extremely valuable to test all the existing promising leads in the critical mouse models and compare efficacy with the clinical calf model. This would be invaluable in establishing a standardized drug development cascade and reducing variability and redundant efforts for future lead identification studies. Further value can be added to these comparisons by understanding correlations between *in vivo* efficacy in various mouse models and efficacy in the parasite persistence assay.

Similarly, there are several different *in vitro* assays used to identify hits, which include immunofluorescence assays, assays using Nluc expressing parasites, RNA

detection using real-time quantitative PCR assay, and assays measuring host cytopathic effect (Bessoff et al., 2013; Castellanos-Gonzalez et al., 2013; Chao et al., 2018; Love et al., 2017; Vinayak et al., 2015). A correlation between assays using a learner set of compounds needs to be established to directly compare hits from the various assays. The assays also use different sources of oocysts, with the *C. parvum* Iowa strain from Bunch Grass Farm and the University of Arizona Sterling Laboratory being the major sources. There have been studies from our group and others to compare activity of promising hits against the Iowa strains and field isolates of *C. parvum*, and *C. hominis* TU502 strain as well. This should be a requirement for *Cryptosporidium* drug development, and studies against *C. hominis* field strains should also be performed, given the variation in virulence across strains. The latter studies are usually hindered due to lack of availability.

4.4. Prioritization Assays

The life stage assays have been used in this thesis to determine diversity based on predominant effect on compounds on the life stages. There is a possibility that the compounds grouped in the same cluster by this method could have different mechanisms of action, i.e., compounds could be affecting different pathways that provide the same life stage affect. This method has a caveat that it could potentially eliminate useful drug candidates at an early stage. However, the current prioritization method is random and this provides a logical method that has worked well for other neglected tropical diseases (NTDs). Based on experience with other NTDs, the lack of

prioritization has led to numerous cases wherein chemical series were pursued far too long, wasting precious resources, time and careers that could have been spent much more wisely. Since there are now an ample supply of early-stage *Cryptosporidium* inhibitors, the risk associated with a high attrition rate in drug development outweighs the initial risks of losing a few potential drug candidates.

The life cycle stage assays used the effective concentration that inhibited 90% of parasites in the regular asexual stage assay (EC_{90}) to determine the predominant effect of the compounds. At this concentration (EC_{90}), activity against no single life stage alone correlated with efficacy *in vivo*. This method is extremely useful in grouping hits for obtaining diversity, but does not mean that the compounds do not have any activity in the other stages. A dose response study against all stages would help better understand the effect on specific stages, and this could be more helpful in determining correlations between stage activity and *in vivo* efficacy. This is even more critical for the DMC1 assay as the life cycle of cryptosporidiosis has not been validated. It is not clear if targeting the asexual (or sexual) stages alone is sufficient for clearing the infection *in vivo*. Although MMV665917 had a similar potency against the asexual stages and DMC1 *in vitro*, many of the compounds tested had a shifted dose response curve with no compound more potent against the DMC1 stage. Interestingly, all compounds that were active *in vivo* had > 70% at or below a concentration of $9\times EC_{90}$ from asexual stage.

The results from these assays provide valuable starting point information to determine if compounds could be potentially synergistic or antagonistic based on life

stage activity. Checkerboard assays with representative compounds from each group can be used to test this idea. These assays also open up doors to explore the biology of the parasite.

The parasite persistence assay for a number of these hits showed that all compounds with *in vivo* efficacy had an exponential or linear rate of parasite elimination. None of the static compounds were active in the NSG mouse model. Not all of the exponential and linear compounds were active *in vivo,* which indicates the importance of other factors including PK and effects on the microbiome, among others.

In summary, we report MMV65917 as a highly promising lead, a parasite persistence assay to determine *in vitro* rate of kill and concentration desired to maximize rate of parasite elimination that can aid in hit-to-lead prioritization studies and in designing *in vivo* experiments. We also report a range of *in vitro* life stage assays that can aide in prioritization of anti-*Cryptosporidium* hits based on diversity.

4.5. References

Arnold, S. L. M., Choi, R., Hulverson, M. A., Schaefer, D. A., Vinayak, S., Vidadala, R. S. R., . . . Van Voorhis, W. C. (2017). Necessity of Bumped Kinase Inhibitor Gastrointestinal Exposure in Treating Cryptosporidium Infection. *J Infect Dis, 216*(1), 55-63. doi:10.1093/infdis/jix247

Bessoff, K., Sateriale, A., Lee, K. K., & Huston, C. D. (2013). Drug repurposing screen reveals FDA-approved inhibitors of human HMG-CoA reductase and isoprenoid synthesis that block Cryptosporidium parvum growth. *Antimicrob Agents Chemother, 57*(4), 1804-1814. doi:10.1128/AAC.02460-12

Bessoff, K., Spangenberg, T., Foderaro, J. E., Jumani, R. S., Ward, G. E., & Huston, C. D. (2014). Identification of Cryptosporidium parvum active chemical series by Repurposing the open access malaria box. *Antimicrob Agents Chemother, 58*(5), 2731-2739. doi:10.1128/AAC.02641-13

Burrows, J. N., Duparc, S., Gutteridge, W. E., Hooft van Huijsduijnen, R., Kaszubska, W., Macintyre, F., . . . Wells, T. N. C. (2017). New developments in anti-malarial target candidate and product profiles. *Malaria journal, 16*(1), 26. doi:10.1186/s12936-016-1675-x

Burrows, J. N., van Huijsduijnen, R. H., Mohrle, J. J., Oeuvray, C., & Wells, T. N. (2013). Designing the next generation of medicines for malaria control and eradication. *Malaria journal, 12*, 187. doi:10.1186/1475-2875-12-187

Castellanos-Gonzalez, A., White, A. C., Jr., Ojo, K. K., Vidadala, R. S., Zhang, Z., Reid, M. C., . . . Van Voorhis, W. C. (2013). A novel calcium-dependent protein kinase inhibitor as a lead compound for treating cryptosporidiosis. *J Infect Dis, 208*(8), 1342-1348. doi:10.1093/infdis/jit327

Chao, A. T., Lee, B. H., Wan, K. F., Selva, J., Zou, B., Gedeck, P., . . . Manjunatha, U. H. (2018). Development of a Cytopathic Effect-Based Phenotypic Screening Assay against Cryptosporidium. *ACS Infect Dis*. doi:10.1021/acsinfecdis.7b00247

Downey, A. S., Chong, C. R., Graczyk, T. K., & Sullivan, D. J. (2008). Efficacy of pyrvinium pamoate against Cryptosporidium parvum infection in vitro and in a neonatal mouse model. *Antimicrob Agents Chemother, 52*(9), 3106-3112. doi:10.1128/aac.00207-08

Gorla, S. K., Kavitha, M., Zhang, M., Liu, X., Sharling, L., Gollapalli, D. R., . . . Cuny, G. D. (2012). Selective and potent urea inhibitors of cryptosporidium parvum inosine 5'-monophosphate dehydrogenase. *Journal of medicinal chemistry, 55*(17), 7759-7771. doi:10.1021/jm3007917

Gorla, S. K., McNair, N. N., Yang, G., Gao, S., Hu, M., Jala, V. R., . . . Hedstrom, L. (2014). Validation of IMP dehydrogenase inhibitors in a mouse model of cryptosporidiosis. *Antimicrob Agents Chemother, 58*(3), 1603-1614. doi:10.1128/aac.02075-13

Jumani, R. S., Bessoff, K., Love, M. S., Miller, P., Stebbins, E. E., Teixeira, J. E., . . . Huston, C. D. (2018). A Novel Piperazine-Based Drug Lead for

Cryptosporidiosis from the Medicines for Malaria Venture Open Access Malaria Box. *Antimicrob Agents Chemother*. doi:10.1128/aac.01505-17

Kato, N., Comer, E., Sakata-Kato, T., Sharma, A., Sharma, M., Maetani, M., . . . Schreiber, S. L. (2016). Diversity-oriented synthesis yields novel multistage antimalarial inhibitors. *Nature, 538*(7625), 344-349. doi:10.1038/nature19804

Katsuno, K., Burrows, J. N., Duncan, K., Hooft van Huijsduijnen, R., Kaneko, T., Kita, K., . . . Slingsby, B. T. (2015). Hit and lead criteria in drug discovery for infectious diseases of the developing world. *Nat Rev Drug Discov, 14*(11), 751-758. doi:10.1038/nrd4683

Love, M. S., Beasley, F. C., Jumani, R. S., Wright, T. M., Chatterjee, A. K., Huston, C. D., . . . McNamara, C. W. (2017). A high-throughput phenotypic screen identifies clofazimine as a potential treatment for cryptosporidiosis. *PLoS Negl Trop Dis, 11*(2), e0005373. doi:10.1371/journal.pntd.0005373

Manjunatha, U. H., Vinayak, S., Zambriski, J. A., Chao, A. T., Sy, T., Noble, C. G., . . . Diagana, T. T. (2017). A Cryptosporidium PI(4)K inhibitor is a drug candidate for cryptosporidiosis. *Nature, 546*(7658), 376-380. doi:10.1038/nature22337

Ndao, M., Nath-Chowdhury, M., Sajid, M., Marcus, V., Mashiyama, S. T., Sakanari, J., . . . Caffrey, C. R. (2013). A cysteine protease inhibitor rescues mice from a lethal Cryptosporidium parvum infection. *Antimicrob Agents Chemother, 57*(12), 6063-6073. doi:10.1128/aac.00734-13

Pawlowic, M. C., Vinayak, S., Sateriale, A., Brooks, C. F., & Striepen, B. (2017). Generating and Maintaining Transgenic Cryptosporidium parvum Parasites. *Curr Protoc Microbiol, 46*, 20B 22 21-20B 22 32. doi:10.1002/cpmc.33

Savitski, M. M., Reinhard, F. B., Franken, H., Werner, T., Savitski, M. F., Eberhard, D., . . . Drewes, G. (2014). Tracking cancer drugs in living cells by thermal profiling of the proteome. *Science, 346*(6205), 1255784. doi:10.1126/science.1255784

Shibata, S., Gillespie, J. R., Kelley, A. M., Napuli, A. J., Zhang, Z., Kovzun, K. V., . . . Buckner, F. S. (2011). Selective inhibitors of methionyl-tRNA synthetase have potent activity against Trypanosoma brucei Infection in Mice. *Antimicrob Agents Chemother, 55*(5), 1982-1989. doi:10.1128/aac.01796-10

Stebbins, E., Jumani, R. S., Klopfer, C., Barlow, J., Miller, P., Campbell, M. A., . . . Huston, C. D. (2018). Clinical and microbiologic efficacy of the piperazine-based drug lead MMV665917 in the dairy calf cryptosporidiosis model. *PLoS Negl Trop Dis, 12*(1), e0006183. doi:10.1371/journal.pntd.0006183

Vinayak, S., Pawlowic, M. C., Sateriale, A., Brooks, C. F., Studstill, C. J., Bar-Peled, Y., . . . Striepen, B. (2015). Genetic modification of the diarrhoeal pathogen Cryptosporidium parvum. *Nature, 523*(7561), 477-480. doi:10.1038/nature14651

COMPREHENSIVE BIBLIOGRAPHY

Abubakar, I., Aliyu, S. H., Arumugam, C., Hunter, P. R., & Usman, N. K. (2007). Prevention and treatment of cryptosporidiosis in immunocompromised patients. *Cochrane Database Syst Rev*(1), CD004932. doi:10.1002/14651858.CD004932.pub2

Akiyoshi, D. E., Feng, X., Buckholt, M. A., Widmer, G., & Tzipori, S. (2002). Genetic analysis of a Cryptosporidium parvum human genotype 1 isolate passaged through different host species. *Infect Immun, 70*(10), 5670-5675.

Akiyoshi, D. E., Mor, S., & Tzipori, S. (2003). Rapid displacement of Cryptosporidium parvum type 1 by type 2 in mixed infections in piglets. *Infect Immun, 71*(10), 5765-5771.

Amadi, B., Mwiya, M., Musuku, J., Watuka, A., Sianongo, S., Ayoub, A., & Kelly, P. (2002). Effect of nitazoxanide on morbidity and mortality in Zambian children with cryptosporidiosis: a randomised controlled trial. *The Lancet, 360*(9343), 1375-1380. doi:10.1016/s0140-6736(02)11401-2

Amadi, B., Mwiya, M., Sianongo, S., Payne, L., Watuka, A., Katubulushi, M., & Kelly, P. (2009). High dose prolonged treatment with nitazoxanide is not effective for cryptosporidiosis in HIV positive Zambian children: a randomised controlled trial. *BMC infectious diseases, 9*, 195. doi:10.1186/1471-2334-9-195

Andrews, K. T., Fisher, G., & Skinner-Adams, T. S. (2014). Drug repurposing and human parasitic protozoan diseases. *Int J Parasitol Drugs Drug Resist, 4*(2), 95-111. doi:10.1016/j.ijpddr.2014.02.002

Angulo-Barturen, I., Jimenez-Diaz, M. B., Mulet, T., Rullas, J., Herreros, E., Ferrer, S., . . . Gargallo-Viola, D. (2008). A murine model of falciparum-malaria by in vivo selection of competent strains in non-myelodepleted mice engrafted with human erythrocytes. *PLoS One, 3*(5), e2252. doi:10.1371/journal.pone.0002252

Arnold, S. L. M., Choi, R., Hulverson, M. A., Schaefer, D. A., Vinayak, S., Vidadala, R. S. R., . . . Van Voorhis, W. C. (2017). Necessity of Bumped Kinase Inhibitor Gastrointestinal Exposure in Treating Cryptosporidium Infection. *J Infect Dis, 216*(1), 55-63. doi:10.1093/infdis/jix247

Arrowood, M. J. (2002). In vitro cultivation of cryptosporidium species. *Clin Microbiol Rev, 15*(3), 390-400.

Arrowood, M. J., & Sterling, C. R. (1987). Isolation of Cryptosporidium oocysts and sporozoites using discontinuous sucrose and isopycnic Percoll gradients. *J Parasitol, 73*(2), 314-319.

Barkhuff, W. D., Gilk, S. D., Whitmarsh, R., Tilley, L. D., Hunter, C., & Ward, G. E. (2011). Targeted disruption of TgPhIL1 in Toxoplasma gondii results in altered parasite morphology and fitness. *PLoS One, 6*(8), e23977. doi:10.1371/journal.pone.0023977

Bessoff, K., Sateriale, A., Lee, K. K., & Huston, C. D. (2013). Drug repurposing screen reveals FDA-approved inhibitors of human HMG-CoA reductase and

isoprenoid synthesis that block Cryptosporidium parvum growth. *Antimicrob Agents Chemother, 57*(4), 1804-1814. doi:10.1128/AAC.02460-12

Bessoff, K., Spangenberg, T., Foderaro, J., Jumani, R. S., Ward, G. E., & Huston, C. D. (2014). Identification of Cryptosporidium parvum active chemical series by repurposing the Open Access Malaria Box. *Antimicrob Agents Chemother*. doi:10.1128/AAC.02641-13

Burrows, J. N., Duparc, S., Gutteridge, W. E., Hooft van Huijsduijnen, R., Kaszubska, W., Macintyre, F., . . . Wells, T. N. C. (2017). New developments in anti-malarial target candidate and product profiles. *Malaria journal, 16*(1), 26. doi:10.1186/s12936-016-1675-x

Burrows, J. N., van Huijsduijnen, R. H., Mohrle, J. J., Oeuvray, C., & Wells, T. N. (2013). Designing the next generation of medicines for malaria control and eradication. *Malaria journal, 12*, 187. doi:10.1186/1475-2875-12-187

Bushen, O. Y., Kohli, A., Pinkerton, R. C., Dupnik, K., Newman, R. D., Sears, C. L., . . . Guerrant, R. L. (2007). Heavy cryptosporidial infections in children in northeast Brazil: comparison of Cryptosporidium hominis and Cryptosporidium parvum. *Transactions of the Royal Society of Tropical Medicine and Hygiene, 101*(4), 378-384. doi:10.1016/j.trstmh.2006.06.005

Cabada, M. M., & White, A. C., Jr. (2010). Treatment of cryptosporidiosis: do we know what we think we know? *Current opinion in infectious diseases, 23*(5), 494-499. doi:10.1097/QCO.0b013e32833de052

Cacciò, S. M. (2005). Molecular epidemiology of human cryptosporidiosis. *Parassitologia, 47*(2), 185-192.

Campbell, L. D., Stewart, J. N., & Mead, J. R. (2002). Susceptibility to Cryptosporidium parvum infections in cytokine- and chemokine-receptor knockout mice. *J Parasitol, 88*(5), 1014-1016. doi:10.1645/0022-3395(2002)088[1014:STCPII]2.0.CO;2

Castellanos-Gonzalez, A., White, A. C., Jr., Ojo, K. K., Vidadala, R. S., Zhang, Z., Reid, M. C., . . . Van Voorhis, W. C. (2013). A novel calcium-dependent protein kinase inhibitor as a lead compound for treating cryptosporidiosis. *J Infect Dis, 208*(8), 1342-1348. doi:10.1093/infdis/jit327

Chalmers, R. M., & Katzer, F. (2013). Looking for Cryptosporidium: the application of advances in detection and diagnosis. *Trends in parasitology, 29*(5), 237-251. doi:10.1016/j.pt.2013.03.001

Chao, A. T., Lee, B. H., Wan, K. F., Selva, J., Zou, B., Gedeck, P., . . . Manjunatha, U. H. (2018). Development of a Cytopathic Effect-Based Phenotypic Screening Assay against Cryptosporidium. *ACS Infect Dis*. doi:10.1021/acsinfecdis.7b00247

Chatelain, E. (2015). Chagas disease drug discovery: toward a new era. *Journal of biomolecular screening : the official journal of the Society for Biomolecular Screening, 20*(1), 22-35. doi:10.1177/1087057114550585

Chatelain, E., & Ioset, J. R. (2011). Drug discovery and development for neglected diseases: the DNDi model. *Drug Des Devel Ther, 5*, 175-181. doi:10.2147/DDDT.S16381

Checkley, W., White, A. C., Jr., Jaganath, D., Arrowood, M. J., Chalmers, R. M., Chen, X. M., . . . Houpt, E. R. (2015). A review of the global burden, novel diagnostics, therapeutics, and vaccine targets for cryptosporidium. *Lancet Infect Dis, 15*(1), 85-94. doi:10.1016/s1473-3099(14)70772-8

Chen, X. M., Huang, B. Q., Splinter, P. L., Orth, J. D., Billadeau, D. D., McNiven, M. A., & LaRusso, N. F. (2004). Cdc42 and the actin-related protein/neural Wiskott-Aldrich syndrome protein network mediate cellular invasion by Cryptosporidium parvum. *Infect Immun, 72*(5), 3011-3021.

Chen, X. M., Keithly, J. S., Paya, C. V., & LaRusso, N. F. (2002). Cryptosporidiosis. *N Engl J Med, 346*(22), 1723-1731. doi:10.1056/NEJMra013170

Cryptosporidiosis: assessment of chemotherapy of males with acquired immune deficiency syndrome (AIDS). (1982). *MMWR. Morbidity and mortality weekly report, 31*(44), 589-592.

Current, W. L., & Reese, N. C. (1986). A comparison of endogenous development of three isolates of Cryptosporidium in suckling mice. *J Protozool, 33*(1), 98-108.

De Rycker, M., Hallyburton, I., Thomas, J., Campbell, L., Wyllie, S., Joshi, D., . . . Gray, D. W. (2013). Comparison of a high-throughput high-content intracellular Leishmania donovani assay with an axenic amastigote assay. *Antimicrob Agents Chemother, 57*(7), 2913-2922. doi:10.1128/aac.02398-12

Delves, M., Plouffe, D., Scheurer, C., Meister, S., Wittlin, S., Winzeler, E. A., . . . Leroy, D. (2012). The activities of current antimalarial drugs on the life cycle stages of Plasmodium: a comparative study with human and rodent parasites. *PLoS Med, 9*(2), e1001169. doi:10.1371/journal.pmed.1001169

Dillingham, R. A., Pinkerton, R., Leger, P., Severe, P., Guerrant, R. L., Pape, J. W., & Fitzgerald, D. W. (2009). High early mortality in patients with chronic acquired immunodeficiency syndrome diarrhea initiating antiretroviral therapy in Haiti: a case-control study. *Am J Trop Med Hyg, 80*(6), 1060-1064.

Disease, G. B. D., Injury, I., & Prevalence, C. (2016). Global, regional, and national incidence, prevalence, and years lived with disability for 310 diseases and injuries, 1990-2015: a systematic analysis for the Global Burden of Disease Study 2015. *Lancet, 388*(10053), 1545-1602. doi:10.1016/S0140-6736(16)31678-6

Downey, A. S., Chong, C. R., Graczyk, T. K., & Sullivan, D. J. (2008). Efficacy of pyrvinium pamoate against Cryptosporidium parvum infection in vitro and in a neonatal mouse model. *Antimicrob Agents Chemother, 52*(9), 3106-3112. doi:10.1128/aac.00207-08

Duffy, S., Sykes, M. L., Jones, A. J., Shelper, T. B., Simpson, M., Lang, R., . . . Avery, V. M. (2017). Screening the Medicines for Malaria Venture Pathogen Box across Multiple Pathogens Reclassifies Starting Points for Open-Source Drug Discovery. *Antimicrob Agents Chemother, 61*(9). doi:10.1128/aac.00379-17

DuPont, H. L., Chappell, C. L., Sterling, C. R., Okhuysen, P. C., Rose, J. B., & Jakubowski, W. (1995). The Infectivity of Cryptosporidium parvum in Healthy Volunteers. *New England Journal of Medicine, 332*(13), 855-859. doi:doi:10.1056/NEJM199503303321304

Eder, J., Sedrani, R., & Wiesmann, C. (2014). The discovery of first-in-class drugs: origins and evolution. *Nat Rev Drug Discov, 13*(8), 577-587. doi:10.1038/nrd4336

Elliott, D. A., Coleman, D. J., Lane, M. A., May, R. C., Machesky, L. M., & Clark, D. P. (2001). Cryptosporidium parvum infection requires host cell actin polymerization. *Infect Immun, 69*(9), 5940-5942.

Fayer, R., & Xiao, L. (2007). *Cryptosporidium and Cryptosporidiosis, Second Edition*: Taylor & Francis.

Flanigan, T., Whalen, C., Turner, J., Soave, R., Toerner, J., Havlir, D., & Kotler, D. (1992). Cryptosporidium Infection and CD4 Counts. *Annals of Internal Medicine, 116*(10), 840-842. doi:10.7326/0003-4819-116-10-840

Gamo, F. J., Sanz, L. M., Vidal, J., de Cozar, C., Alvarez, E., Lavandera, J. L., . . . Garcia-Bustos, J. F. (2010). Thousands of chemical starting points for antimalarial lead identification. *Nature, 465*(7296), 305-310. doi:10.1038/nature09107

Gollapalli, D. R., Macpherson, I. S., Liechti, G., Gorla, S. K., Goldberg, J. B., & Hedstrom, L. (2010). Structural determinants of inhibitor selectivity in prokaryotic IMP dehydrogenases. *Chemistry & biology, 17*(10), 1084-1091. doi:10.1016/j.chembiol.2010.07.014

Gorla, S. K., Kavitha, M., Zhang, M., Liu, X., Sharling, L., Gollapalli, D. R., . . . Cuny, G. D. (2012). Selective and potent urea inhibitors of cryptosporidium parvum inosine 5'-monophosphate dehydrogenase. *Journal of medicinal chemistry, 55*(17), 7759-7771. doi:10.1021/jm3007917

Gorla, S. K., McNair, N. N., Yang, G., Gao, S., Hu, M., Jala, V. R., . . . Hedstrom, L. (2014). Validation of IMP dehydrogenase inhibitors in a mouse model of cryptosporidiosis. *Antimicrob Agents Chemother, 58*(3), 1603-1614. doi:10.1128/aac.02075-13

Griffiths, J. K., Theodos, C., Paris, M., & Tzipori, S. (1998). The gamma interferon gene knockout mouse: a highly sensitive model for evaluation of therapeutic agents against Cryptosporidium parvum. *J Clin Microbiol, 36*(9), 2503-2508.

Guerrant, D. I., Moore, S. R., Lima, A. A., Patrick, P. D., Schorling, J. B., & Guerrant, R. L. (1999). Association of early childhood diarrhea and cryptosporidiosis with impaired physical fitness and cognitive function four-seven years later in a poor urban community in northeast Brazil. *Am J Trop Med Hyg, 61*(5), 707-713.

Guiguemde, W. A., Shelat, A. A., Bouck, D., Duffy, S., Crowther, G. J., Davis, P. H., . . . Guy, R. K. (2010). Chemical genetics of Plasmodium falciparum. *Nature, 465*(7296), 311-315. doi:10.1038/nature09099

Hlavsa, M. C., Roberts, V. A., Anderson, A. R., Hill, V. R., Kahler, A. M., Orr, M., . . . Yoder, J. S. (2011). Surveillance for waterborne disease outbreaks and other health events associated with recreational water --- United States, 2007--2008. *MMWR. Surveillance summaries : Morbidity and mortality weekly report. Surveillance summaries / CDC, 60*(12), 1-32.

Hobbs, C. V., Neal, J., Conteh, S., Donnelly, L., Chen, J., Marsh, K., . . . Duffy, P. E. (2014). HIV treatments reduce malaria liver stage burden in a non-human

primate model of malaria infection at clinically relevant concentrations in vivo. *PLoS One*, *9*(7), e100138. doi:10.1371/journal.pone.0100138

Human cryptosporidiosis--Alabama. (1982). *MMWR. Morbidity and mortality weekly report*, *31*(19), 252-254.

Hunter, P. R., Hughes, S., Woodhouse, S., Nicholas, R., Syed, Q., Chalmers, R. M., . . . Goodacre, J. (2004). Health Sequelae of Human Cryptosporidiosis in Immunocompetent Patients. *Clinical Infectious Diseases*, *39*(4), 504-510. doi:10.1086/422649

Hunter, P. R., & Thompson, R. C. A. (2005). The zoonotic transmission of Giardia and Cryptosporidium. *Int J Parasitol*, *35*(11–12), 1181-1190. doi:http://dx.doi.org/10.1016/j.ijpara.2005.07.009

Huston, C. D., Spangenberg, T., Burrows, J., Willis, P., Wells, T. N., & van Voorhis, W. (2015). A Proposed Target Product Profile and Developmental Cascade for New Cryptosporidiosis Treatments. *PLoS Negl Trop Dis*, *9*(10), e0003987. doi:10.1371/journal.pntd.0003987

Ito, M., Hiramatsu, H., Kobayashi, K., Suzue, K., Kawahata, M., Hioki, K., . . . Nakahata, T. (2002). NOD/SCID/gamma(c)(null) mouse: an excellent recipient mouse model for engraftment of human cells. *Blood*, *100*(9), 3175-3182. doi:10.1182/blood-2001-12-0207

Jain, V., Yogavel, M., Kikuchi, H., Oshima, Y., Hariguchi, N., Matsumoto, M., . . . Sharma, A. (2017). Targeting Prolyl-tRNA Synthetase to Accelerate Drug Discovery against Malaria, Leishmaniasis, Toxoplasmosis, Cryptosporidiosis, and Coccidiosis. *Structure*, *25*(10), 1495-1505.e1496. doi:10.1016/j.str.2017.07.015

Jumani, R. S., Bessoff, K., Love, M. S., Miller, P., Stebbins, E. E., Teixeira, J. E., . . . Huston, C. D. (2018). A Novel Piperazine-Based Drug Lead for Cryptosporidiosis from the Medicines for Malaria Venture Open Access Malaria Box. *Antimicrob Agents Chemother*. doi:10.1128/aac.01505-17

Kato, N., Comer, E., Sakata-Kato, T., Sharma, A., Sharma, M., Maetani, M., . . . Schreiber, S. L. (2016). Diversity-oriented synthesis yields novel multistage antimalarial inhibitors. *Nature*, *538*(7625), 344-349. doi:10.1038/nature19804

Katsuno, K., Burrows, J. N., Duncan, K., Hooft van Huijsduijnen, R., Kaneko, T., Kita, K., . . . Slingsby, B. T. (2015). Hit and lead criteria in drug discovery for infectious diseases of the developing world. *Nat Rev Drug Discov*, *14*(11), 751-758. doi:10.1038/nrd4683

Khanna, I. (2012). Drug discovery in pharmaceutical industry: productivity challenges and trends. *Drug discovery today*, *17*(19-20), 1088-1102. doi:10.1016/j.drudis.2012.05.007

Korpe, P. S., Haque, R., Gilchrist, C., Valencia, C., Niu, F., Lu, M., . . . Petri, W. A., Jr. (2016). Natural History of Cryptosporidiosis in a Longitudinal Study of Slum-Dwelling Bangladeshi Children: Association with Severe Malnutrition. *PLoS Negl Trop Dis*, *10*(5), e0004564. doi:10.1371/journal.pntd.0004564

Kotloff, K. L., Nataro, J. P., Blackwelder, W. C., Nasrin, D., Farag, T. H., Panchalingam, S., . . . Levine, M. M. (2013). Burden and aetiology of diarrhoeal

disease in infants and young children in developing countries (the Global Enteric Multicenter Study, GEMS): a prospective, case-control study. *Lancet, 382*(9888), 209-222. doi:10.1016/S0140-6736(13)60844-2

Lasser, K. H., Lewin, K. J., & Ryning, F. W. (1979). Cryptosporidial enteritis in a patient with congenital hypogammaglobulinemia. *Human pathology, 10*(2), 234-240.

Liu, J., Platts-Mills, J. A., Juma, J., Kabir, F., Nkeze, J., Okoi, C., . . . Houpt, E. R. (2016). Use of quantitative molecular diagnostic methods to identify causes of diarrhoea in children: a reanalysis of the GEMS case-control study. *Lancet, 388*(10051), 1291-1301. doi:10.1016/S0140-6736(16)31529-X

Love, M. S., Beasley, F. C., Jumani, R. S., Wright, T. M., Chatterjee, A. K., Huston, C. D., . . . McNamara, C. W. (2017). A high-throughput phenotypic screen identifies clofazimine as a potential treatment for cryptosporidiosis. *PLoS Negl Trop Dis, 11*(2), e0005373. doi:10.1371/journal.pntd.0005373

Mac Kenzie, W. R., Hoxie, N. J., Proctor, M. E., Gradus, M. S., Blair, K. A., Peterson, D. E., . . . Davis, J. P. (1994). A Massive Outbreak in Milwaukee of Cryptosporidium Infection Transmitted through the Public Water Supply. *New England Journal of Medicine, 331*(3), 161-167. doi:doi:10.1056/NEJM199407213310304

Macfarlane, D. E., & Horner-Bryce, J. (1987). Cryptosporidiosis in well-nourished and malnourished children. *Acta Paediatr Scand, 76*(3), 474-477.

Malebranche, R., Arnoux, E., Guerin, J. M., Pierre, G. D., Laroche, A. C., Pean-Guichard, C., . . . et al. (1983). Acquired immunodeficiency syndrome with severe gastrointestinal manifestations in Haiti. *Lancet, 2*(8355), 873-878.

Manjunatha, U. H., Chao, A. T., Leong, F. J., & Diagana, T. T. (2016). Cryptosporidiosis Drug Discovery: Opportunities and Challenges. *ACS Infect Dis, 2*(8), 530-537. doi:10.1021/acsinfecdis.6b00094

Manjunatha, U. H., Vinayak, S., Zambriski, J. A., Chao, A. T., Sy, T., Noble, C. G., . . . Diagana, T. T. (2017). A Cryptosporidium PI(4)K inhibitor is a drug candidate for cryptosporidiosis. *Nature, 546*(7658), 376-380. doi:10.1038/nature22337

Maurya, S. K., Gollapalli, D. R., Kirubakaran, S., Zhang, M., Johnson, C. R., Benjamin, N. N., . . . Cuny, G. D. (2009). Triazole inhibitors of Cryptosporidium parvum inosine 5'-monophosphate dehydrogenase. *J Med Chem, 52*(15), 4623-4630. doi:10.1021/jm900410u

Mauzy, M. J., Enomoto, S., Lancto, C. A., Abrahamsen, M. S., & Rutherford, M. S. (2012). The Cryptosporidium parvum transcriptome during in vitro development. *PLoS One, 7*(3), e31715. doi:10.1371/journal.pone.0031715

Meisel, J. L., Perera, D. R., Meligro, C., & Rubin, C. E. (1976). Overwhelming watery diarrhea associated with a cryptosporidium in an immunosuppressed patient. *Gastroenterology, 70*(6), 1156-1160.

Meuten, D. J., Van Kruiningen, H. J., & Lein, D. H. (1974). Cryptosporidiosis in a calf. *Journal of the American Veterinary Medical Association, 165*(10), 914-917.

Mlambo, G., Coppens, I., & Kumar, N. (2012). Aberrant sporogonic development of Dmc1 (a meiotic recombinase) deficient Plasmodium berghei parasites. *PLoS One, 7*(12), e52480. doi:10.1371/journal.pone.0052480

Molina, I., Gomez i Prat, J., Salvador, F., Trevino, B., Sulleiro, E., Serre, N., . . . Pahissa, A. (2014). Randomized trial of posaconazole and benznidazole for chronic Chagas' disease. *N Engl J Med, 370*(20), 1899-1908. doi:10.1056/NEJMoa1313122

Morada, M., Lee, S., Gunther-Cummins, L., Weiss, L. M., Widmer, G., Tzipori, S., & Yarlett, N. (2016). Continuous culture of Cryptosporidium parvum using hollow fiber technology. *Int J Parasitol, 46*(1), 21-29. doi:10.1016/j.ijpara.2015.07.006

Mortality, G. B. D., & Causes of Death, C. (2016). Global, regional, and national life expectancy, all-cause mortality, and cause-specific mortality for 249 causes of death, 1980-2015: a systematic analysis for the Global Burden of Disease Study 2015. *Lancet, 388*(10053), 1459-1544. doi:10.1016/S0140-6736(16)31012-1

Murphy, R. C., Ojo, K. K., Larson, E. T., Castellanos-Gonzalez, A., Perera, B. G., Keyloun, K. R., . . . Maly, D. J. (2010). Discovery of Potent and Selective Inhibitors of Calcium-Dependent Protein Kinase 1 (CDPK1) from C. parvum and T. gondii. *ACS Med Chem Lett, 1*(7), 331-335. doi:10.1021/ml100096t

Murtagh, F., & Legendre, P. (2014). Ward's Hierarchical Agglomerative Clustering Method: Which Algorithms Implement Ward's Criterion? . *Journal of Classification, 31*(3), 274-295.

Navin, T. R., Weber, R., Vugia, D. J., Rimland, D., Roberts, J. M., Addiss, D. G., . . . Bryan, R. T. (1999). Declining CD4+ T-lymphocyte counts are associated with increased risk of enteric parasitosis and chronic diarrhea: results of a 3-year longitudinal study. *J Acquir Immune Defic Syndr Hum Retrovirol, 20*(2), 154-159.

Ndao, M., Nath-Chowdhury, M., Sajid, M., Marcus, V., Mashiyama, S. T., Sakanari, J., . . . Caffrey, C. R. (2013). A cysteine protease inhibitor rescues mice from a lethal Cryptosporidium parvum infection. *Antimicrob Agents Chemother, 57*(12), 6063-6073. doi:10.1128/aac.00734-13

Nime, F. A., Burek, J. D., Page, D. L., Holscher, M. A., & Yardley, J. H. (1976). Acute enterocolitis in a human being infected with the protozoan Cryptosporidium. *Gastroenterology, 70*(4), 592-598.

Nwaka, S., & Hudson, A. (2006). Innovative lead discovery strategies for tropical diseases. *Nat Rev Drug Discov, 5*(11), 941-955. doi:10.1038/nrd2144

Nwaka, S., Ramirez, B., Brun, R., Maes, L., Douglas, F., & Ridley, R. (2009). Advancing drug innovation for neglected diseases-criteria for lead progression. *PLoS Negl Trop Dis, 3*(8), e440. doi:10.1371/journal.pntd.0000440

Nwaka, S., & Ridley, R. G. (2003). Virtual drug discovery and development for neglected diseases through public-private partnerships. *Nat Rev Drug Discov, 2*(11), 919-928. doi:10.1038/nrd1230

Panciera, R. J., Thomassen, R. W., & Garner, F. M. (1971). Cryptosporidial Infection in a Calf. *Veterinary Pathology Online, 8*(5-6), 479-484. doi:10.1177/030098587100800 5-00610

Pawlowic, M. C., Vinayak, S., Sateriale, A., Brooks, C. F., & Striepen, B. (2017). Generating and Maintaining Transgenic Cryptosporidium parvum Parasites. *Curr Protoc Microbiol, 46*, 20B 22 21-20B 22 32. doi:10.1002/cpmc.33

Payne, D. J., Gwynn, M. N., Holmes, D. J., & Pompliano, D. L. (2007). Drugs for bad bugs: confronting the challenges of antibacterial discovery. *Nat Rev Drug Discov, 6*(1), 29-40. doi:10.1038/nrd2201

Perkins, F. O., Barta, J. R., Clopton, R. E., Peirce, M. A., & Upton, S. J. (2000). *Phylum Apicomplexa* (2nd ed.): Society of Protozoologists.

Peterson, J. R., Bickford, L. C., Morgan, D., Kim, A. S., Ouerfelli, O., Kirschner, M. W., & Rosen, M. K. (2004). Chemical inhibition of N-WASP by stabilization of a native autoinhibited conformation. *Nature structural & molecular biology, 11*(8), 747-755. doi:10.1038/nsmb796

Pham, J. S., Dawson, K. L., Jackson, K. E., Lim, E. E., Pasaje, C. F., Turner, K. E., & Ralph, S. A. (2014). Aminoacyl-tRNA synthetases as drug targets in eukaryotic parasites. *Int J Parasitol Drugs Drug Resist, 4*(1), 1-13. doi:10.1016/j.ijpddr.2013.10.001

Pink, R., Hudson, A., Mouries, M. A., & Bendig, M. (2005). Opportunities and challenges in antiparasitic drug discovery. *Nat Rev Drug Discov, 4*(9), 727-740. doi:10.1038/nrd1824

Platts-Mills, J. A., Babji, S., Bodhidatta, L., Gratz, J., Haque, R., Havt, A., . . . Investigators, M.-E. N. (2015). Pathogen-specific burdens of community diarrhoea in developing countries: a multisite birth cohort study (MAL-ED). *Lancet Glob Health, 3*(9), e564-575. doi:10.1016/S2214-109X(15)00151-5

Plouffe, D., Brinker, A., McNamara, C., Henson, K., Kato, N., Kuhen, K., . . . Winzeler, E. A. (2008). In silico activity profiling reveals the mechanism of action of antimalarials discovered in a high-throughput screen. *Proc Natl Acad Sci U S A, 105*(26), 9059-9064. doi:10.1073/pnas.0802982105

Reese, N. C., Current, W. L., Ernst, J. V., & Bailey, W. S. (1982). Cryptosporidiosis of Man and Calf: a Case Report and Results of Experimental Infections in Mice and Rats. *Am J Trop Med Hyg, 31*(2), 226-229.

Rider, S. D., Jr., Cai, X., Sullivan, W. J., Jr., Smith, A. T., Radke, J., White, M., & Zhu, G. (2005). The protozoan parasite Cryptosporidium parvum possesses two functionally and evolutionarily divergent replication protein A large subunits. *J Biol Chem, 280*(36), 31460-31469. doi:10.1074/jbc.M504466200

Rose, J. B., Huffman, D. E., & Gennaccaro, A. (2002). Risk and control of waterborne cryptosporidiosis. *FEMS microbiology reviews, 26*(2), 113-123.

Salic, A., & Mitchison, T. J. (2008). A chemical method for fast and sensitive detection of DNA synthesis in vivo. *Proc Natl Acad Sci U S A, 105*(7), 2415-2420. doi:10.1073/pnas.0712168105

Savitski, M. M., Reinhard, F. B., Franken, H., Werner, T., Savitski, M. F., Eberhard, D., . . . Drewes, G. (2014). Tracking cancer drugs in living cells by thermal profiling of the proteome. *Science, 346*(6205), 1255784. doi:10.1126/science.1255784

Schaefer, D. A., Betzer, D. P., Smith, K. D., Millman, Z. G., Michalski, H. C., Menchaca, S. E., . . . Riggs, M. W. (2016). Novel Bumped Kinase Inhibitors Are Safe and Effective Therapeutics in the Calf Clinical Model for Cryptosporidiosis. *J Infect Dis, 214*(12), 1856-1864. doi:10.1093/infdis/jiw488

Schuster, F. L. (2002). Cultivation of plasmodium spp. *Clin Microbiol Rev, 15*(3), 355-364.

Shibata, S., Gillespie, J. R., Kelley, A. M., Napuli, A. J., Zhang, Z., Kovzun, K. V., . . . Buckner, F. S. (2011). Selective inhibitors of methionyl-tRNA synthetase have potent activity against Trypanosoma brucei Infection in Mice. *Antimicrob Agents Chemother, 55*(5), 1982-1989. doi:10.1128/aac.01796-10

Shirley, D. A., Moonah, S. N., & Kotloff, K. L. (2012). Burden of disease from cryptosporidiosis. *Current opinion in infectious diseases, 25*(5), 555-563. doi:10.1097/QCO.0b013e328357e569

Shoultz, D. A., de Hostos, E. L., & Choy, R. K. (2016). Addressing Cryptosporidium Infection among Young Children in Low-Income Settings: The Crucial Role of New and Existing Drugs for Reducing Morbidity and Mortality. *PLoS Negl Trop Dis, 10*(1), e0004242. doi:10.1371/journal.pntd.0004242

Shultz, L. D., Lyons, B. L., Burzenski, L. M., Gott, B., Chen, X., Chaleff, S., . . . Handgretinger, R. (2005). Human lymphoid and myeloid cell development in NOD/LtSz-scid IL2R gamma null mice engrafted with mobilized human hemopoietic stem cells. *J Immunol, 174*(10), 6477-6489.

Slavin, D. (1955). Cryptosporidium meleagridis (sp. nov.). *J Comp Pathol, 65*(3), 262-266.

Sonzogni-Desautels, K., Renteria, A. E., Camargo, F. V., Di Lenardo, T. Z., Mikhail, A., Arrowood, M. J., . . . Ndao, M. (2015). Oleylphosphocholine (OlPC) arrests Cryptosporidium parvum growth in vitro and prevents lethal infection in interferon gamma receptor knock-out mice. *Front Microbiol, 6*, 973. doi:10.3389/fmicb.2015.00973

Sow, S. O., Muhsen, K., Nasrin, D., Blackwelder, W. C., Wu, Y., Farag, T. H., . . . Levine, M. M. (2016). The Burden of Cryptosporidium Diarrheal Disease among Children < 24 Months of Age in Moderate/High Mortality Regions of Sub-Saharan Africa and South Asia, Utilizing Data from the Global Enteric Multicenter Study (GEMS). *PLoS Negl Trop Dis, 10*(5), e0004729. doi:10.1371/journal.pntd.0004729

Stebbins, E., Jumani, R. S., Klopfer, C., Barlow, J., Miller, P., Campbell, M. A., . . . Huston, C. D. (2018). Clinical and microbiologic efficacy of the piperazine-based drug lead MMV665917 in the dairy calf cryptosporidiosis model. *PLoS Negl Trop Dis, 12*(1), e0006183. doi:10.1371/journal.pntd.0006183

Swinney, D. C. (2013). Phenotypic vs. target-based drug discovery for first-in-class medicines. *Clin Pharmacol Ther, 93*(4), 299-301. doi:10.1038/clpt.2012.236

Theodos, C. M., Griffiths, J. K., D'Onfro, J., Fairfield, A., & Tzipori, S. (1998). Efficacy of nitazoxanide against Cryptosporidium parvum in cell culture and in animal models. *Antimicrob Agents Chemother, 42*(8), 1959-1965.

Trotz-Williams, L. A., Jarvie, B. D., Peregrine, A. S., Duffield, T. F., & Leslie, K. E. (2011). Efficacy of halofuginone lactate in the prevention of cryptosporidiosis in dairy calves. *Vet Rec, 168*(19), 509. doi:10.1136/vr.d1492

Trouiller, P., Olliaro, P., Torreele, E., Orbinski, J., Laing, R., & Ford, N. (2002). Drug development for neglected diseases: a deficient market and a public-health policy failure. *Lancet, 359*(9324), 2188-2194. doi:10.1016/S0140-6736(02)09096-7

Tyzzer, E. E. (1907). A sporozoan found in the peptic glands of the common mouse. *Proc. Soc. Exp. Biol. Med., 5*, 12-13.

Tyzzer, E. E. (1910). An extracellular Coccidium, Cryptosporidium Muris (Gen. Et Sp. Nov.), of the gastric Glands of the Common Mouse. *The Journal of medical research, 23*(3), 487-510 483.

Tzipori, S., Rand, W., & Theodos, C. (1995). Evaluation of a two-phase scid mouse model preconditioned with anti-interferon-gamma monoclonal antibody for drug testing against Cryptosporidium parvum. *J Infect Dis, 172*(4), 1160-1164.

U.S. Cancer Statistics Working Group, (2017). United States Cancer Statistics: 1999-2014 Incidence and Mortality Web-based Report. Atlanta: U.S. Department of Health and Human Services, Centers for Disease Control and Prevention and National Cancer Institute. Retrieved from www.cdc.gov/uscs

Van Voorhis, W. C., Adams, J. H., Adelfio, R., Ahyong, V., Akabas, M. H., Alano, P., . . . Willis, P. A. (2016). Open Source Drug Discovery with the Malaria Box Compound Collection for Neglected Diseases and Beyond. *PLoS Pathog, 12*(7), e1005763. doi:10.1371/journal.ppat.1005763

Vinayak, S., Pawlowic, M. C., Sateriale, A., Brooks, C. F., Studstill, C. J., Bar-Peled, Y., . . . Striepen, B. (2015). Genetic modification of the diarrhoeal pathogen Cryptosporidium parvum. *Nature, 523*(7561), 477-480. doi:10.1038/nature14651

Ward Jr, J. H. (1963). Hierarchical grouping to optimize an objective function. *Journal of the American statistical association, 58*(301), 236-244.

Weisburger, W. R., Hutcheon, D. F., Yardley, J. H., Roche, J. C., Hillis, W. D., & Charache, P. (1979). Cryptosporidiosis in an immunosuppressed renal-transplant recipient with IgA deficiency. *American journal of clinical pathology, 72*(3), 473-478.

You, X., Schinazi, R. F., Arrowood, M. J., Lejkowski, M., Juodawlkis, A. S., & Mead, J. R. (1998). In-vitro activities of paromomycin and lasalocid evaluated in combination against Cryptosporidium parvum. *J Antimicrob Chemother, 41*(2), 293-296.

Zambriski, J. A., Nydam, D. V., Bowman, D. D., Bellosa, M. L., Burton, A. J., Linden, T. C., . . . Mohammed, H. O. (2013). Description of fecal shedding of Cryptosporidium parvum oocysts in experimentally challenged dairy calves. *Parasitol Res, 112*(3), 1247-1254. doi:10.1007/s00436-012-3258-2

Zhang, J. H. (1999). A Simple Statistical Parameter for Use in Evaluation and Validation of High Throughput Screening Assays. *Journal of Biomolecular Screening, 4*(2), 67-73. doi:10.1177/108705719900400206

APPENDIX I: UPDATES ON DEVELOPMENT OF MMV006169 AND ITS VARIANTS FOR TREATMENT OF CRYPTOSPORIDIOSIS

The screen of the Medicines for Malaria Ventures Open Access Malaria Box also identified MMV006169 (B-1) as a promising hit with several potent variants (2,4-diaminoquinazoline series) (Bessoff et al., 2014) and this chapter will discuss some of our efforts towards developing these hits for cryptosporidiosis. Chemical structure search using the SciFinder database (https://scifinder.cas.org/) identified the series to be related to DBeQ, which is a reversible inhibitor of the p97 ATPase (Chou et al., 2011). The protein p97 belongs to the ATPase associated with diverse cellular activities (AAA) family, and is conserved across eukaryotic species. In fact, retrospectively we found that DBeQ was one of the active variants identified from our structural activity relationship studies (B-23). This compound behaved similarly to all other 2,4-diaminoquinazolines in the various life stage assays tested in chapter 3. The protein p97 is involved in a variety of functions, including shuttling of protein across the endoplasmic reticulum (ER) membrane as part of the ER-associated degradation pathway (ERAD), and is essential for viability in budding yeast (Giaever et al., 2002) and mice (Muller, Deinhardt, Rosewell, Warren, & Shima, 2007). Interestingly, this pathway has been explored for drug targets in malaria as several protozoan pathogens contain a minimal ERAD pathway when compared to the mammalian host making them more sensitive to drugs targeting this pathway (Harbut et al., 2012). The yeast p97 (called cdc48 or YDL126C) protein sequence from lab strain W303 was obtained from the Saccharomyces genome database (https://www.yeastgenome.org/) and a

protein BLAST was performed against *C. parvum* Iowa and *C. hominis* TU502 genomes on the CryptoDB website (http://cryptodb.org/). This identified cgd1_330 in *C. parvum* Iowa and Chro.10043 in *C. hominis* with 63% identity.

The protein is vital for yeast survival and temperature sensitive mutants of this protein have been used to study its function in yeast (Hsieh & Chen, 2011). We intended to make use of this yeast system to study the *C. parvum* p97 gene and test the hypothesis that B-1 inhibits the *C. parvum* p97. The high temperature sensitive cdc-48 mutant strain (cdc48-3) that cannot grow at 37 °C since the cdc48 is not functional along with control W303 strain were a kind gift from Dr, Rey-Huei Chen (Institute of Molecular Biology, Academia Sinica, and National Defense Medical Center, Taipei, Taiwan). Growth can be rescued in these strains with expression of wild type cdc48 using a shuttle vector. We plan to transfect the yeast cdc48-3 mutants with a plasmid expressing the *C. parvum* p97 gene under a gal promotor, and check if this gene complements the function of the yeast cdc48-3 mutant at the high temperatures. The cdc48-3 mutant is in the W303 strain background and the genotype of W303 is as follows:

Genotype: MATa/MATα leu2-3,112 trp1-1 can1-100 ura3-1 ade2-1 his3-11,15

Dr. Doug Johnson provided us with low expressing shuttle vectors p416 and high expression shuttle vector p426 (Mumberg, Muller, & Funk, 1994). When induced with galactose the temperature sensitive mutant (cdc48-3) transformed with vectors expressing yeast cdc48 grew normally at 30 °C and the growth was partially rescued growth at 37 °C with both p416 (Fig. 1) and p426 vactors (Fig. 2). Surprisingly, the

cdc48-3 mutants with vectors containing *C. parvum* p97 in p416 (Fig. 1) and p426 vectors (Fig. 2) did not grow at 30 °C and 37 °C in the presence of galactose. All these strains grew fine in the absence of galactose indicating inhibition of yeast growth upon expression of *C. parvum* p97.

We also collaborated with Dr. Adam Sateriale in Dr. Boris Striepen's lab to transiently overexpress *C. parvum* p97 *in vitro* and check for decrease in MMV006169 potency. However, the overexpression did not decrease MMV006169 potency. The transient system is not an ideal system due to low transfection efficiencies combined with short window of parasite culture. It is rather recommended to perform stable overexpression, but is more cumbersome as it involves surgeries and passage in mice to select the population desired. We have also collaborated with Dr. Bart Staker to express this protein as its ATPase activity can be tested *in vitro* to determine direct inhibition by the compound.

We also tested three scaffolds from this series, namely B-1, B-5 and B-13 in our chronic NOD SCID gamma mouse model of cryptosporidiosis, but the compounds did not have any efficacy (data not shown).

Transmission electron microscopy to visualize parasites after compound addition in the parasite persistence assay did not reveal any obvious differences in the parasitophorous vacuoles between MMV0061619 and DMSO treated samples (data not shown).

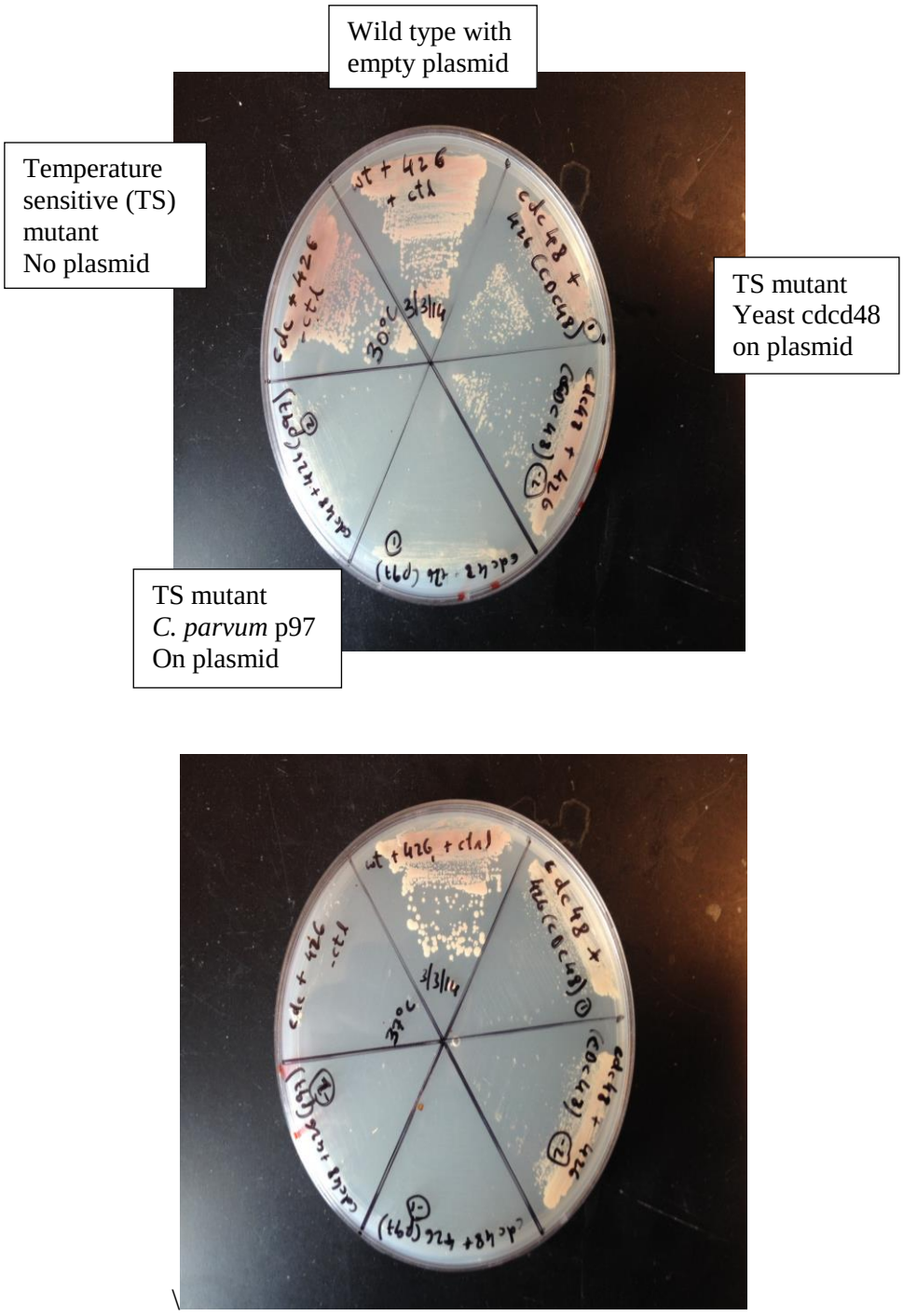

Figure 1. Attempt to complement yeast with *C. parvum* p97 using p416 vector.

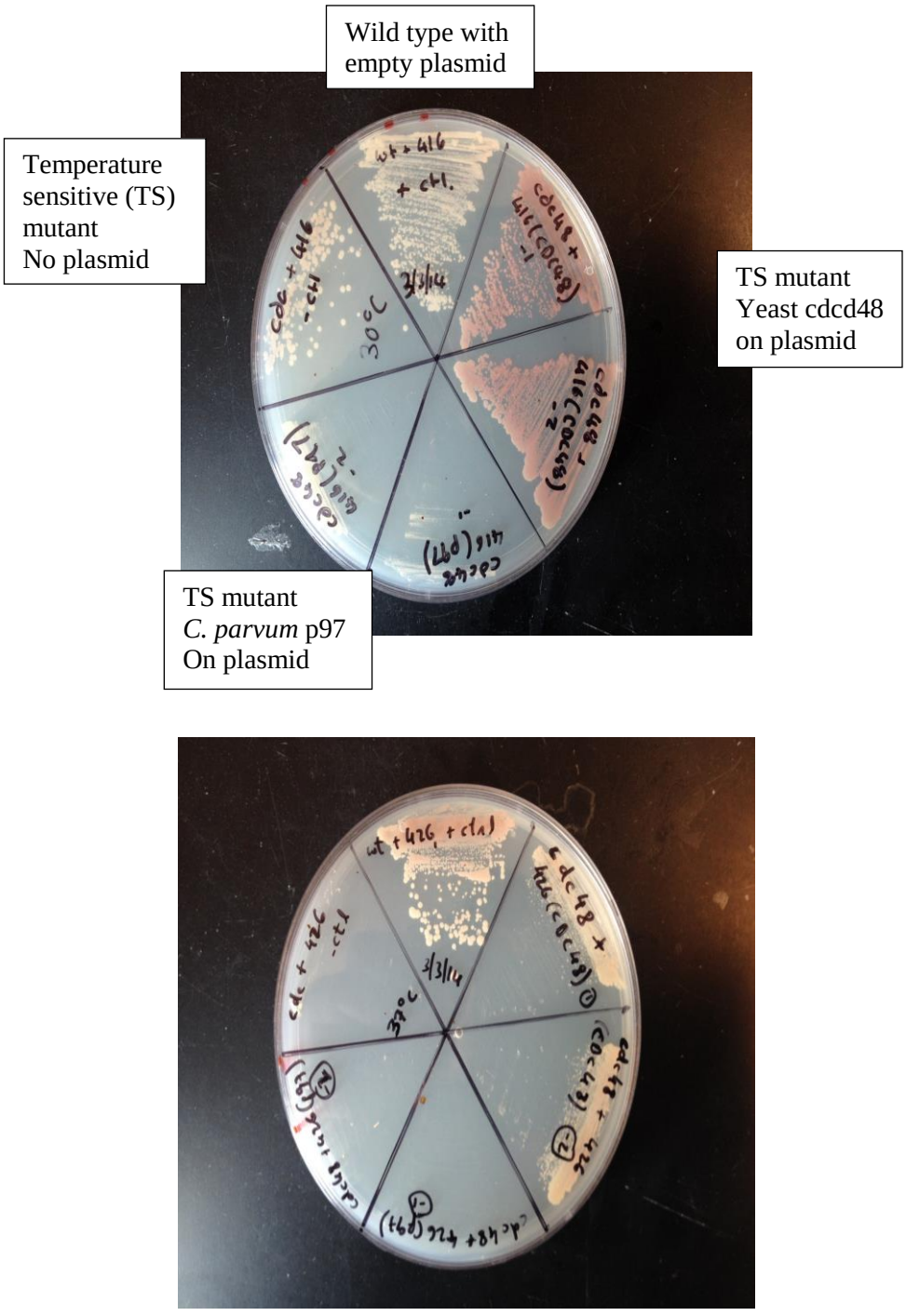

Figure 2. Attempt to complement yeast with *C. parvum* p97 using p426 vector.

References

Bessoff, K., Spangenberg, T., Foderaro, J. E., Jumani, R. S., Ward, G. E., & Huston, C. D. (2014). Identification of Cryptosporidium parvum active chemical series by Repurposing the open access malaria box. *Antimicrob Agents Chemother, 58*(5), 2731-2739. doi:10.1128/AAC.02641-13

Chou, T. F., Brown, S. J., Minond, D., Nordin, B. E., Li, K., Jones, A. C., . . . Deshaies, R. J. (2011). Reversible inhibitor of p97, DBeQ, impairs both ubiquitin-dependent and autophagic protein clearance pathways. *Proc Natl Acad Sci U S A, 108*(12), 4834-4839. doi:10.1073/pnas.1015312108

Giaever, G., Chu, A. M., Ni, L., Connelly, C., Riles, L., Veronneau, S., . . . Johnston, M. (2002). Functional profiling of the Saccharomyces cerevisiae genome. *Nature, 418*(6896), 387-391. doi:10.1038/nature00935

Harbut, M. B., Patel, B. A., Yeung, B. K., McNamara, C. W., Bright, A. T., Ballard, J., . . . Greenbaum, D. C. (2012). Targeting the ERAD pathway via inhibition of signal peptide peptidase for antiparasitic therapeutic design. *Proc Natl Acad Sci U S A, 109*(52), 21486-21491. doi:10.1073/pnas.1216016110

Hsieh, M. T., & Chen, R. H. (2011). Cdc48 and cofactors Npl4-Ufd1 are important for G1 progression during heat stress by maintaining cell wall integrity in Saccharomyces cerevisiae. *PLoS One, 6*(4), e18988. doi:10.1371/journal.pone.0018988

Muller, J. M., Deinhardt, K., Rosewell, I., Warren, G., & Shima, D. T. (2007). Targeted deletion of p97 (VCP/CDC48) in mouse results in early embryonic lethality. *Biochem Biophys Res Commun, 354*(2), 459-465. doi:10.1016/j.bbrc.2006.12.206

Mumberg, D., Muller, R., & Funk, M. (1994). Regulatable promoters of Saccharomyces cerevisiae: comparison of transcriptional activity and their use for heterologous expression. *Nucleic acids research, 22*(25), 5767-5768.

APPENDIX II: UPDATES ON DEVELOPMENT OF MMV403679 AND ITS VARIANTS FOR TREATMENT OF CRYPTOSPORIDIOSIS

MMV40679 (C-1) is an allopurinol-based scaffold identified as a promising hit from the Medicines for Malaria Venture Open Access Malaria Box (Bessoff et al., 2014). This section is going to outlay the developments made towards progressing this series for cryptosporidiosis. There were several promising variants with nanomolar potency against *C. parvum* identified ((Bessoff, Sateriale, Lee, & Huston, 2013) and data not shown). The washout experiment determined it to be a fast acting drug (Bessoff et al., 2013). It also displayed an exponential rate of parasite decay in the parasite persistence assay with maximum rate of parasite elimination achieved at $3\times EC_{90}$. Morphology of parasites were also visualized using transmission electron microscopy (TEM) using the parasite persistence assay experimental design (Fig. 1). TEM images showed that a higher proportion of parasites were in the meront stage compared to DMSO control. Furthermore, C-1 treated vacuoles were degenerating (Fig. 1). These data indicate that C-1 is cidal and possibly inhibits parasite egress when added at 24 hours on a mixed culture. However, the DNA synthesis assay showed that C-1 inhibits DNA synthesis when added earlier in infection cycle (3 hours post-infection), and hence, was active in the egress, motility and re-invasion assay (Chapter 3, Fig. 3). This was not known when the below mouse experiments were being conducted and it was assumed that C-1 is an egress inhibitor.

We tested several variants of C-1 in our chronic NOD SCID gamma mouse model of cryptosporidiosis and measured plasma levels of the compounds in these

experiments with a view to understand the pharmacokinetic (PK) properties that drive *in vivo* efficacy for this series. All the variants got absorbed to different degrees with 20 to 2830 × EC_{90} plasma levels achieved within 4 hours of a single oral dose of 100 mg/kg (Fig. 2). Nevertheless, none of the compounds reduced parasite shedding even after 7 days of dosing 100 mg/kg once daily (Fig. 3). Similar results were found when twice-daily dose, each of 50 mg/kg was given to mice for 4 days (data not shown). None of the compounds showed any signs of *in vitro* toxicity against host HCT-8 cells up to 100 μM (data not shown). Surprisingly, C-2 (F5091-0186) was toxic to mice at once daily dose of 100 mg/kg and killed mice 3 out of the 4 mice about 7 days after cessation of treatment. However, in the second experiment, it did not have any toxicity when 50 mg/kg was given twice a day (total of 100 mg/kg per day) for 4 days. This indicates that the compound is toxic when given at a higher single dose of 100 mg/kg or when given for a longer duration of 7 days or both. Based on the results we planned follow-up experiments such that each dose is ≤ 50 mg with not more than 100 mg given per day and mice not treated for more than 4 days.

We hypothesized that the C scaffold requires compounds to be continuously available in intestinal (apical side of cells) to be effective. Since C-2 was poorly absorbed compared to other variants, we wanted to test if the compound would be active when dosed frequently, such that high levels are continuously available in the intestine. Furthermore, to test the effect of drug on egress, we wanted to target the first stage of parasite life cycle *in vivo*; hence, mice were treated the same day after oral gavage with *C. parvum* oocysts (similar to acute mouse models of *C. parvum* infection

experiments wherein mice are treated soon after infection (Gorla et al., 2014)). In a modification of the egress, motility re-invasion assay, C-1 seemed to be ineffective when washed out after ~9.5 hours after infection, but appeared to be partially active when added ~9.5 hours post-infection as compared to addition at 3 hours post-infection (Fig. 4). Based on this experiment, *in vivo* dosing regimens were decided (Table 1). Based on gut transit times in mice from published literature (Padmanabhan, Grosse, Asad, Radda, & Golay, 2013), mice were treated either with 8 doses every 2 hours (to mimic complete exposure with compound added 3 hours post-infection *in vitro*), or given 4 doses every 2 hours after infection (mimic the in vitro washout experiment) (4 doses a.m.), or given 4 doses every 2 hours from ~10 hours post-infection (to mimic in vitro compound addition before egress). The total dose given was the same in all cases, that is, 100 mg/kg, which was divided into 4 doses or 8 doses. Mice were treated only on this day 1, and then mice were allowed to incubate as these mice start reliably shedding oocysts in the feces only after 6 days post-infection. Interestingly, all doses reduced oocysts shedding, but unfortunately, the mice starting getting sick about 6 days after treated. The mice treated with 4 doses soon after infection (4 doses am) were the worst hit and mice died on day 8 post infection. Mice treated with 4 days from ~10 hours post-infection did not die but were lethargic, with mice treated with 8 doses the least sick. Hence, although C-2 reduced oocysts shedding in all conditions (Fig. 5), the data are inconclusive as the compound could be indirectly altering oocysts shedding as it was lethal to mice. However, the data is indicative of apical exposure requirement for this series, and this should be confirmed with a different non-toxic variant and/or

tested with multiple doses on an established infection. The timing did not seem to make a difference (except for toxicity which could be due to higher amounts per dose in 4 doses) The increased toxicity might be related to the age of the mice, as these mice were treated approximately a week earlier than the previous experiments. The toxicity might be also due to co-infection of mice.

To test the apical or basolateral exposure requirement, we developed a transwell assay using HCT-8 and measurement of transwell resistance (Fig 6). The differentiated Caco2 cells were first tested in this assay, but an acceptable level of infection could not be established (data not shown). Hence, the assay was established with HCT-8 cells, which has the advantage of direct comparison with our regular assay and also, the assay is quick with only 2-3 days required to establish the resistance. The resistance of the monolayer decreases when the parasites egress and destroy the monolayer. Therefore, the assay cannot be used for compounds that act on stages after egress. But for C-1, an inhibitor of DNA synthesis, this assay is perfect. The only caution that the transport of C-1 across the monolayer is not known and might need to be determined to interpret the assay results. This assay can also be used to identify egress inhibitors. Furthermore, parasites could be stained using immunofluorescence by the regular assay method and imaged (data not shown) adding further value to the assay.

Scifinder search identified C-1 to be related to a human phosphodiesterase (PDE) inhibitor (Meng et al., 2012). A protein BLAST on CryptoDB of human PDE (GenBank: AAC39778.1) identified cgd6_500 as a homolog with E value 3e-35 on October 26, 2015. As with p97, Dr. Adam Sateriale transiently overexpressed *C.*

parvum cgd6_500 *in vitro* and tested C-1, but the potency did not decrease. The gene needs to be stably expressed to confirm the result. We have also collaborated with Dr. Bart Staker at the Center for Infectious Disease Research to express, purify and crystalize the *Cryptosporidium* protein. Potential future experiments include determining the effect of C-1 and its structural variants on phosphodiesterase activity of the protein *in vitro* using purified protein, and co-crystal structures of the protein with compound bound.

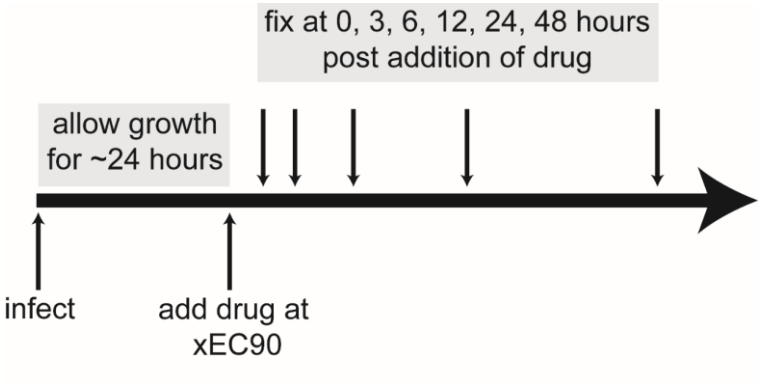

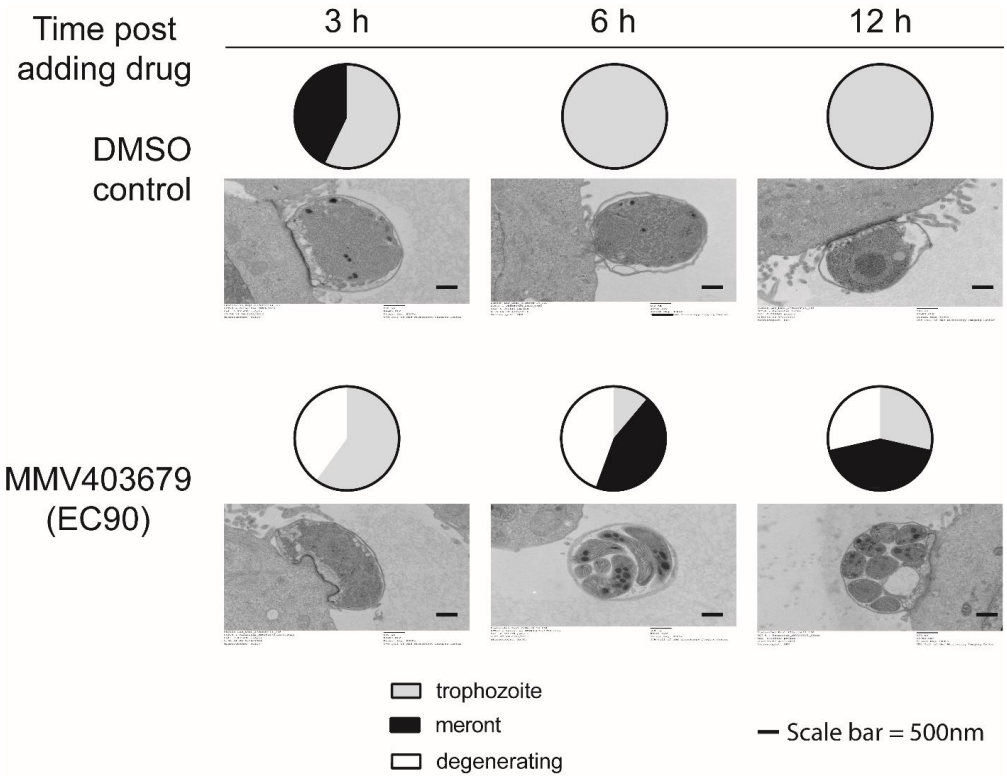

Figure 1. Transmission electron microscopy to get an insight into mechanism of action.

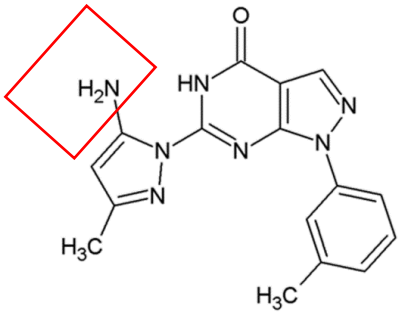

C-35

Mean serum levels

4.8µM (**25 x EC90**) at 0.5 h

3.8µM (**20 x EC90**) at 4 h

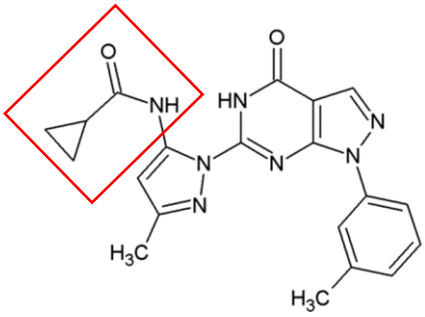

C-4

Mean serum levels

67µM (**1460 x EC90**) at 0.5 h

130µM (**2830 x EC90**) at 4 h

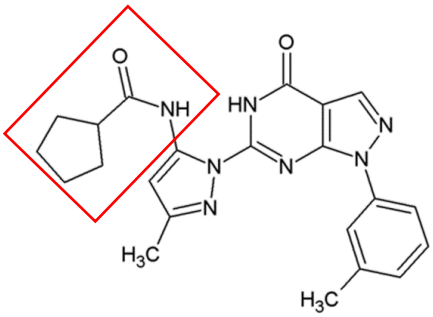

C-5

Mean serum levels

21µM (**330 x EC90**) at 0.5 h

29µM (**460 x EC90**) at 4 h

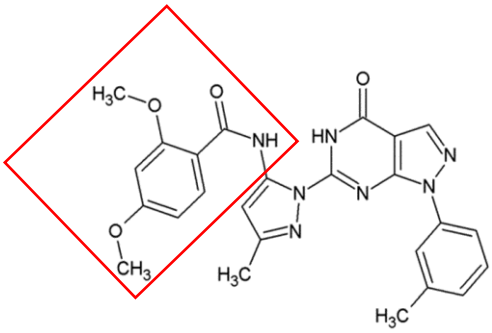

C-2

Mean serum levels

2.5µM (**60 x EC90**) at 0.5 h

13µM (**330 x EC90**) at 4 h

Figure 2. Plasma levels of MMV665917 variants in *C. parvum* infected NSG mice.

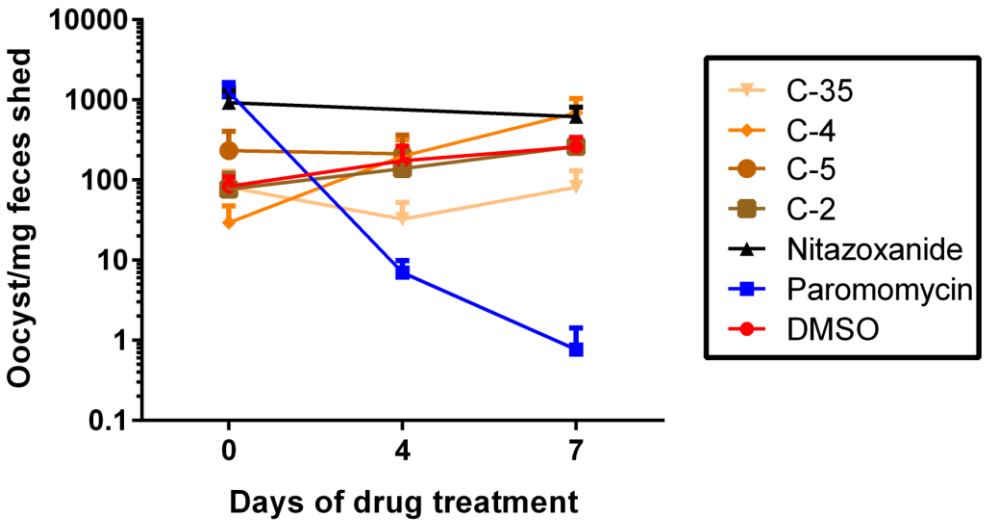

Figure 3. ***In vivo C. parvum*** **efficacy study of MMV403679 variants on an established infection in NSG mice.**

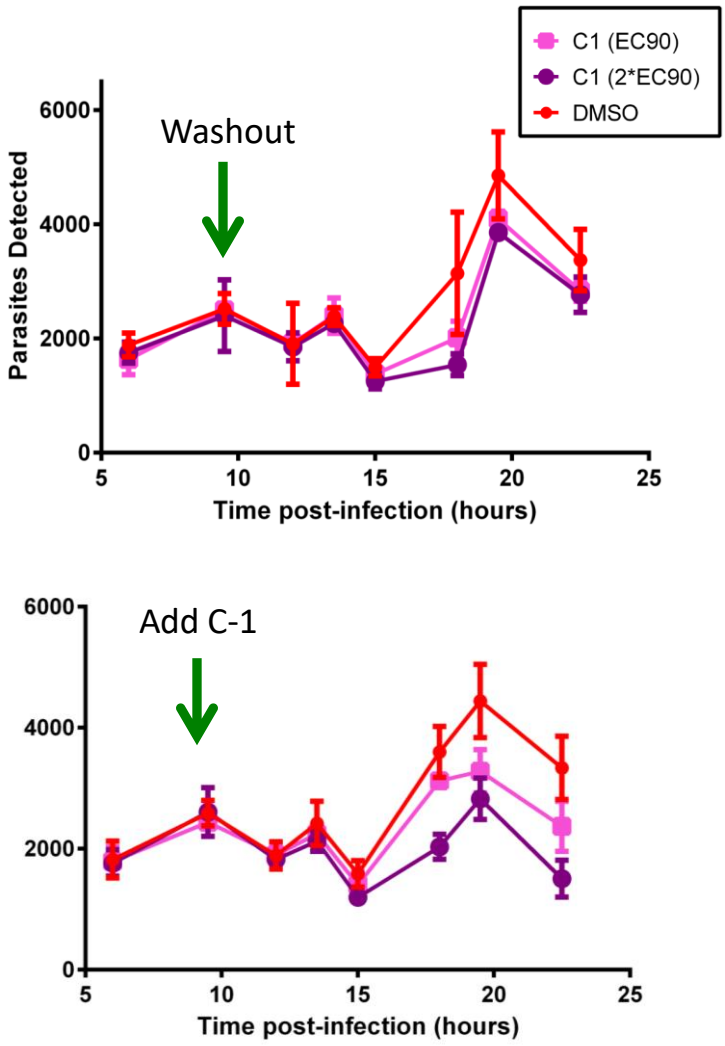

Figure 4. Washout or addition of MMV403679 (C-1) before initiation of parasite egress.

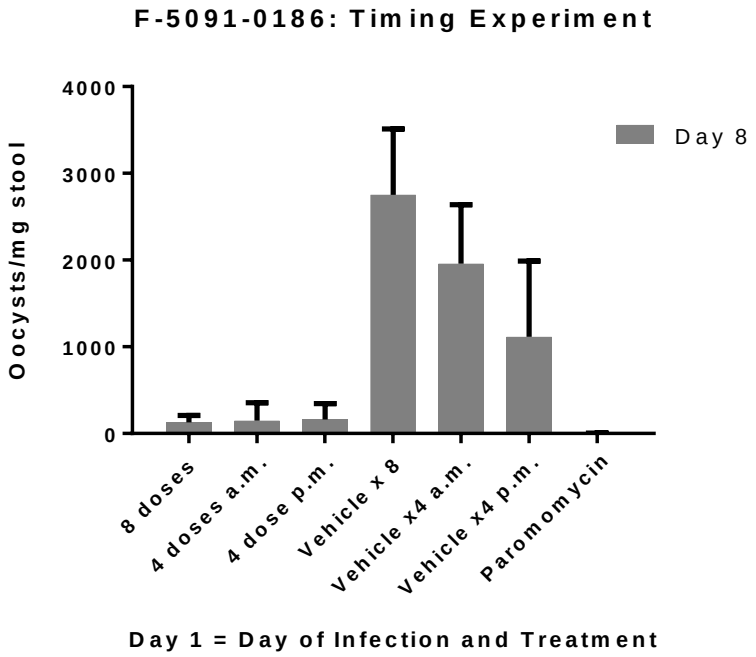

Figure 5. ***In vivo*** **efficacy of MMV403679 variant, F5091-0186 (C-2) soon after infection of NSG mice.**

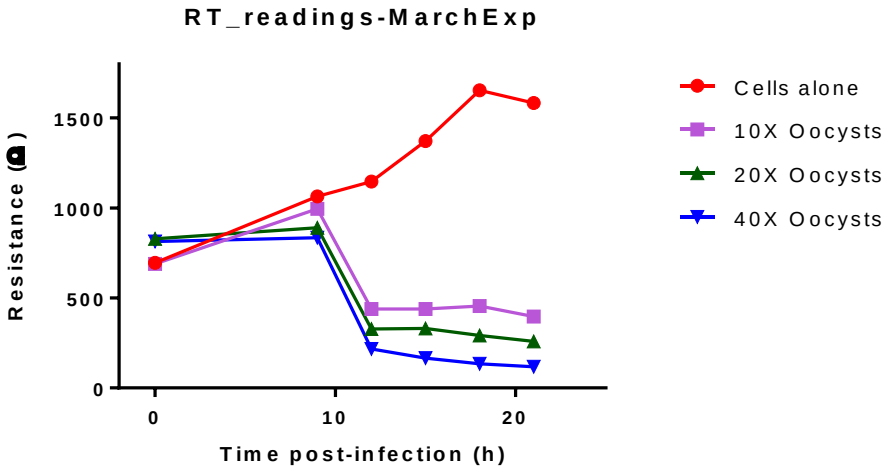

Figure 6. Transwell assay to measure effect of apical or basolateral exposure of compound on parasites.

Table 1. Compound C-2 dosing regime soon after infection

		8:00 AM	10:00 AM	12:00 PM	2:00 PM	4:00 PM	6:00 PM	8:00 PM	10:00 PM	12:00 AM
		10^5 oocysts	Compound treatemnt							
C-2 Compound	**A**	+	X	X	X	X	X	X	X	X
C-2 Compound	**B**	+	X	X	X	X	-	-	-	-
C-2 Compound	**C**	+	-	-	-	-	X	X	X	X
DMSO	**D**	+	X	X	X	X	X	X	X	X
DMSO	**E**	+	X	X	X	X	-	-	-	-
DMSO	**F**	+	-	-	-	-	X	X	X	X
Paromomycin	**G**	+	X	-	-	-	-	-	-	-

References

Bessoff, K., Sateriale, A., Lee, K. K., & Huston, C. D. (2013). Drug Repurposing Screen Reveals FDA-Approved Inhibitors of Human HMG-CoA Reductase and Isoprenoid Synthesis that Block Cryptosporidium parvum Growth. *Antimicrobial agents and chemotherapy*. doi:10.1128/AAC.02460-12

Bessoff, K., Spangenberg, T., Foderaro, J. E., Jumani, R. S., Ward, G. E., & Huston, C. D. (2014). Identification of Cryptosporidium parvum active chemical series by Repurposing the open access malaria box. *Antimicrob Agents Chemother, 58*(5), 2731-2739. doi:10.1128/AAC.02641-13

Gorla, S. K., McNair, N. N., Yang, G., Gao, S., Hu, M., Jala, V. R., . . . Hedstrom, L. (2014). Validation of IMP dehydrogenase inhibitors in a mouse model of cryptosporidiosis. *Antimicrob Agents Chemother, 58*(3), 1603-1614. doi:10.1128/aac.02075-13

Meng, F., Hou, J., Shao, Y. X., Wu, P. Y., Huang, M., Zhu, X., . . . Ke, H. (2012). Structure-based discovery of highly selective phosphodiesterase-9A inhibitors and implications for inhibitor design. *Journal of medicinal chemistry, 55*(19), 8549-8558. doi:10.1021/jm301189c

Padmanabhan, P., Grosse, J., Asad, A. B., Radda, G. K., & Golay, X. (2013). Gastrointestinal transit measurements in mice with 99mTc-DTPA-labeled activated charcoal using NanoSPECT-CT. *EJNMMI Res, 3*(1), 60. doi:10.1186/2191-219x-3-60

APPENDIX III: STRATEGIES TO IDENTIFY DRUG COMBINATIONS FOR TREATING CRYPTOSPORIDOSIS

Evolution of drug resistance to monotherapy is a major problem for infectious disease, particularly malaria. We anticipate similar problems with cryptosporidiosis in the future. Hence, efforts should be made to identify drug combinations to treat cryptosporidiosis. To this end, we have tested combinations of drug using our regular 48 hours asexual assay, wherein compounds are added, alone or in combinations at 3 hours post-infection and parasite number measured 48 hours post-infection. This strategy has not been very successful in identifying synergistic combinations, with itraconazole and tegaserod to be the most synergistic combination determined to date (Table 1). Since we have developed specific life stage assays, we wanted to logically combine representative compounds from each cluster to identify potentially synergistic or antagonistic set of compounds. But the invasion assay involves addition of compound before infection of host monolayer. Addition of compounds after 3 hours of invasion would lose the effect of compounds on this stage. One strategy would be to design the experiments with compounds added before infection. We tested this experimental design using a combination of nitazoxanide (inactive in the invasion assay) and clofazimine (invasion inhibitor) with compounds added before infection. The compounds were more potent than in this assay with only few lower concentrations providing a window to look for combinatorial effect. There seemed to be some hint of antagonism (Table 2).

Addition of compounds early might potentially give an advantage for certain compounds that act on the early stages, negating the effect of compounds that act later. Also, early on the infection is roughly synchronized with only trophozoites available in culture. It would be more relevant to look for combination of compounds on a mixed culture. Hence, we plan to test compound combinations on an established culture, with compounds added at about 24 hours post-infection and parasite number readout taken at 48 and 72 hours post-infection to cover almost all stages of the life cycle. Furthermore, we also have data from the parasite persistence assay, which similarly tests effects of compounds on an established infection. This assay also differentiates compounds to be potentially static while others to be potentially cidal. It would be ingesting to test if potentially static and cidal compounds would look different when combined.

Table 1. Checkerboard assay using the regular 48 h assay with compounds added 3 h post-infection.

	% inhibition						
	0 5 10 15 20 25 30 35 40 45 50 55 60 65 70 75 80 85 90 95 ###						
[Itraconazole] µM							
7.24	67	50	52	51	75	84	96
3.62	82	76	94	85	83	76	92
1.81	14	70	94	80	89	81	90
0.91	-8	5	40	90	93	86	92
0.45	27	-2	44	61	82	94	85
0.23	-15	-14	21	25	76	87	91
0	0	2	8	25	30	91	88
	0	0.3225	0.645	1.29	2.58	5.16	10.32
	[Tegaserod] µM						

Table 2. Checkerboard assay with compounds added before infection and parasite numbers measure 48 h post-infection.

	% inhibition						
	0 5 10 15 20 25 30 35 40 45 50 55 60 65 70 75 80 85 90 95 ##						
Clofazimine (CFZ)							
19.6	97	97	98	98	97	96	96
9.8	88	93	95	96	96	95	95
4.9	79	89	94	95	96	95	95
2.45	67	76	89	95	95	95	95
1.2	51	71	86	93	94	96	95
0.6	43	69	80	90	94	95	95
0	0	48	66	78	87	94	96
	0	0.11	0.22	0.44	0.88	1.76	3.52
	[Nitazoxanide] µM						